PROPOSAL OF WIRELESS CHARGING METHOD AND ARCHITECTURE TO INCREASE RANGE IN ELECTRIC VEHICLES

by

Omar Nezamuddin

A Dissertation

Submitted to the Faculty of Purdue University

In Partial Fulfillment of the Requirements for the degree of

Doctor of Philosophy

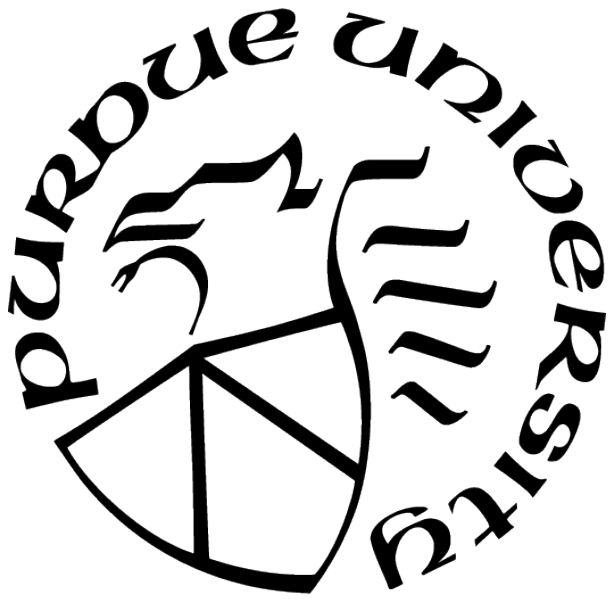

Department of Electrical and Computer Engineering

Indianapolis, Indiana

May 2021

THE PURDUE UNIVERSITY GRADUATE SCHOOL
STATEMENT OF COMMITTEE APPROVAL

Dr. Euzeli dos Santos Jr., Chair

Department of Engineering and Technology

Dr. Brian King

Department of Engineering and Technology

Dr. Maher Rizkalla

Department of Engineering and Technology

Dr. Lingxi Li

Department of Engineering and Technology

Approved by:

Dr. Brian King

For the best parents anyone could ask for:
Dr. Nabeel Nezamuddin and Dr. Farida Mirza.

ACKNOWLEDGMENTS

First and foremost, I would like to thank God for all the things in my life, and for bringing me to this point in particular. I want to take this opportunity to thank my parents for all their love, encouragement, and never ending support on everything. To them I owe so much and could never return the favor. I dedicate all this work to you, Dad & Mom. Now and always, Thank You. I also would like to thank my lovely wife, Cansu Sener, for supporting me and always being by my side. I can't express how much you have done for me; thank you for your unconditional love and encouragement. And to my awesome siblings, Sarah, Ibraheem, and Nora, thank you for your support of my education, encouragement, and continuously providing me with the help and mental support I need. I could have never done this without all your support. And I extend this sincere gratitude to the Alnamanakni, Mirza, and Sener families - thank you all for providing me with support and aide.

I would also like to thank the whole ECE department, with special thanks to the following: To Dr. Euzeli dos Santos Jr, for his continuous support, the great opportunities he has opened for me, and for supporting and guiding me in my educational endeavor. Thank you Dr. Santos, for helping me get to where I am today in my graduate education and for always pushing me to do better. To Dr. Maher Rizkalla, for all his support, his constant belief in me, and for encouraging me to pursue my masters degree. Dr. Rizkalla, you are the reason why I was convinced to get a masters degree, and I appreciate all your support in all my academic journey. To Dr. Lingxi Li, for all his support during my undergraduate years, and for believing in my pursuit of higher education. To Dr. Brian King for his support through out my academic career, for always there to give good advice, and always looking out for funding opportunities for me. To Sherrie Tucker, space is too limited to list everything she has done and all the help she's provided me throughout my undergraduate and graduate career, but I will mention this - if it was not for her, I would have missed so many important opportunities and don't get me started on deadlines. I truly thank you Sherrie for all your support and constant guidance throughout my time as a student.

Additionally, I would like to mention some of my good friends who have been through what I have, and shared some memorable time together in the lab. To Maryam Alibeik,

thank you for being there and going through the process with me, it was very nice to always be comforted by you when things got stressful. It was also a pleasure to have done research with you in our lab. To Rishikesh Bagwe, thanks for the many lab experiments we conducted together, there were a lot of nights filled with work, laughter, too much coffee, and arguments of which operating system is better. I'm sure Maryam will be happy that we are out of her hair. To Waiel Tariq for going through a lot of the courses with me during his Masters degree, stopping by the lab for coffee, and for giving me some competition in FIFA and Futsal. To Emre Arman, thanks for being a good study partner while you were taking your step 1 exam and I was studying for my qualification exam. We had some good memorable long nights on DS, CS, and arguing over Lucky(aka Sherafeddin). Also, to Mohammed Almutary, Jouse Arude, Gregory Almeida, Nustenil Marinus, Eduardo de Souza, Gregory Strum, Nathan Wheeler, Cloris Tang, Bharath Kumar, Prajakta Moghe, Jonah Crespo, Mayuresh Bhasagare, Maricio, Felipe and the soccer crew. We have shared some good memories together, and I'm very happy that you guys were part of my graduate career and life.

Finally, to the Futsal YMCA friends who made my stay here in Indianapolis memorable: Abdul Mustafa, Kemo, Basheer, Mubarak, Nani, Bagio, Ahmed, Evan and Andy. You guys know that I always look forward for our Futsal matches. I would like to also thank the late Majesty King Abdullah Bin Abdulaziz Al-Saud, and the Government of Saudi Arabia, for providing me the opportunity to conduct my studies through their generous support during my bachelors and masters degree.

PREFACE

This basis for this dissertation is stemmed for developing better alternatives for electric vehicles to prolong their trip. As the world embraces an era of electric vehicles, there will be a greater need to address some of the problems that prevents them in becoming a convenient solution over vehicles with an internal combustion engine. This dissertation will discuss some of those issues and propose two unique solutions.

This dissertation is ultimately based on a patent, a journal paper, and three published conference papers for the author Omar Nezamuddin.

TABLE OF CONTENTS

LIST OF TABLES

LIST OF FIGURES

LIST OF SYMBOLS

v	velocity
P_{out}	output power
P_{in}	input power
V_s	voltage source
V_1	voltage applied to transmitter
V_2	voltage at load of receiver
R_s	resistance of voltage source
R_1	parasitic resistances of transmitter coil
R_2	parasitic resistances of receiver coil
k	coupling coefficient
L_1	inductance or transmitter coil
L_2	inductance or receiver coil
r_1	radius of transmitter coil
r_2	radius of receiver coil
C_1	Capacitance of the transmitter coil
C_2	Capacitance of the receiver coil
C_{rated}	rated energy capacity of the battery
I_{bat}	battery current
V_{i}	internal voltage of battery
R_{i}	internal resistance of battery
P_{Bat}	output power of the battery
P_{motor}	output power of the motor
$P_{accessory}$	power consumed by the accessory load
η	efficiency of a motor
F_{trac}	total tractive force
F_{in}	inertial force
F_G	grade force
F_{rr}	rolling resistance force

F_{aero}	aerodynamic drag force
θ	incline angle
f_0	linear resonance frequency
ω_0	angular resonance frequency
η_1	efficiency of motor 1
η_2	efficiency of motor 2
η_3	efficiency of motor 3
T_{req}	requested torque
T_{Motor_i}	torque obtained from motor i
T_{Motor_j}	torque obtained from motor j
k_{Motor_i}	percentages of the total requested torque for motor i
k_{Motor_j}	percentages of the total requested torque for motor j
V_{int}	nonlinear internal voltage
E_0	constant voltage
$\mathrm{e}xp$	exponential zone dynamics
K	polarization constant
i^*	low-frequency current dynamics
$\mathrm{i}t$	extracted capacity
Q	maximum battery capacity
A	exponential voltage
B	exponential capacity

ABBREVIATIONS

EV	electric vehicle
HEV	hybrid electric vehicle
ICE	internal combustion engine
VVR	vehicle to vehicle recharging
WPT	wireless power transfer
TX	transmitter coil (or pad)
RX	receiver coil (or pad)
SOC	state of charge
GGE	gasoline gallon equivalent
CoM	charge on the move
IPT	inductive power transfer
EMF	electromagnetic field
DC	direct current
AC	alternating current
V2V	vehicle-to-vehicle
V2I	vehicle-to-infrastructure
MPC	model predictive controller
PMBDCM	permanent magnet brushless dc motors
APP	accelerator pedal position
BPP	brake pedal position
CPT	capacitive power transfer
RBS	rule based strategy
ORBS	optimized rule based strategy
PMSM	permanent magnet synchronous machine
FTP	federal test procedure
UDDS	urban dynamometer driving schedule
Li-ion	Lithium ion

ABSTRACT

Electric vehicles (EVs) face a major issue before becoming the norm of society, that is, their lack of range when it comes to long trips. Fast charging stations are a good step forward to help make it simpler for EVs, but it is still not as convenient when compared to vehicles with an internal combustion engine (ICE). Plenty of infrastructure changes have been proposed in the literature attempting to tackle this issue, but they typically tend to be either an expensive solution or a difficult practical implementation.

This dissertation presents two solutions to help increase the range of EVs: a novel wireless charging method and a multi-motor architecture for EVs. The first proposed solution involves the ability for EVs to charge while en route from another vehicle, which will be referred to from here on as vehicle-to-vehicle recharging (VVR). The aim of this system is to bring an innovative way for EVs to charge their battery without getting off route on a highway. The electric vehicle can request such a service from a designated charger vehicle on demand and receive electric power wirelessly while en route. The vehicles that provide energy (charger vehicles) through wireless power transfer (WPT) only need to be semi-autonomous in order to "engage" or "disengage" during a trip. Also, a novel method for wireless power transfer will be presented, where the emitter (TX) or receiver (RX) pads can change angles to improve the efficiency of power transmission. This type of WPT system would be suitable for the VVR system presented in this dissertation, along with other applications.

The second solution presented here will be an architecture for EVs with three or more different electric motors to help prolong the state of charge (SOC) of the battery. The key here is to use motors with different high efficiency regions. The proposed control algorithm optimizes the use of the motors on-board to keep them running in their most efficient regions. With this architecture, the powertrain would see a combined efficiency map that incorporates the best operating points of the motors. Therefore, the proposed architecture will allow the EV to operate with a higher range for a given battery capacity.

The state-of-the-art is divided into four subsections relevant to the proposed solutions and where most of the innovations to reduce the burden of charging EVs can be found: (1) infrastructure changes, (2) device level innovations, (3) autonomous vehicles, and (4) electric

vehicle architectures. The infrastructure changes highlight some of the proposed systems that aim to help EVs become a convenient solution to the public. Device level innovations covers some of the literature on technology that addresses EVs in terms of WPT. The autonomous vehicle subsection covers the importance of such technology in terms of safety and reliability, that could be implemented on the VVR system. Finally, the EV architectures covers the current typologies used in EVs. Furthermore, modeling, analysis, and simulation is presented to validate the feasibility of the proposed VVR system, the WPT system, and the multi-motor architecture for EVs.

1. INTRODUCTION

The move towards a society where electric vehicles (EVs) and hybrid electric vehicles (HEVs) dominate the roads is within the near future [1], [2]. This push has been affected mainly by environmental concerns, primarily regarding the rate of fuel consumption around the world [3], which would inevitably cause an increase in the price of fuel. Of the biggest drawbacks preventing EVs from populating the roads is the time it takes to charge them. This becomes a greater burden when going on trips requiring more than one pit-stop for recharging, which can represent a large portion of the trip time.

While the introduction of fast charging stations represents a good step forward [4], [5], the pit-stop time lacks the convenience of conventional vehicles with internal combustion engines (ICE). The current technology for high speed charging systems is considered as "Level 3" or "DC fast charging", which is capable of delivering 50 kW of power in 0.5 hr [6]. Indeed, the amount of energy contained in a typical gasoline tank is considerably higher than other sources [7], [8]. Gasoline gallon equivalent (GGE) is the amount of electric energy needed to equal the energy content of one liquid gallon of gasoline, e.g., 1 GGE = 33.40 kWh. With most compact cars, tanks around 15 gallons of capacity and an electric compact car with a battery size of 75 kWh [9], a direct comparison indicates that such conventional vehicles carry almost seven times more energy than those electric vehicles. Moreover, with fast charging stations already in existence, and the demand for more to help push EVs on the roads, their effects on the utility grid will be of concern [10]–[20].

This struggle for EVs to be a convenient solution on longer trip has been addressed mainly in terms of infrastructure change, with several of those solutions to be discussed in detail in the next chapter. A common issue that those proposed infrastructures have is that they are expensive and/or would require drastic change in terms of roads and highway re-construction. This dissertation proposes two novel solutions: a new method for vehicles to charge their battery via another vehicle while en route, and a multi-motor architecture for EVs.

The the first solution to be discussed in this dissertation will be denoted from here on as a vehicle-to-vehicle recharging (VVR) system. In the VVR system, a user driving on a trip

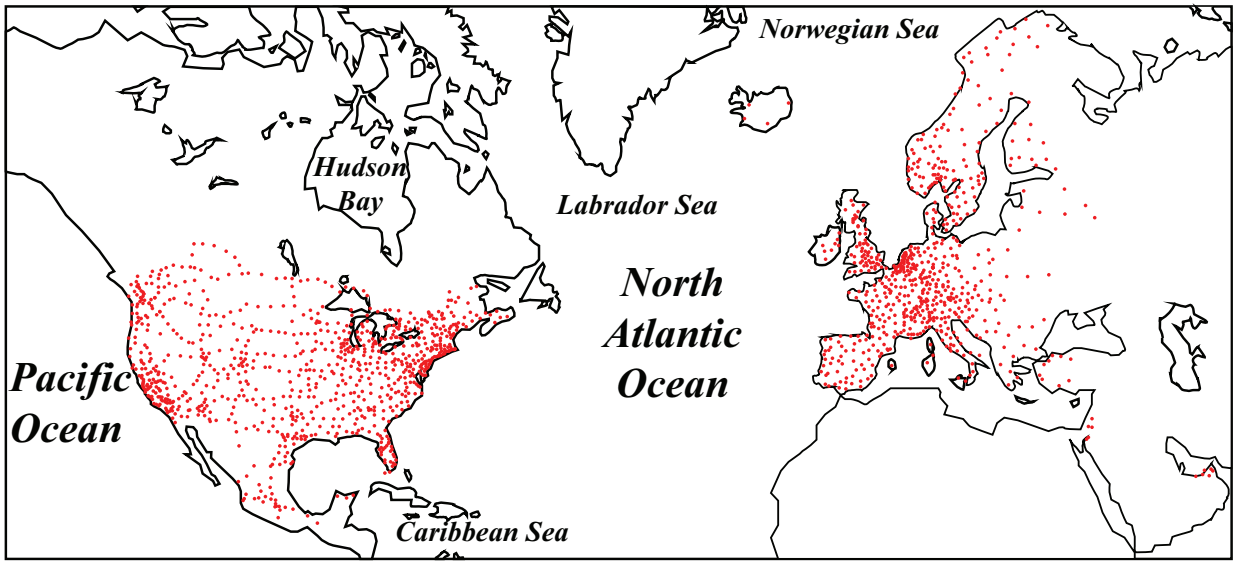

Figure 1.1. Tesla's fast charging network map for 2020.

can get extra energy on-demand throughout a trip to help give a boost of energy without needing to stop at a charging station. The vehicles requesting energy will be known as "user vehicles" in this dissertation, while the vehicles that charge the user vehicles will be known as "charger vehicles". Figure 1.2 illustrates the operation of the VVR system. It can be seen in Figure 1.2a that the user vehicle is on the highway with a full charge, and in Figure 1.2b the vehicle runs low on charge and requests for the VVR system. Then, the charger vehicle joins the highway as it gets close by and "engages" with the user vehicle as shown in Figure 1.2c. Finally, in Figure 1.2d the vehicle is either fully charged or no longer need the VVR system, and the charger vehicle "disengages" from the user vehicle. These charger vehicles would be located throughout the highways either in designated depots or at current charging stations. Also, the number of charger vehicles throughout the highways would depend on the demand. Notice that there is an infrastructure already in place to guarantee fast charging conditions to the EVs. Figure 1.1 shows the current map for Tesla's fast charging infrastructure in 2020 [21]. The proposed charging system is not expected to replace charging stations, but to work as a premium service available for those customers who value the time spent in a trip more than extra payment for the service. The proposed system could also be used for emergencies for police cars or ambulances that are EVs and running low on battery,

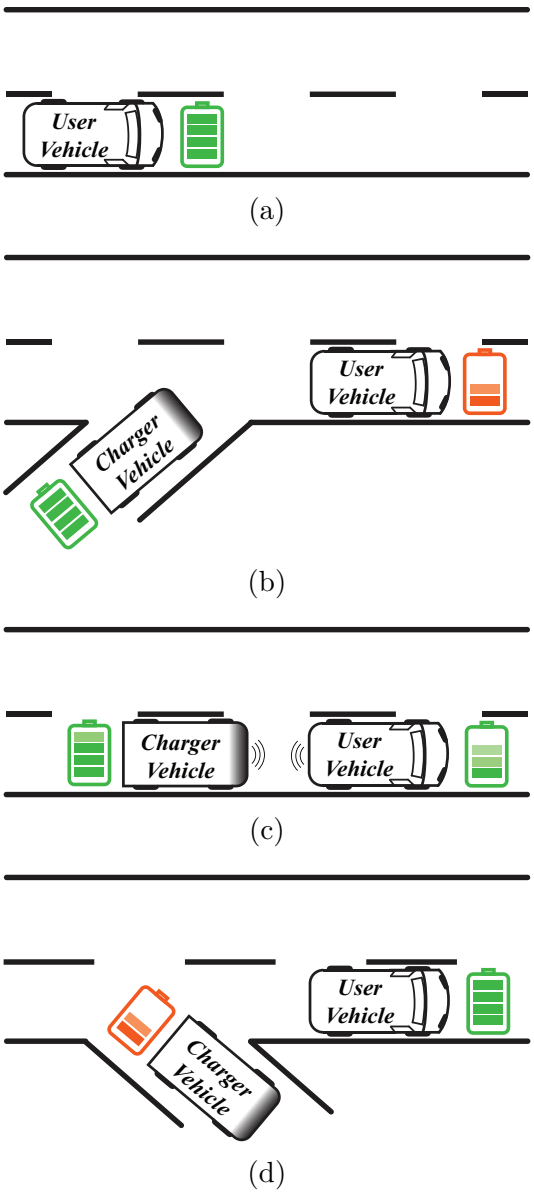

Figure 1.2. (a) User vehicle en route. (b) User vehicle requesting VVR. (c) VVR application. (d) Charger vehicle disengaging/leaving route.

since time is of the essence for such vehicles that are on duty. In-fact, some argue that police stations would have a difficult time transitioning to fully EVs due to limitations of the current battery technology [22], which the VVR system could help overcome in some situations. This would be a similar concept to that of refueling the military planes while in the air without the need for landing to re-fuel. To aid and improve the VVR system that will be presented, this dissertation also proposes a wireless power transfer (WPT) system

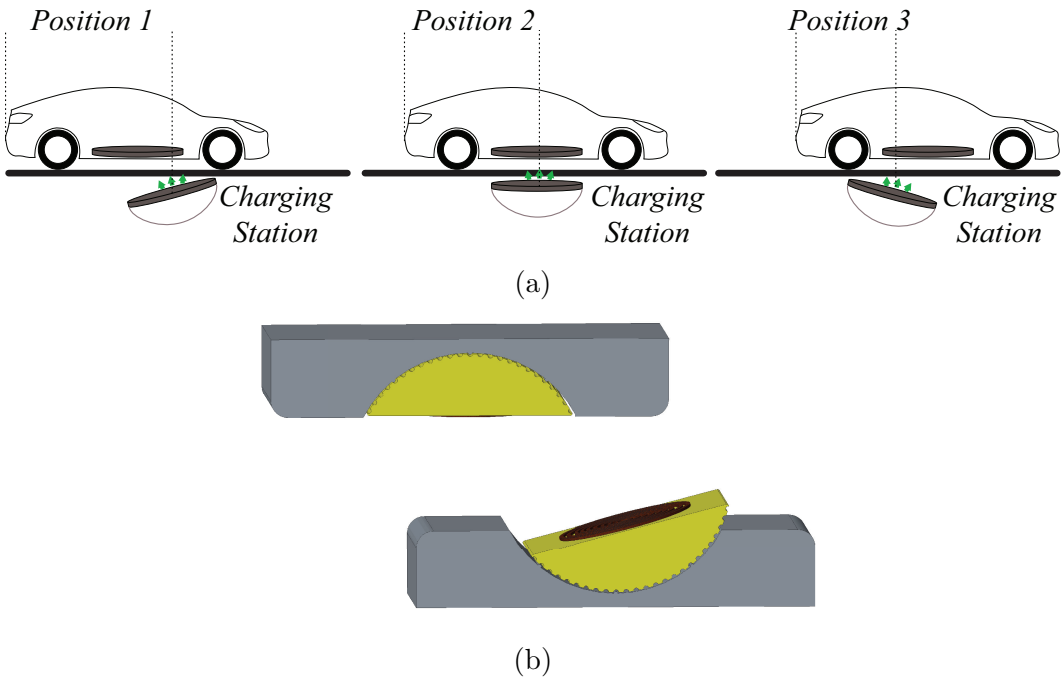

Figure 1.3. (a) Different relative position between vehicle and a charging station with dynamic self-alignment system. (b) 3D view in perspective.

with a dynamic positioning mechanism that allows power transfer with high efficiency for a large range of relative position between the transmitter (TX) and receiver (RX) coils. The system would incorporate a self-alignment feature for tracking the optimum angle to maximize power transfer between both coils. This type of wireless power transfer system can be suitable for the VVR system as well as other applications (e.g., charging stations). Figure 1.3 shows how the application of such WPT system can be incorporated at a charging station.

The second solution in this dissertation proposes an architecture for EVs that incorporates three electric motors with different operating regions to be used for propulsion. The main advantage is that at different operating regions, a controller can determine which motor would be running based on their efficiency map. The operating region is defined as the demanded torque to achieve the current speed. This way the motor with maximum efficiency at the current speed will be used for propulsion, or a combination of motors that would be considered a more efficient solution for the current operating region. Figure 1.4a shows an EV with a single motor power train, Figure 1.4b shows an EV with a power train that

incorporates three motors, and Figure 1.4c shows an EV power train that has n-motors. Note that in Figure1.4b and 1.4c, the power train would see a combined motor map efficiency of all the motors on board. More details including modeling and simulation will be presented later in the text. In addition to the comprehensive modeling, analysis, and simulation of the proposed systems, this dissertation will address the current state-of-the-art of the solutions proposed or EVs. This dissertation is organized as follows: a review on the scientific outcomes will be discussed in Chapter 2. The literature review will be presented in Chapter 3 and is divided into 3.1 *Infrastructure Changes*, 3.2 *Device Level Innovations*, 3.3 *Autonomous Vehicles*, and 3.4 *Hybrid and Electric Vehicles*. Chapter 4 will present the first solution to be discussed in this dissertation, that is, the vehicle-to-vehicle recharging system. Following that, Chapter 5 will present a wireless transfer method that can be incorporated in the VVR system. Then, Chapter 6 will discuss the second solution, a multi-motor architecture for EVs. Finally, Chapter 7 will present the summary of this dissertation.

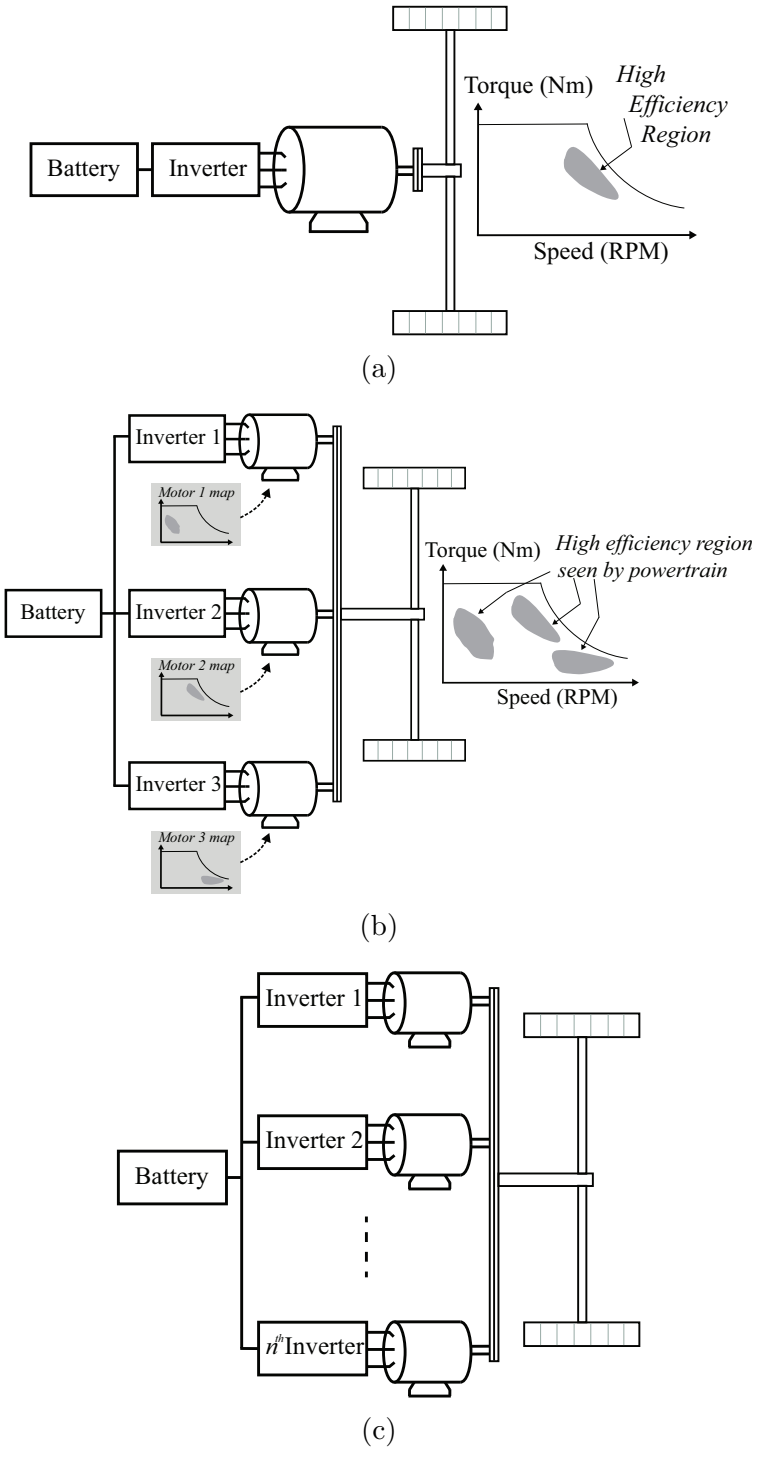

Figure 1.4. (a) Single motor EV architecture, (b) proposed three-motor architecture, and (c) proposed multi-motor architecture with n-motors.

2. SCIENTIFIC OUTCOMES

This will be a brief chapter presenting the contributions (scientific outcome) covered in this dissertation. The first outcome was a published journal by the author in the *IEEE Transactions on Intelligent Transportation Systems*. That paper presents a comprehensive literature review with focus on the difficulties electric vehicles (EVs) face to charge the battery while on a trip, and proposed a solution without the need of an expensive change in infrastructure. The proposed method charges EVs while en route from another vehicle, which was the vehicle-to-vehicle recharging (VVR). The aim of the system is to bring an innovative way for EVs to charge their battery without getting off route on a highway. This type of system would also not require drastic infrastructure change in terms of roadway re-construction, but rather exist with the current charging stations available. This concept of the VVR was also filed for a patent on Jan 6, 2021 with a title "*CARAVANNING AUTONOMOUS VEHICLE TRAIN*" by The Trustees of Indiana University, in which the author of this dissertation is also a co-inventor.

The second outcome from this dissertation was a paper published in the *2020 IEEE Transportation Electrification Conference and Expo (ITEC)*, which proposes a wireless power transfer system with a dynamic positioning mechanism that allows power transfer with high efficiency for a large range of relative position between emitting and receiving coils. The system would have a self-alignment feature for tracking the optimum angle and resonant frequency to maximize power transfer between both coils. This dynamic wireless power transfer system is suitable for applications such as the VVR, ground charging station, or a superior dock charging system.

Finally, this dissertation was the outcome of a paper published in the *2019 IEEE Transportation Electrification Conference and Expo (ITEC)*, which proposes a multi-motor architecture for EVs that help prolong the battery's state of charge (SOC) throughout a trip. The proposed architecture incorporates 3 or more motors, with different high efficiency regions. A control strategy can be implemented to decide which motor (or combination of motors) to use based on the current operating region. This would guarantee that the motors are running in their most efficient regions. With this architecture, the powertrain would see a

combined efficiency map that incorporates the best operating points of all motors on-board. Therefore, the proposed architecture will allow the EV to operate with a higher range for the same given battery capacity.

3. STATE-OF-THE-ART

This chapter presents a literature review covering methodologies and technologies related to the attempts from industry and academia to tackle the problem of small range in electrical vehicles. The following narrative reviews the current knowledge including substantive findings as well as theoretical and methodological contributions to topics presented in this dissertation. Those topics are divided into four subsections relevant to the proposed solutions and where most of the innovations to reduce the burden of charging EVs can be found: (1) infrastructure changes, (2) device level innovations, (3) autonomous vehicles, and (4) electric vehicle architectures.

3.1 Infrastructure Changes

This section includes the proposal of infrastructures that would ease the way for EVs on the road. Although such infrastructure would be expensive to implement, it would have advantages such as: (1) increasing driving range, (2) decreasing battery size, and (3) improving convenience [23]–[27]. In [28], a metering and wireless charging system was proposed that can account for the exact amount of electric power received by each vehicle, with a billing strategy. It is presented for infrastructures where wireless pads are placed under designated regions of the roads and vehicles can charge wirelessly while passing by. As multiple vehicles (that are close to each other) pass by a specific transmitter, it would be difficult to account for the energy consumed by each vehicle. The authors propose identification and metering equipment, charge control unit, and a dedicated software installed on the EV's to help alleviate this issue.

Other types of infrastructures have been proposed to help vehicles to charge-on-the-move (CoM). The idea of CoM for EVs is not a new concept, in fact it has been implemented for years as an overhead catenary system. Such system was used on busses, trams, and trains as well as road freight vehicles. In 2011, Siemens developed a refined catenary system that was tested on hybrid electric trucks [29]. In this system, using a pantograph type conductors, the vehicles can autonomously connect and charge from electrified parts of the highway as seen in Figure 3.1. The amount of power these vehicles can receives from the two wire overhead

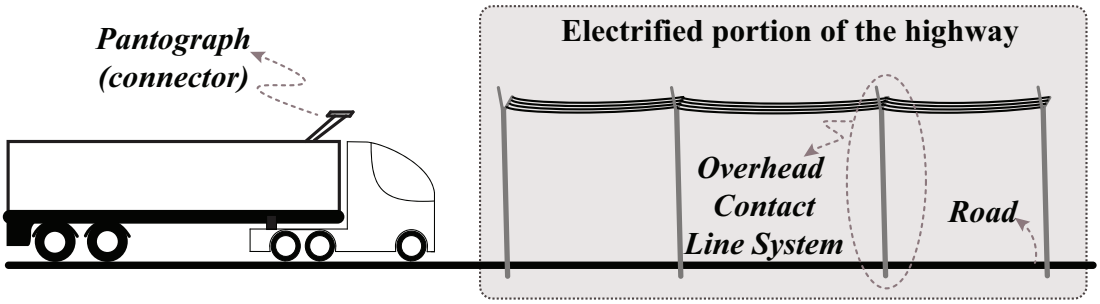

Figure 3.1. Siemens catenary system for hybrid electric trucks.

system is about 260 kW. This Siemens catenary system was introduced to a public road in Sweden (in June 2016) for two years of testing. The system was set up on a highway north of Stockholm, within a two-kilometer stretch. They used two diesel hybrid vehicles to operate under the Siemens catenary system for testing.

A change in the current infrastructure was proposed in [30] where cars could CoM as illustrated in Figure 3.2. The authors discuss the two major parts for such system which are the inductive power transfer (IPT) devices for both vehicles and roads. The IPTs on the road would be 1.5 m in length and spaced out on highways and rural roads. The authors also present a comprehensive consideration of the infrastructure updates, with an estimated cost of 76 billion euros for about 86% of the car-miles in Great Britain. The majority of this cost is due to the integration of IPT devices on the roads on a national scale. A study on the feasibility of such infrastructure was conducted in [31], where true decarbonization of the national road freight system was presented. The authors also highlight a logistic concept for road freight operations that is divided into four categories along with the proposal of different vehicles and charging methods for each.

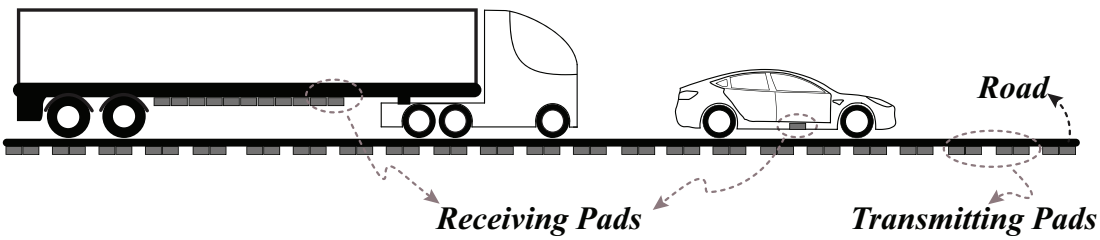

Figure 3.2. Charge-on-the-Move infrastructure illustration.

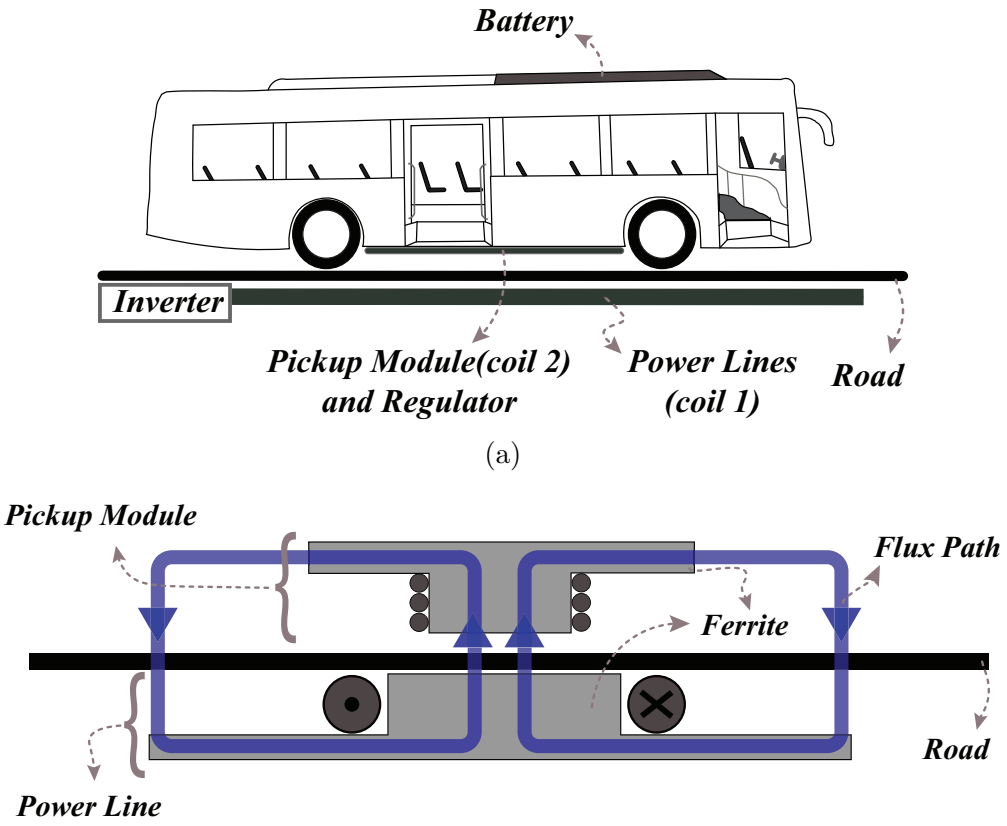

Figure 3.3. (a) On-line EV system. (b) Vertical magnetic flux pickup coil and design of power line.

In [32], an On-Line Electric Vehicle system is presented that incorporates high efficient and low electromagnetic field (EMF) wireless power transfer. This system (presented in Figure 3.3a) is comprised of power lines connected to an inverter that extends under ground to generate resonant magnetic field, while the EVs have a pickup modules, batteries, capacitors and electric motors. The authors use vertical magnetic flux type pickup coil along with a proper design of power lines to achieve 80% efficiency as highlighted in Figure 3.3b. The authors also propose two methods for EMF shielding for the design.

Another proposal of infrastructure change for EVs was presented in [33] (Figure 3.4) that consists of WPT, supercapacitors and electric motors. The author highlights the importance of using WPT based on magnetic resonance for high efficiency along with supercapacitors as buffer devices instead of Li-ion batteries. The claim is that the incorporation of such devices

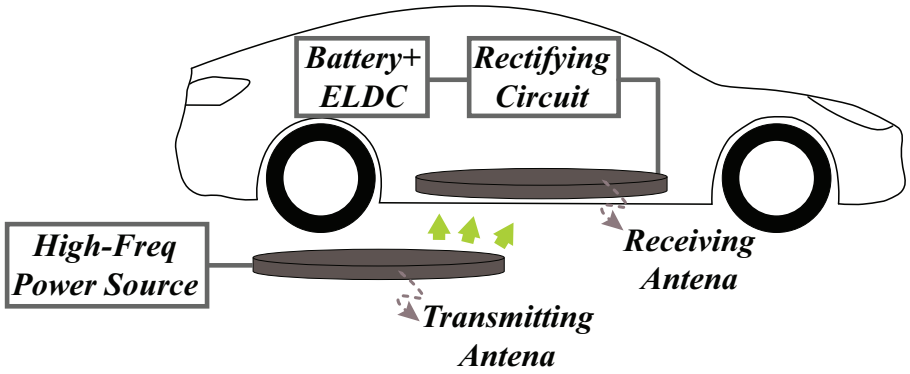

Figure 3.4. Infrastructure with EV's that consists of supercapacitors (ELDC) and batteries on-board.

will allow the feasibility of a convenient EV infrastructure. The author also showcases experimental results for WPT with 90% efficiency at an operating frequency of 10 MHz. It is worth mentioning that in this setup the vehicles would charge while stationary to get a boost of energy. A similar setup which requires adding transmitting coils under the roads was discussed in [34]. Herein, the authors propose an innovative way of WPT using multiple transmitting coils that are connected together and can turn off/on selectively. They derive an expression for the efficiency of the proposed system, and also provide simulation and experimental results. In [35], another system which involves charging vehicles while on the move via dielectric coupling is presented. Here, the vehicle's tires have a steel belt around them that interacts with electrified roadways while on the move to allow for WPT (as illustrated in Figure 3.5). The Authors show experimental results with a 1/32 scale models of EVs, and assert that this approach is promising since it can achieve high efficiency with impedance matching circuits. Another take on EV infrastructure (similar to that discussed in this paper) was introduced in [36], [37]. The authors use large vehicles (like a truck or bus) on highways to transfer energy to other vehicles on the road, therefore overcoming the need for EVs to stop for a charge. The system presented in this paper, however, proposes a better solution with an optimized charger vehicle.

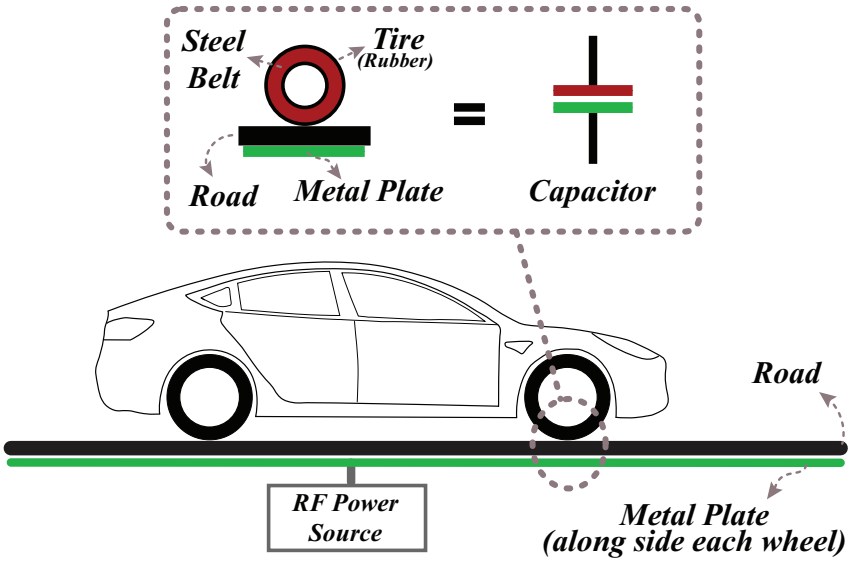

Figure 3.5. CoM infrastructure via dielectric coupling.

3.2 Device Level Innovations

The topic itself of WPT in electric vehicles has become more popular, and many methods and different approaches of WPT have been introduced and discussed in detail [38]–[44]. A study for evaluating different power pads used for electric vehicles based on their power transfer efficiency was conducted in [45]. It's a bigger challenge to charge vehicle on the move (dynamic wireless energy transfer), and most of the studies conducted are for static wireless charging as presented in a detailed review in [46]. They also present a unique issue to dynamic wireless energy transfer, that is the need for alignment between the two coils which greatly affects the transmission power.

The main technologies for WPT are through radio waves [47], resonances coupling and inductive power transfer. In recent years though, the WPT based on resonance coupling has been explored and became more popular due to its high efficiency [48]–[54], and was first discussed in [55].

Even with such technologies, one of the challenges that wireless charging faces is when the energy transfer is done with coils that are not aligned and with a dynamic changing distance between them (dynamic WPT) [56]. In [57], the authors show that the worry of the change in distance between the two coils can be overcome by choosing an optimal transmission

frequency for the WPT with coupled-mode and resonance theory. The analysis there is based on a circuit model of a strongly magnetic resonance WPT. Another study in [58] highlights the WPT systems' dependency on the complex impedance of the receiver. The authors propose a complex impedance tuning method that comprises of a DC/DC converter and LC filters. They show that it is possible to tune the receiver load resistance in a wide range of values from the circuits low-frequency region.

One important aspect of control in WPT systems is certainly maximizing the power efficiency, and plenty of research on that topic has been conducted [59]–[66]. Another aspect of dynamic WPT is the consideration and estimation of the coupling coefficient as presented in [59]. Herein, the authors present a method for real time coupling coefficient estimation, along with a controller to maximize the WPT efficiency using the DC/DC converter on the receiver side. In [67], a state feedback controller was designed to watch out for the changes of mutual inductance that helps improve the general stability of the system. The authors mention that such controller could be usable in applications of dynamic WPT on EVs.

Dynamic WPT technologies also face an issue when there is a tilt between the two coils. In fact, a study conducted in [68] shows the effects of the tilt angle between the transmitting and receiving coils. The authors showcase three different scenarios and propose a method to obtain the optimal tilt angle for high WPT efficiency, with respect to their relative position. The analysis for power efficiency was based on a circuit model (illustrated in Figure 3.6a) with a single transmitter (TX) and receiver (RX). The coupling coefficient (k) was calculated considering a misalignment both in angle and horizontal position as shown in Figure 3.6b.

Moreover, research on the effects of the vehicle's speed at which it passes a WPT area was conducted in [69].The authors show that different speeds affect the efficiency of the WPT, and propose a control method to optimize the energy transfer with respect to the driving speed. This control method is focused on adjusting the voltage of the transmission or the vehicle-side equivalent load resistance. With the topic of dynamic WPT becoming more popular, recent research control methods for dynamic WPT have been proposed in the literature such as [70]. Herein, a power control method that changes the amount of power being transferred based on the state of charge (SOC) of the battery is presented. The authors

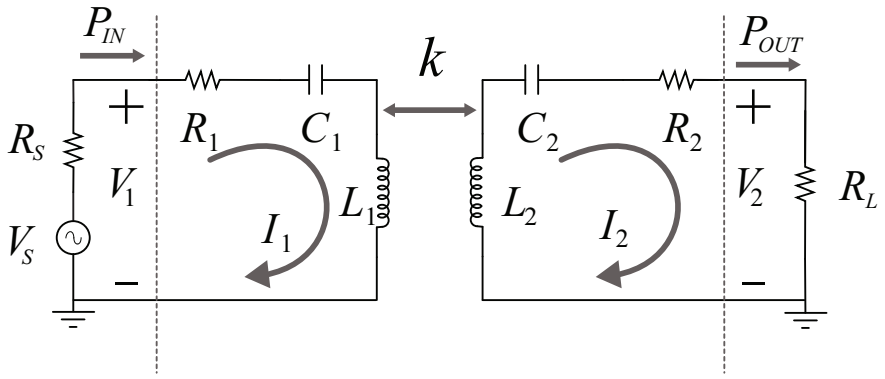

(a)

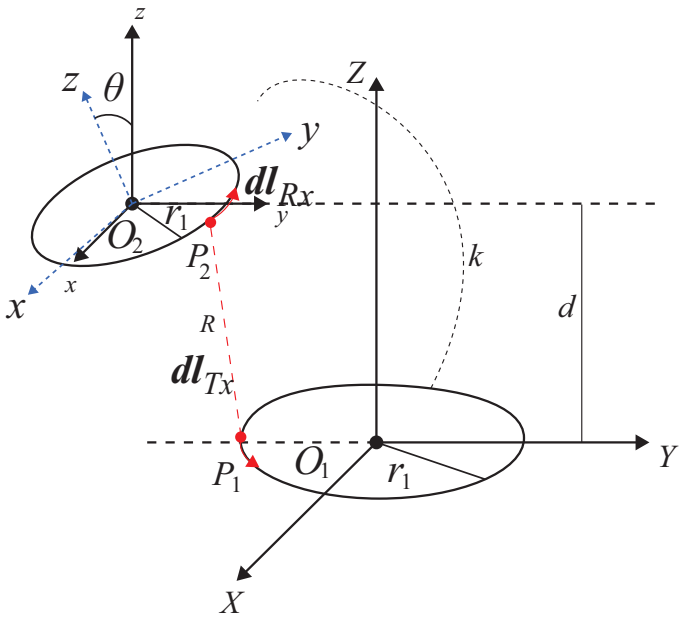

(b)

Figure 3.6. (a) Circuit model of WPT system with a single TX and RX. (b) WPT system with angle and horizontal misalignment.

argue that with such method, dual-sided communication is avoided. They also provide some experimental results from a built prototype that can transmit about 1.5 kW of power.

3.3 Autonomous Vehicles

As mentioned in the last section, the concept of the VVR system is that a user vehicle can get extra energy on-demand to prolong the duration of the trip without having to pit-stop. This is similar to the concept of vehicular platooning, where one vehicle follows another safely

with a small distance between each other at high speeds. In the VVR system, the charger vehicle only needs to be semi-autonomous in order for it to guarantee a constant distance while charging, and this level of "semi-autonomous" is currently available in the market. Although, research on vehicular platooning has attracted attention as vehicles get higher level of autonomy, specifically with connected autonomous vehicles [71]–[73]. Also, plenty of research has been conducted on vehicular platooning in terms of safety [74]–[78]. It is worth mentioning that it is possible to achieve vehicular platooning safely at small distances between vehicles, with no information or communication from the lead vehicle [79]–[85].

Fully autonomous vehicles (self driving cars) are vehicles that are equipped with sensors to identify and navigate through the environment nearby with no human input at all. If both the user vehicle and the charger vehicle have full autonomous capability, it would make for a stronger case in terms reliability and safety. Recently, the concept of autonomous vehicles have become more popular [86]–[90]. The automotive industry, along with research institutions, are also playing a role in advocating some of the highlights of autonomous (or semi-autonomous) vehicles in terms of safety. At the present time, multiple studies have been conducted on the improvement of the self driving cars in terms of safety [91]–[93] and control [94]–[97].

Autonomous vehicles always need to answer the question of "what to do next?". These vehicles need to use information gathered by their localization center to answer that question. The localization techniques used in autonomous vehicles can be summed up in two categories [98]: sensor based, and cooperative localization techniques. The first technique is comprised of vehicles that only rely on on-board sensors to make decisions. Although the sensors used in such a technique are typically more accurate and reliable, they come with an increase of cost. The second technique makes decisions based on communications of vehicle-to-vehicle (V2V), vehicle-to-infrastructure (V2I), and on-board sensors. The authors in [99] show that such a cooperative localization technique can indeed increase the system performance, robustness, and a general better awareness of the surrounding environment. In recent years, the exploration of autonomous vehicles have also expanded to the airspace [100]–[106], and also underwater [63], [107]–[110].

One of the most important features that autonomous vehicles must comprise of is the steering control for path tracking capability. In [111], a model predictive controller (MPC) was introduced for path tracking that reduces that lateral tracking deviation and keeps the vehicle stable for high and low speeds. Due to the computational complexity in which an MPC controller can impose when considering path tracking as an optimization problem, [112]–[114] have suggested combining the MPC with a Laguerre function and/or an exponential weight to reduce such complexity. Another adaptation of an MPC was presented in [115], where a linear MPC is capable of path tracking with minimum side to side deviation at high speeds. In [116], a detailed comparison between a path tracking and a torque-vectoring controller is presented. Although torque-vectoring controllers require vehicles that have motors on each wheel, they still provide a great solution for vehicle stability and performance when compared to path tracking controllers based on steering system actuation.

Modeling of autonomous vehicles is desired to ensure that proposed control systems work as expected. In [117], the authors propose a game theoretic traffic model that can be used to test multiple vehicles' decisions based on safety and correct performance. The authors also state that their developed simulator can be used to tune and calibrate parameters of control policies in autonomous vehicles. Other game theoretic modeling techniques for autonomous vehicles were presented in [118]. Herein, the models were used as a solution to paradigms that are important when considering a driver's interaction with the vehicles active front steering collision avoidance controller. A similar study was also conducted in [119], where the focus of the game theoretic model was to analyze the interaction between the driver and an automated steering system that is based on a cooperative pareto steering strategy. As the topic is still passing its early stages, modeling of autonomous vehicles will continue to be a discussed subject in the literature in the foreseeable future. All the current and new autonomous vehicle developments can be used to make the proposed VVR system more efficient.

3.4 Hybrid and Electric Vehicles

HEVs have a more complex powertrain when compared to EVs, and plenty of propulsion architectures have been proposed for the use in HEVs [120]. The three main types are parallel HEV, series HEV, and a series-parallel HEV. The series-parallel HEV system is more complex than the other two configurations, its main advantage is that it can allow the ICE to run closer to its higher efficiency regions more often [121].

Electric vehicles, on the other hand, couples an electric motor to axle and wheels through transmission/differential and a power electronics module couples the motor to a battery. Architectures with two motors have been studied in the literature and [122] provides a method for optimizing the torque applied by each motor of a dual motor drive system of an all-electric vehicle. The authors in [123] applied the Pontryagin's minimum principle optimization to their dual motor setup. Based on the optimization results, a control strategy is developed which is a combination of mode switching control and power-split control. The research in [124] proposes a brake energy recovery strategy for a dual-motor dual-axis electric powertrain. Their new strategy achieves 9.95% higher regeneration than the front axle braking strategy while keep the same driving behavior. In [125], a novel dual-motor coupling powertrain that couples speed and torque is proposed. Although coupling multiple motors to a driveline could have its own complexity, it is a problem with all HEVs or EVs that incorporate more than one motor or engine and this technology has been well established. The coupling of the motors onto a single powertrain will not be the focus of this paper.

Other architectures have incorporated the motors directly on to the wheels. One main advantage of in-wheel motors is the reduction of distance for power transmission which would provide an increase in efficiency. A driving and control system for a direct-wheel-driven EV is proposed in [126], which employs two permanent-magnet brushless dc motors (PMBDCMs) and a control strategy that simplifies the commonly complex differential algorithm for steering. In [127], a current distribution control for a dual direct driven wheel motors is proposed. The authors determine the necessary amount of input current to each driving wheel with a load disturbance observer, model following controller and a velocity command compensator.

Other control systems have been proposed for an EV with four in-wheel drive systems such as those in [128] and [129]. Although in-wheel drive systems present specific technical advantages, they face considerable challenges. Some of those challenges include limited space to work with, increasing the unsprung weight, and a lack of differential requires a complex torque controller to achieve different wheel speeds [130]. Other notable issues with in-wheel motors include the effects of heat from braking on the motor performance, any shocks and bumps seen on the road by the wheel would affect the motor components connected in the wheel setup. An in-depth review on mechanical causes of failure modes for in-wheel motors in EVs is presented in [131].

4. CONVENTIONAL ELECTRIC VEHICLE: MODELING AND SIMULATION

The first component to be presented in this dissertation is the modeling of an electric vehicle (EV). The EV models are hybrid models that incorporate equation-based modeling similar to that presented in [132]. There are two globally accepted methods for modeling an EV, a forward-facing powertrain model and a backward-facing powertrain model [133]. This paper employs a forward-facing powertrain model and was implemented in MATLAB®/Simulink®.

Figure 4.1 shows the main block diagram representing the model of a typical EV. The first aspect of this model is the drive cycle (or reference vehicle speed), which primarily contains data points that represent the speed of a vehicle versus time. These data points can either be synthetic or real, depending on the type of modeling to be presented. In this dissertation, the data points were either purely synthetic or taken from well known drive cycles used in the literature. The data points from the drive cycle would then be fed into the driver model along with the current vehicle speed.

The driver model block can be seen in detail in Figure 4.2, where the objective here is to ensure that the vehicle speed obtained from the glider model is following the drive cycle data. It does that by getting the difference (error), which is then applied to a PID controller to define the accelerator pedal position (APP) along with the brake pedal position (BPP).

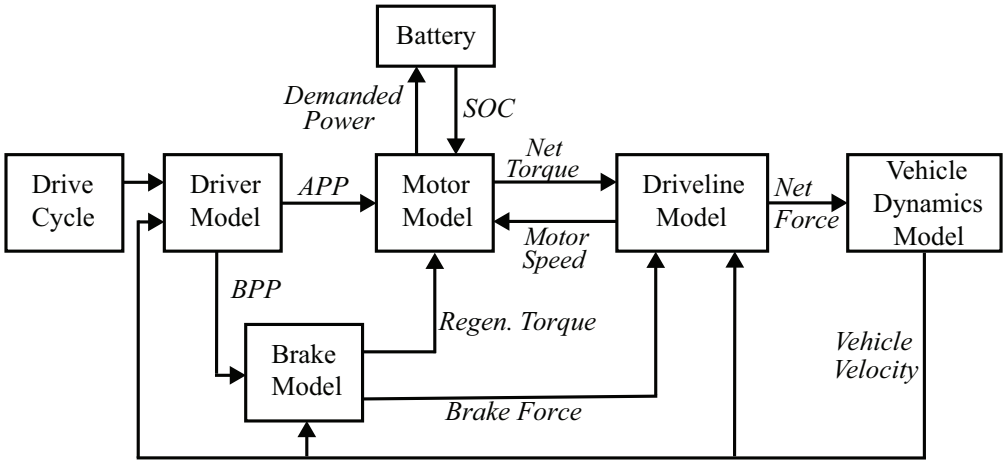

Figure 4.1. Block diagram of the proposed EV.

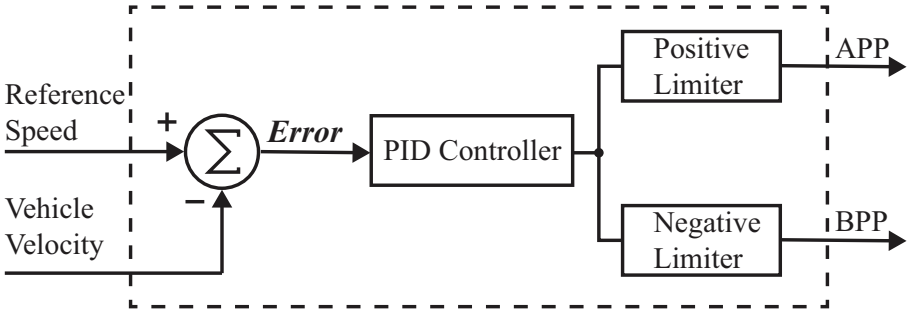

Figure 4.2. Driver model block diagram.

The BPP is then the input of the the brake system along with he vehicle speed, to determine how much regenerative torque can through the motor. The output of the brake model is the regenerative torque, which is an input to the motor block, and the friction brake force that is fed to the driveline model.

On the other hand, the APP from the driver model goes to the motor model shown with more details in Figure 4.3. Herein, the APP requests the amount of torque to reduce the speed difference error, but is limited by a one-dimensional lookup table that defines how much maximum torque is allowed at the current motor speed. The output of the limiter is the positive torque needed for propulsion, subtracted by the regenerative torque (obtained from a brake model) to get the total net tractive torque going to the driveline. This net torque at the current speed is what defines the power needed from the battery based off the motors' efficiency map (a 3D lookup table also highlighted in Figure 4.3).

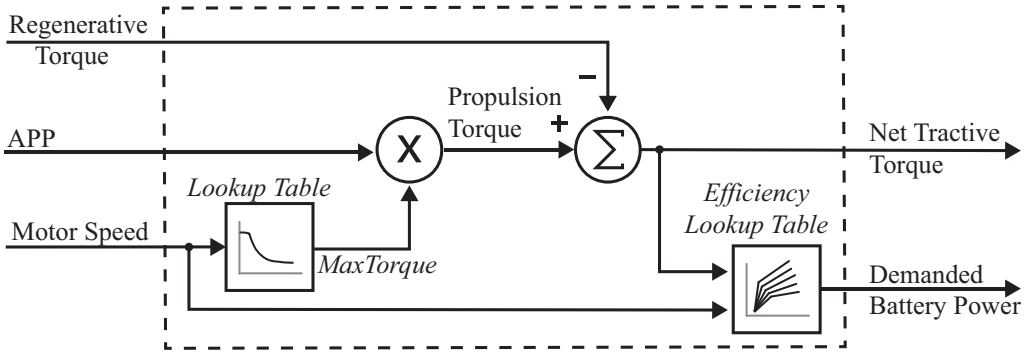

Figure 4.3. Motor model block diagram.

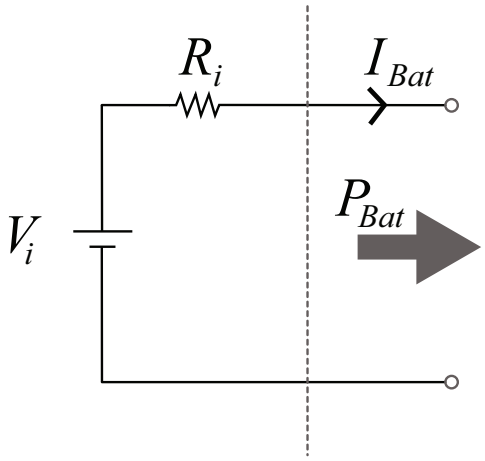

Figure 4.4. Battery model.

The motor model would then have two outputs: the net tractive torque going to the driveline block and the total power requested from the motor to the battery model. The battery model would then use the power demanded to calculate a new value of SOC. The Battery's SOC is calculated using the coulomb counting method as shown in [134], which can be re-written as:

$$SOC = SOC(t_0) - \frac{1}{C_{rated}} \int_{t_0}^{t_{final}} I_{Bat} dt \tag{4.1}$$

where C_{rated} is the rated energy capacity of the battery, t_0 is the initial time, t_{final} is the final time, and I_{Bat} is the battery current. The convention here is that positive current I_{Bat} is coming from the battery. For a simplified battery model (shown in Figure 4.4) consisting of an internal resistance (R_i) and voltage (V_i) connected in series only, the current I_{Bat} is a function of the power output of the battery (P_{Bat}), and can be defined as:

$$I_{Bat} = \frac{V_\mathrm{i} - \sqrt{V_\mathrm{i}^2 - 4R_\mathrm{i}P_{Bat}}}{2R_\mathrm{i}} \tag{4.2}$$

where $P_{Bat} = \frac{1}{\eta} P_{motor} + P_{accessory}$, η is the efficiency of the motor, P_{motor} is the output power of the motor, and $P_{accessory}$ is the power consumed by the accessory load. In this simulation, the battery current is positive when delivering power to the driveline, and negative when there is regenerative energy coming back to it. Research on battery management techniques

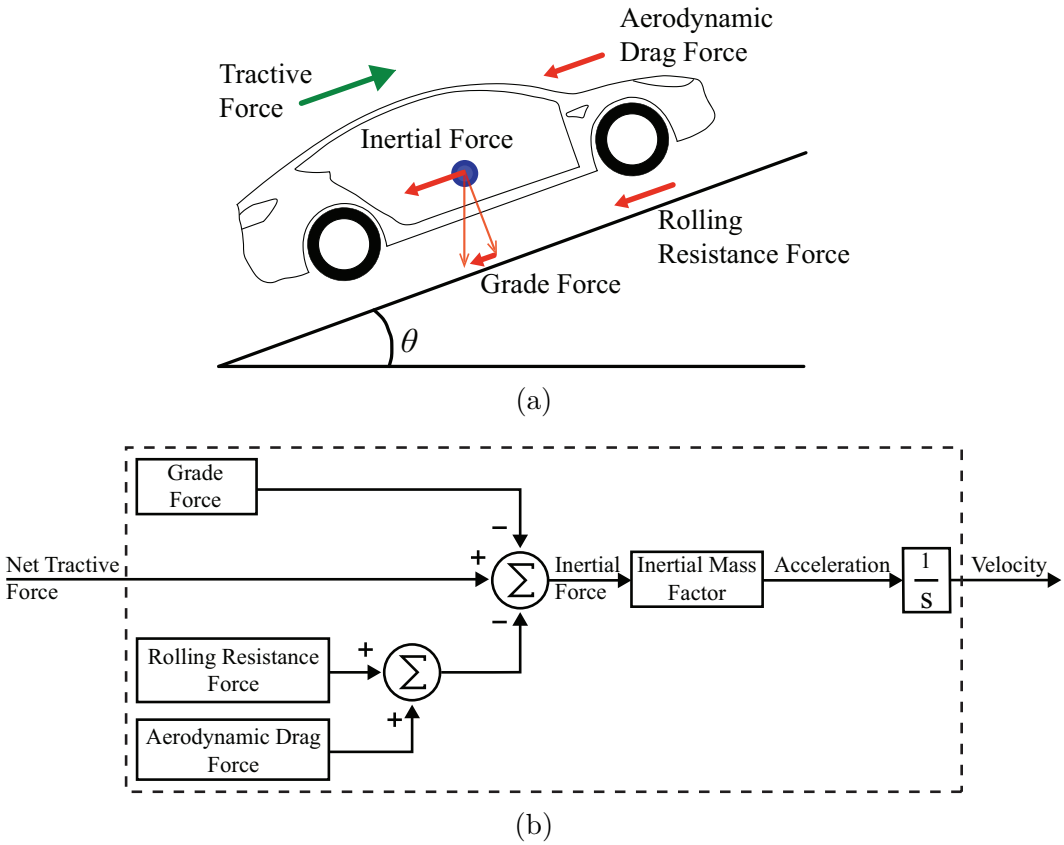

Figure 4.5. (a) Free body diagram of vehicle. (b) Block diagram of vehicle model.

have been discussed in the literature such as in [135], where the authors propose a hierarchical energy management strategy for HEVs that can be used for EVs.

The driveline block converts that total tractive torque it received from the motor block to tractive force, which is then the input of the glider model. The glider model (or vehicle model) is a physics-based model inspired from [136]–[138] where the tractive force overcomes all other forces acting on the vehicle. Figure 4.5a shows the a free body diagram of the vehicle highlighting the forces acting on it, which can be described as:

$$F_{trac} = F_{in} + F_G + F_{rr} + F_{aero} \tag{4.3}$$

where F_{trac} is the total tractive force needed for propulsion, F_{in} is the inertial force, F_G is the grade force, F_rr is the rolling resistance force, and F_aero is the aerodynamic drag force. It is evident that unless the vehicle is slowing down or braking, the F_{trac} must overcome all

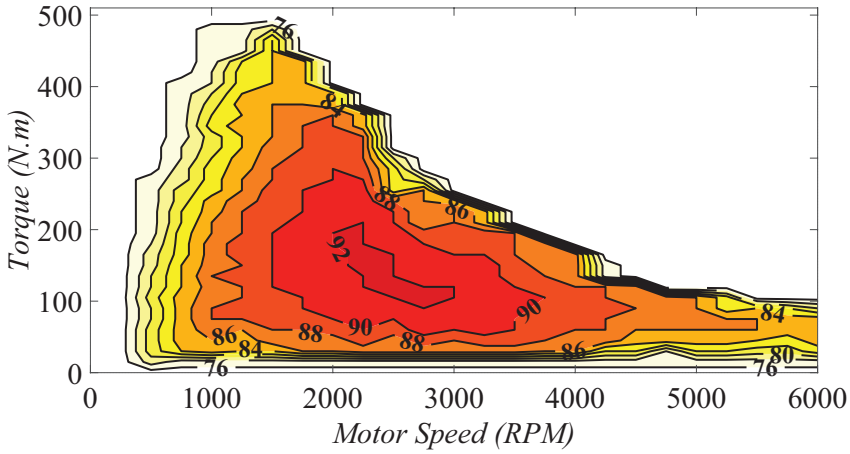

Figure 4.6. An induction motor efficiency map.

the other forces acting on the vehicle in order for it to catch up to the reference speed. A block diagram describing this is shown in Figure 4.5b, where the inertial force is used here to obtain the acceleration, then integrating it to obtain the vehicle velocity.

To show the performance of this model, a simple simulation will be presented in this chapter. The motor map used was similar to that of an induction motor with the following efficiency map presented in Figure 4.6, and the vehicle dynamics for the EV used are presented in Table 4.1. The drive cycle (reference vehicle speed) for this demonstration was the urban dynamometer driving schedule (UDDS), which is approximately 1400 seconds. The first objective to observe is whether the model is following the reference speed provided from the drive cycle data, and as presented in Figure 4.7, it is evident that the model does a good

Table 4.1. Vehicle dynamic parameters used for modeling the EV.

Parameter	Value
Air density	1.23 kg/m^3
Drag coefficient	0.38
Vehicle frontal area	2.1 m^2
Vehicle mass	1560 kg
Gravitational acceleration	9.81 m/s^2
Road angle	0 $Degrees$
Rolling resistance coefficient	0.01

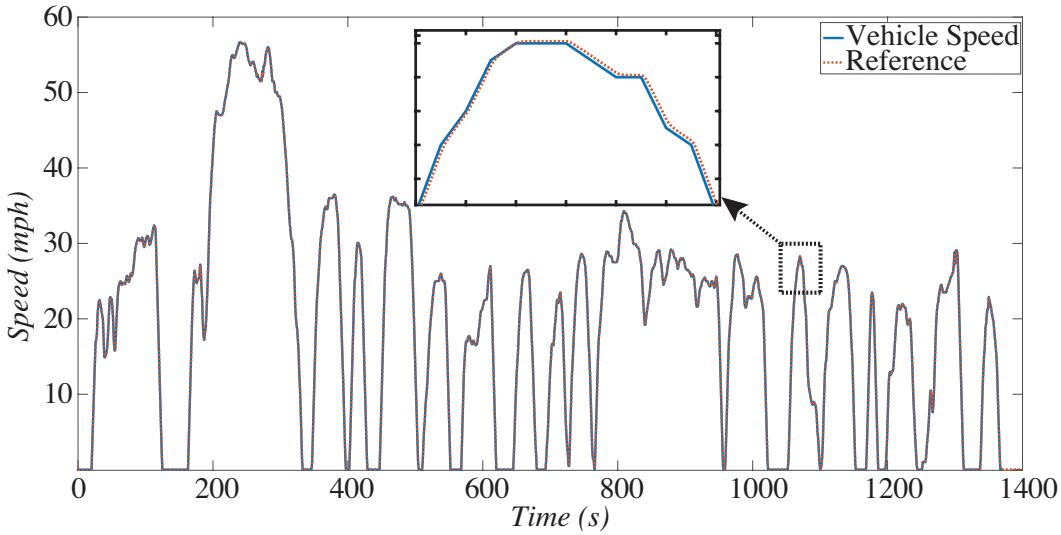

Figure 4.7. Reference speed vs vehicle speed for the urban dynamometer driving schedule (UDDS).

job doing so. Figure 4.8 shows the SOC of the battery for this model after 1400 seconds, which is roughly about 79%.

Justification of battery model

Although this simulation uses a simplistic battery model shown in Figure 4.4, it does well in understanding the effects of other variables in the simulation on the battery's SOC. A

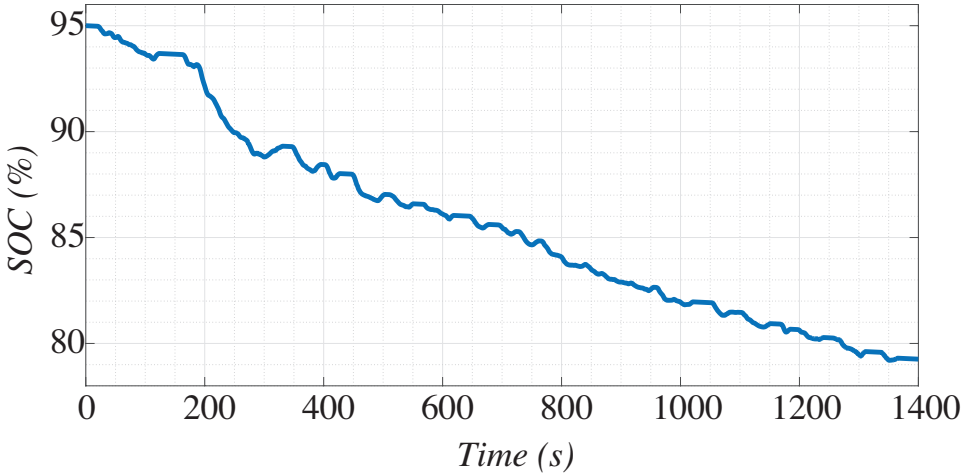

Figure 4.8. State of charge of the battery's EV.

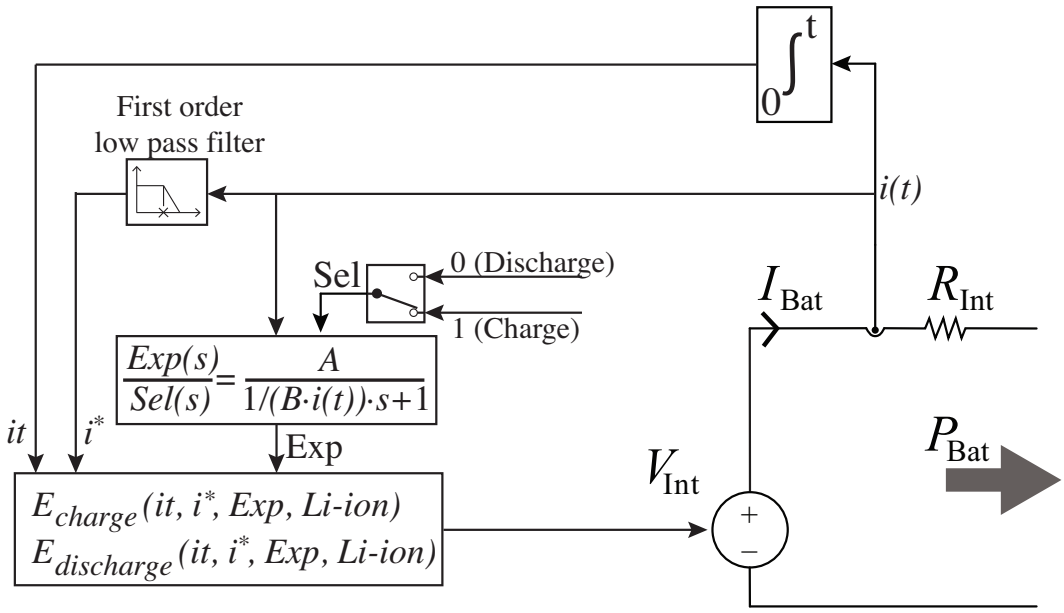

Figure 4.9. Lithium-ion battery model obtained from Simulink.

more complex model presented in Figure 4.9 was used as a comparison. This model is for a lithium ion (Li-ion) battery obtained from Simulink, and was set to have the same capacity as that presented previously. The model was derived from the discharge curve characteristics of a Li-ion battery, and is constituted by the following equations for its internal voltage:
For $i^* > 0$,

$$E_{discharge} = V_{int} = E_0 - K\frac{Q}{Q - it}i^* - K\frac{Q}{Q - it}it + A \cdot exp(-B \cdot it) \tag{4.4}$$

For $i^* < 0$,

$$E_{charge} = V_{int} = E_0 - K\frac{Q}{it + 0.1Q}i^* - K\frac{Q}{Q - it}it + A \cdot exp(-B \cdot it) \tag{4.5}$$

where V_{int} is the nonlinear internal voltage, E_0 is the constant voltage, exp is the exponential zone dynamics, K is the polarization constant, i^* is the low-frequency current dynamics, i is the battery current, it is the extracted capacity, Q is the maximum battery capacity, A is the exponential voltage, and finally B is the exponential capacity.

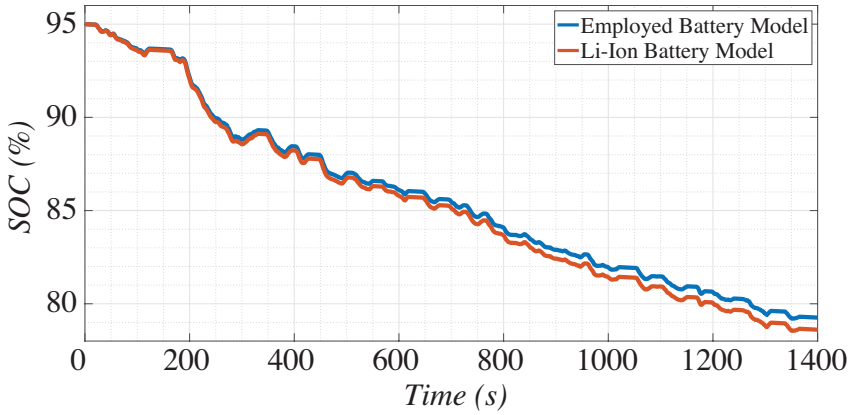

Figure 4.10. Comparison of SOC for employed battery model vs Li-ion battery model.

Figure 4.10 shows a comparison of the SOC with the battery model derived from equation (4.2) vs that of a generic Li-ion battery obtained from Simulink. It can be seen that there is a 1% difference in SOC after about 1400 seconds. Although the Li-ion battery had a different SOC, the time of running the simulation was much longer. This means that the model presented in Figure 4.4 would suffice to illustrate the effects of the rest of the model on the SOC.

5. VEHICLE TO VEHICLE RECHARGING

5.1 Proposed System

As the literature review suggests, the problem of electric vehicle charging remains open ended. Although there are many technical solutions presented in the technical literature, most of them carry inherent economic and/or implementation challenges. This section presents an alternative solution that allows EV batteries to be charged with minimum infrastructure changes and with the ability to reduce the pit-stop time to zero.

The proposed system in constituted by a charger vehicle that is capable of charging another vehicle wirelessly on a highway. The user vehicle would be en route on a trip that would typically require at least one pit-stop. During the trip, the user vehicle can request for the VVR as the SOC of the battery goes low. The logistics of such a system can be further studied and discussed to improve the performance of the over all system, however an introduction to the idea will be discussed in this dissertation. A general overview of how the charger vehicle engages and disengages from the user vehicle is presented in Figure 5.1. It is assumed that the user vehicle starts the trip with a full SOC (see Figure 5.1a). As the vehicle goes about the route, and starts to reach an uncomfortable low level of SOC, it requests for a VVR and the charger vehicle joins the route as highlighted in Figure 5.1b. The charger vehicle would then get close to the user vehicle, and wait for a request to "engage" to start the process of wireless power transfer. Figure 5.1c shows both vehicles during VVR process with both vehicles traveling at a close distance. Finally, in Figure 5.1d, the user vehicle is either fully charged or requests a "disengage" from the VVR, which will find an exit to either recharge its own battery or park and wait for the next user vehicle. It is note worthy to mention the following assumptions of the VVR system for this dissertation: (1) the user and charger vehicle has location information about the other vehicle; (2) the charger vehicle has SOC information on the user vehicle; (3) the charger vehicles only participate in the VVR if they have sufficient amount of energy to provide; and finally (4) the user vehicle will travel on a designated route that has charger vehicles available at depots or charging stations.

As for the charger vehicles, the concept here is that they would have either large batteries or an on-board electric generator that is capable of delivering power to multiple vehicles as

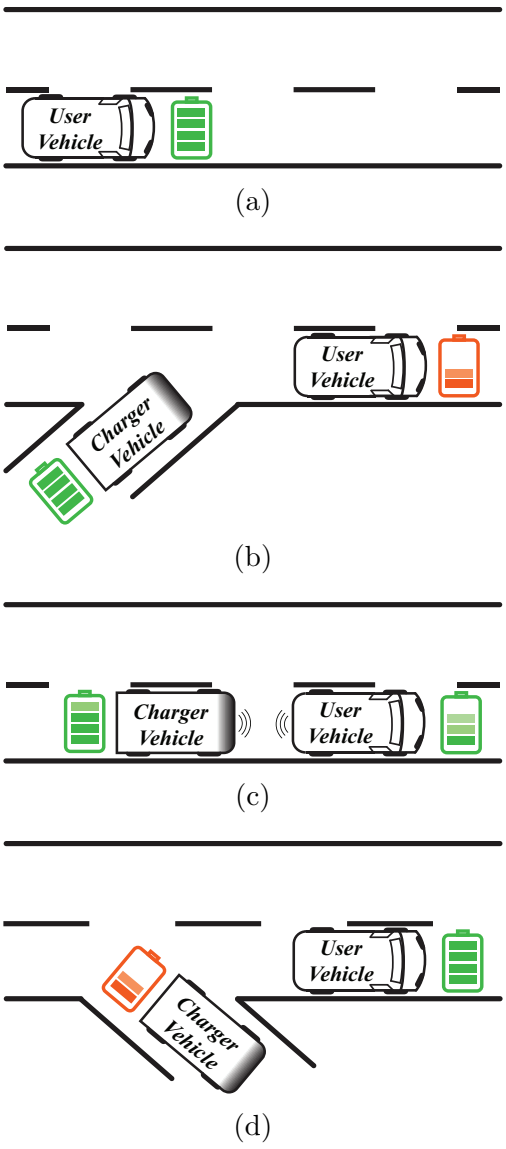

Figure 5.1. (a) User vehicle en route. (b) User vehicle requesting VVR. (c) VVR application. (d) Charger vehicle disengaging/leaving route.

shown in Figure 5.2. Figure 5.2 (left) shows the charger vehicle as 100% electric, implemented with a large battery package, while Figure 5.2 (right) introduces the hybrid charger vehicle with an embedded generator set. The proposed system could be implemented with either option. The hybrid charger vehicle could be implemented first to lower the cost of the entire system, and as batteries costs reduce, then electric charger vehicles would be a substitute to the hybrid counterparts. Note that the WPT charging mechanism can be placed at either the front or back of either of those vehicles.

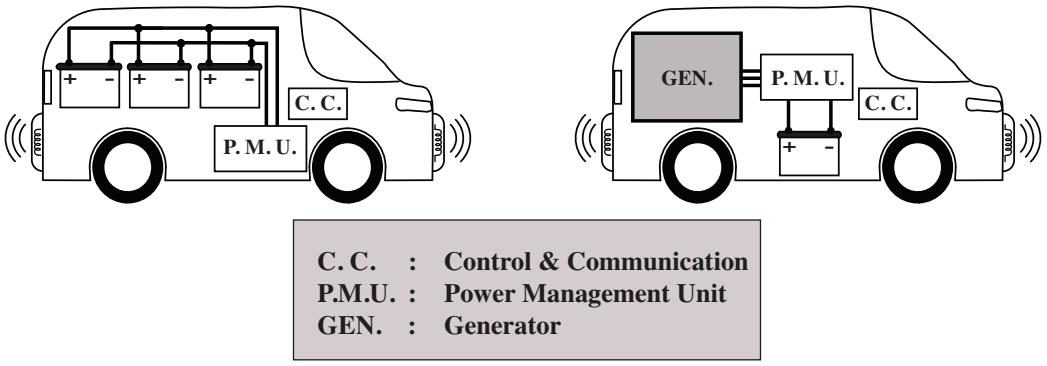

Figure 5.2. Charger vehicle that is either fully EV (left) or HEV (right).

5.2 Modeling and Analysis

In the VVR system presented in this study, the user and charger vehicles are both electric vehicles. Figure 5.3 shows the block diagram of the proposed system. Both the user and charger vehicle models are hybrid models that incorporates equation-based modeling similar to that presented in Chapter 4. The first aspect of this model is also the drive cycle data points. The data points presented in this study was purely synthetic to demonstrate a desired driving condition to be used with the VVR. The data points from the drive cycle would then be fed into the driver model along with the current vehicle speed. As done in Chapter 4,

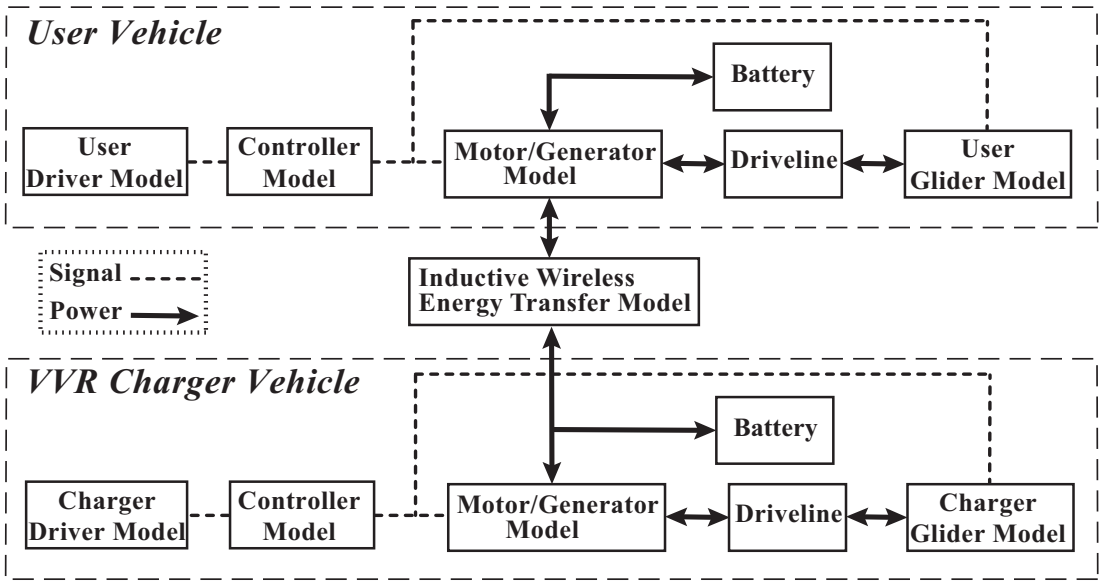

Figure 5.3. Block diagram of the VVR system.

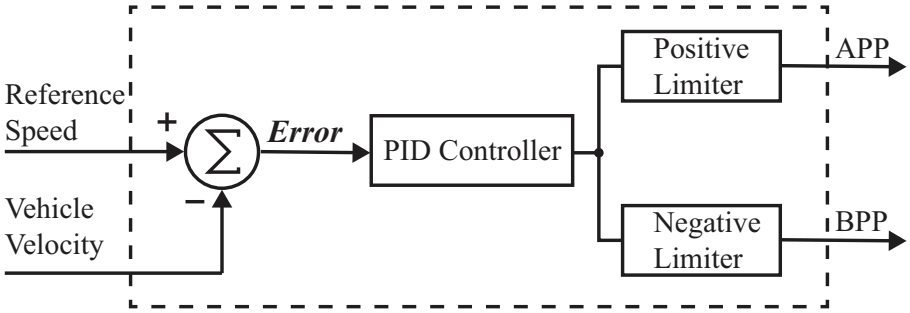

Figure 5.4. Driver model block diagram.

the driver model block (Figure 5.4), ensures that the vehicle speed obtained from the glider model is following the drive cycle data. The BPP is used to determine the regenerative torque, which is an input to the motor block, and the friction brake force that is fed to the driveline model.

The APP from the driver model goes to the motor model (Figure 5.5) and requests the amount of torque to reduce the speed difference error, but is limited by a one-dimensional lookup table that defines how much maximum torque is allowed at the current motor speed. The output of the limiter is the positive torque needed for propulsion, subtracted by the regenerative torque (obtained from a brake model) to get the total net tractive torque going to the driveline. This net torque at the current speed is what defines the power needed from the battery based off the motors' efficiency map (a 3D lookup table also highlighted in Figure 5.5). For this simulation, the motor efficiency map that was implemented was the same induction motor used in Figure 4.6.

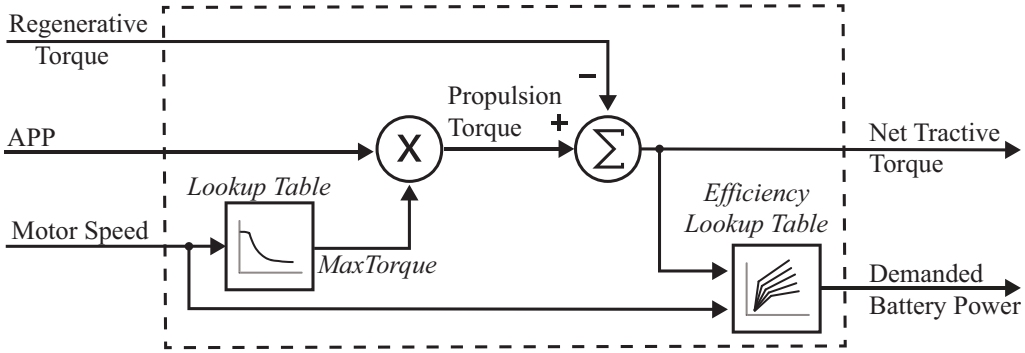

Figure 5.5. Motor model block diagram.

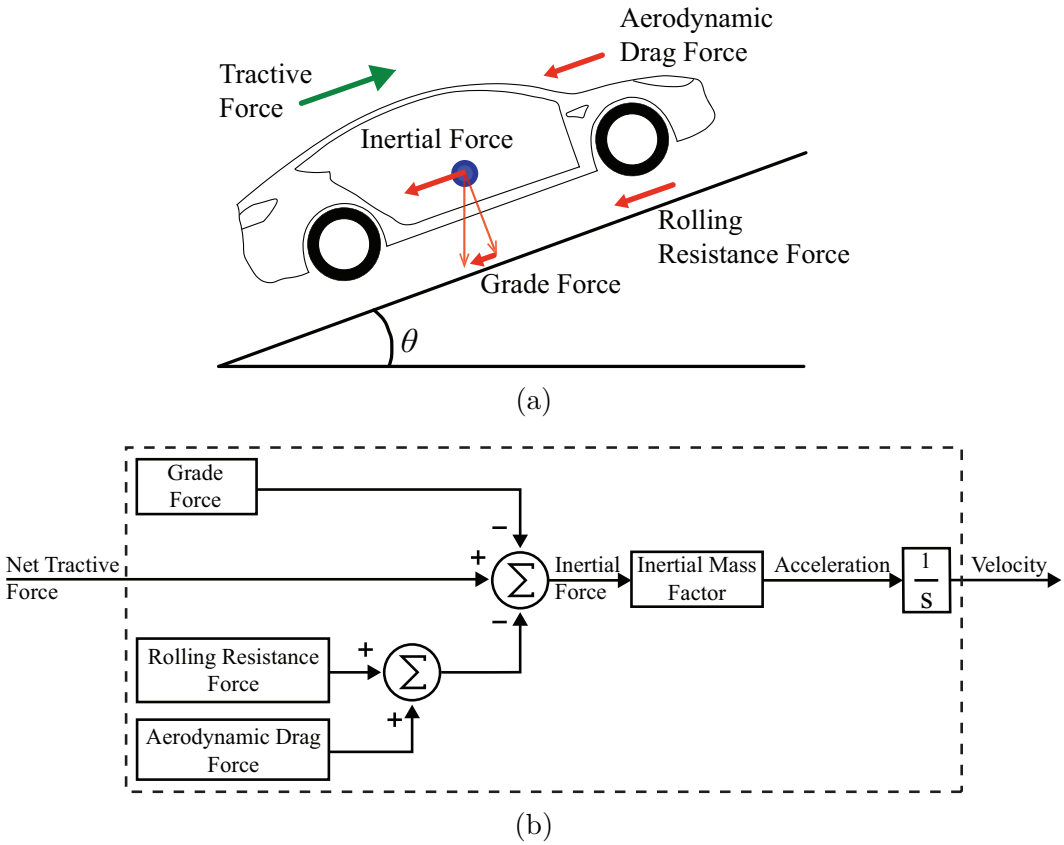

Figure 5.6. (a) Free body diagram of vehicle. (b) Block diagram of vehicle model.

The motor model would output the net tractive torque to the driveline block and the total power requested form the motor to the battery model. The battery model would then use the power demanded to calculate a new value of SOC. The SOC in this chapter was also calculated using the coulomb counting method as shown in [134]. This was also presented in Chapter 4 in equation (4.1), with the current derived from Figure 4.4 and shown in equation (4.2).

The driveline block converts that total tractive torque it received from the motor block to tractive force, which is then the input of the glider model. The glider model (or vehicle model) is also a physics-based model presented in Chapter 4, where the tractive force overcomes all other forces acting on the vehicle. Figure 5.6a re-highlights the free body diagram of the vehicle modeled. Again, the tractive force must overcome all the other forces acting on the vehicle in order for it to catch up to the reference speed. The inertial force is used to obtain the acceleration, then integrating it to obtain the vehicle velocity as shown in Figure 5.6b.

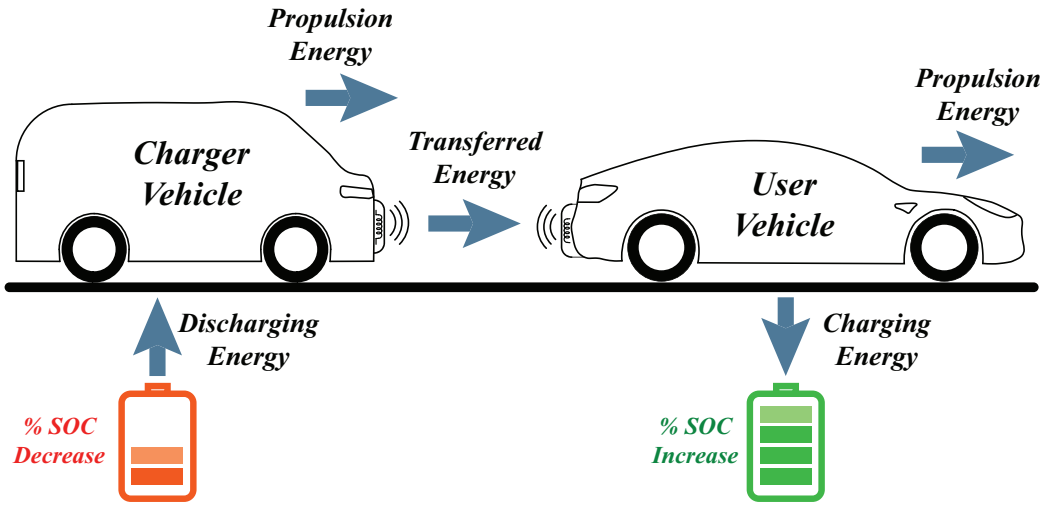

Figure 5.7. Energy distribution throughout the VVR system.

The controller in the VVR model must guarantee that the charger vehicles' battery has an SOC that does not go below 10%, and it must also ensure that only when the system is engaged that it charges the user vehicle. When the vehicle is engaged, the battery of the charger vehicle sends energy through the inductive WPT model simplified here as a constant representing an efficiency of 90%, similar to the efficiency in the literature [48]. Note that in this model, the user and charger vehicle powertrain model work in a similar fashion.

5.3 Results

Energy Analysis

One important aspect to consider for the VVR system is how much energy the charger vehicle will use. This incorporates the power that will be consumed by the charger vehicle and the power being transferred to the user vehicle during the VVR application. Figure 5.7 provides an illustration of energy consumption of the system. Note that in Figure 5.7 the wireless energy transferred must overcome the energy to propel the user vehicle in order to charge its battery.

This type of analysis helps understanding the cost of using the VVR, since the user vehicle will be responsible for the total energy being consumed by the charger vehicle during the VVR. Although the VVR system would be more costly than using a typical charging

Table 5.1. VVR glider model parameters.

Parameters	User Vehicle	Charger Vehicle
Aerodynamic Drag Coeff.	0.38	0.38
Air Density	1.23 kg/m^3	1.23 kg/m^3
Frontal Area	1.8 m^2	2.1 m^2
Gravity	9.81 m/s^2	9.81 m/s^2
Mass of Vehicle	1800 kg	3114 kg
Rolling Resistance Coeff.	0.01	0.012
Incline Angle	0 *Degrees*	0 *Degrees*
Vehicle Inertial Mass	2000 kg	4784 kg

station along the route, the argument here is for a convenient solution since there is no need to pull over and waste time on just charging. An argument can also be made in terms of stress on the grid, since the VVR vehicles can be charged during non-peak times and provide the energy to the user vehicles during peak times. Peak times here is defined as the period of time throughout the day in which the electric utility company is observing the most demand from the consumers. Another point is the charger vehicles don't have to be fully electric vehicles, they can be hybrid with an on-board generator as mentioned previously.

Drive-Cycle Analysis

MATLAB® and Simulink® was used to simulate the proposed system. The block diagram presented in Figure 5.3 was implemented where both the user and charger vehicles are fully electric. As mentioned before, the glider model presented here is a physics based model, and the parameters used are presented in Table 5.1.

The VVR system presented in this paper was simulated with the following scenario for the drive cycles: a lower scale user vehicle is on a trip that requires at least one pit-stop or a VVR request (about 70 miles). Figure 5.8 shows the drive cycle used in the simulation, which was fully synthetic and made up from a combination of well known highway drive cycles also used in [132]. It is evident from Figure 5.8 that the charger vehicle was requested at about 3,450 seconds and joined the user vehicle a little after. Then, as both vehicles are about to get off the highway (at about 4,700 seconds), the charger vehicle disengages and the user

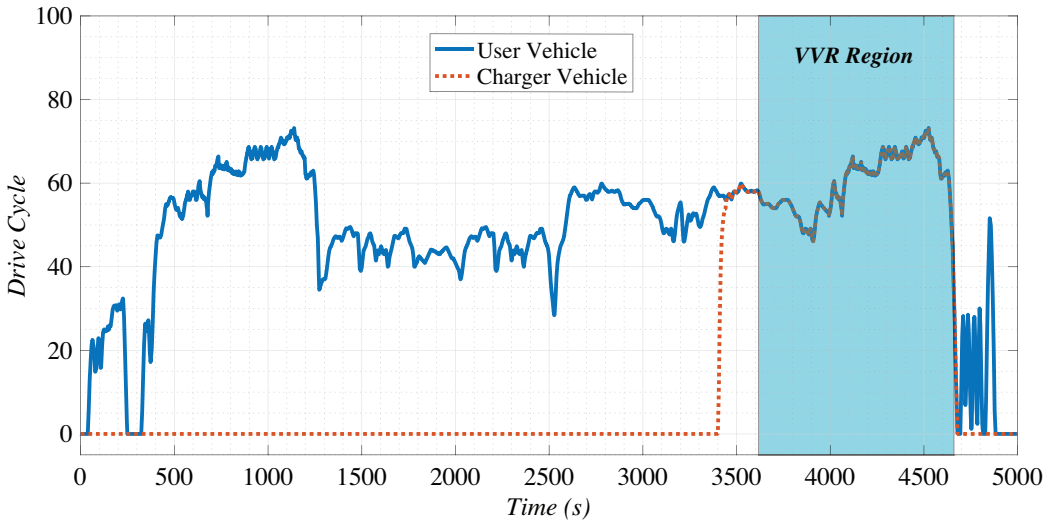

Figure 5.8. Drive cycle of the user and charger vehicles.

continues the trip. The user vehicle here has a battery size of about 23.7 kWh, while the charger vehicle's battery capacity is 35.91 kWh. The SOC of both the user and charger vehicle is presented in Figure 5.9, highlighting the region in which the user vehicle battery is no longer used for its own propulsion. Figure 5.10 shows the power consumed by the user vehicle, charger vehicle, and the power transferred during the application of VVR.

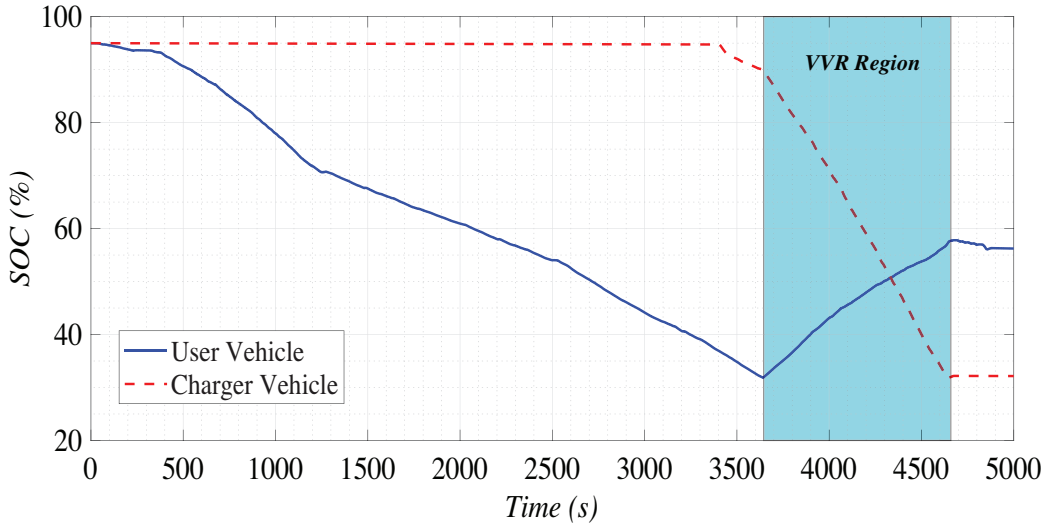

Figure 5.9. SOC of user and charger vehicles.

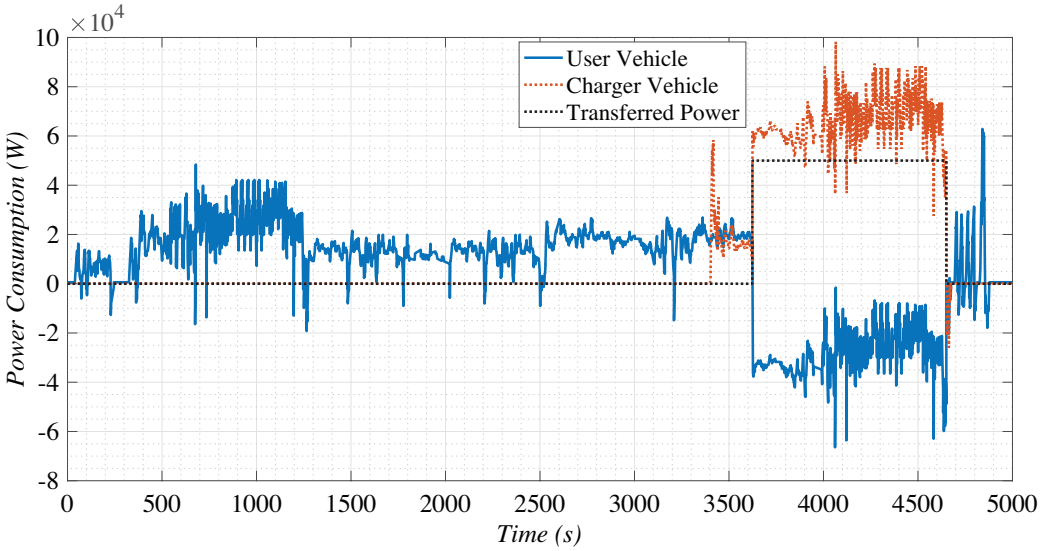

Figure 5.10. Total power consumption of user and charger vehicles (including WPT).

A comparison between an EV using VVR versus stopping by a conventional fast charging station to charge its battery is presented in Figure 5.11. It is clear that the EV charging with VVR would reach the destination 20 minutes earlier than a vehicle that would have stopped at a conventional charging station. It is then a matter of preference on whether customers are willing to pay a premium to reduce such a trip presented in this analysis by 20%.

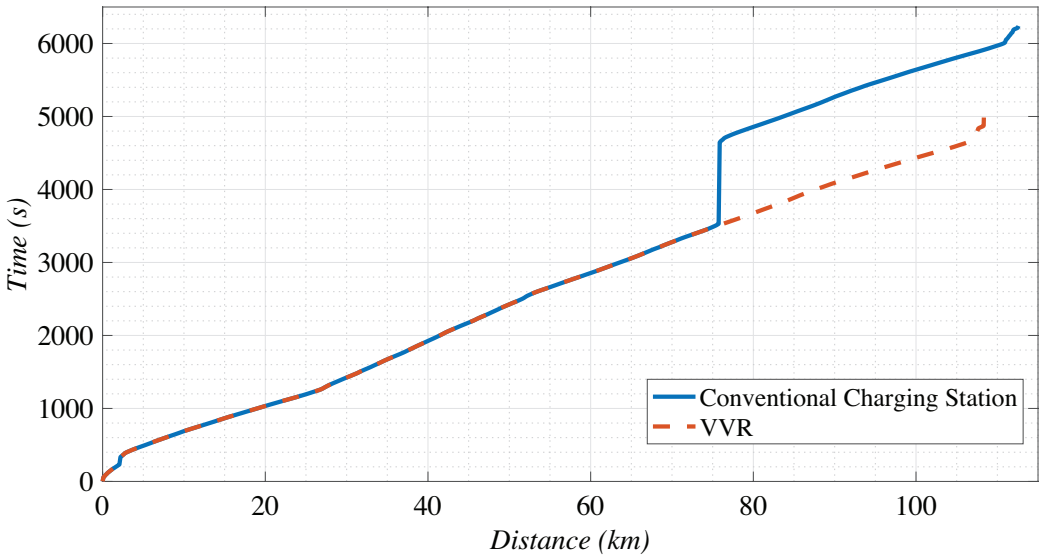

Figure 5.11. Elapsed time versus distance: Comparison between EV using conventional charging station versus the VVR system during the same trip.

6. NOVEL WIRELESS POWER TRANSFER METHOD

6.1 Conventional System

The wireless power transfer methodology can be considered a mature technology today. Different methods and approaches have been proposed by scholars and by the industry to improve the performance of inductive power transfer (IPT) and capacitive power transfer (CPT) systems. These methods include megahertz operation frequency [139], compensation, maintaining system resonance [140], refactoring coil structure [141], and network improvement [142]. The traditional way to implement wireless power transfer is accomplished with considerable high efficiency if both plates with transmitting (TX) and receiving (RX) coils are aligned. The perfect alignment is what it is known as the "sweet spot" within the commercial jargon. Figure 6.1(a) shows the traditional coupling with perfect alignment, i.e., sweet spot. Figure 6.1(b), in turn, shows both plates misaligned. The perfect alignment

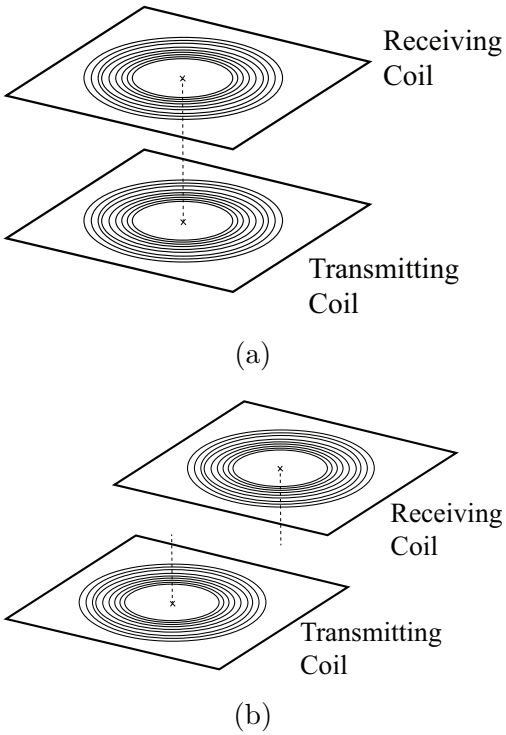

Figure 6.1. Wireless power transfer transmitting and receiving coils with (a) alignment (sweet spot) and (b) misalignment.

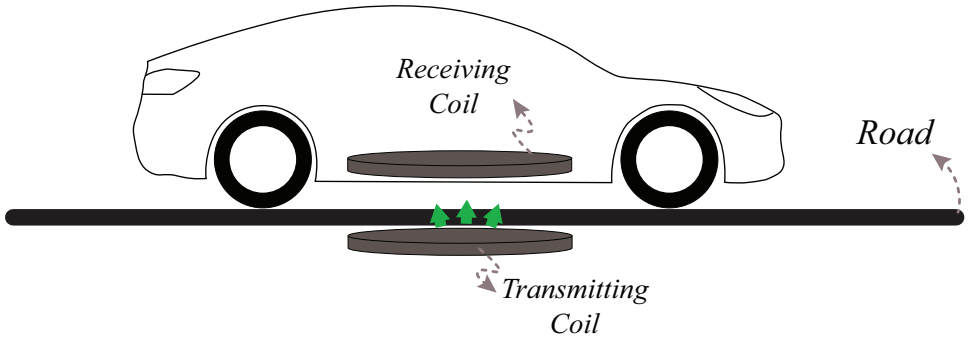

(a)

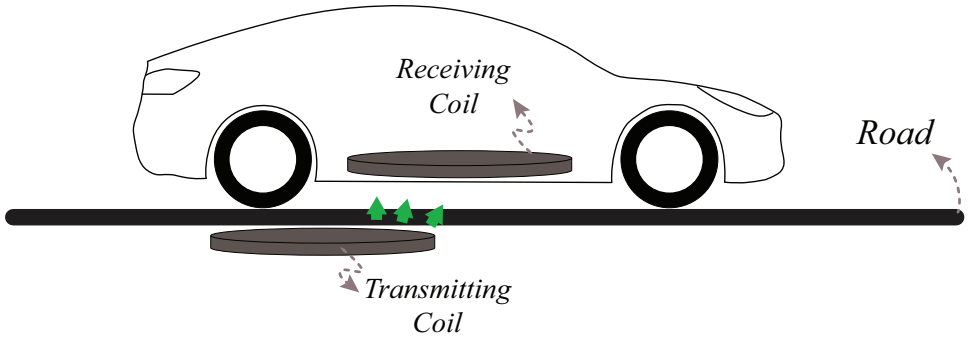

(b)

Figure 6.2. Wireless power transfer system with ground charging: (a) perfect alignment and (b) misalignment.

is relatively easy to achieve with static devices. On the other hand, high-efficient charging devices that change their relative position dynamically is rather challenging.

One of the most promising wireless power transfer technology today for EVs is the one where the electric current is transferred by creating a magnetic field between a TX pad on the ground and a RX pad located under the vehicle. This is an application where the alignment between plates is not easily accomplished. In this wireless charging system, the vehicle needs to stop at the sweet spot to guarantee maximum efficiency, as shown in Figure 6.2. Companies like BMW has proposed a system with cameras and positioning devices at the bottom of the vehicle to guarantee the sweet spot and therefore ensure higher efficiency while transferring power [143], which adds cost and complexity to the final product. Figure 6.3 shows a typical graph of efficiency and power supply versus horizontal distance. In this graph when there are no displacements in the horizontal direction both maximum efficiency and supply powers are achieved. The state where both the TX and RX coils' center match-up is

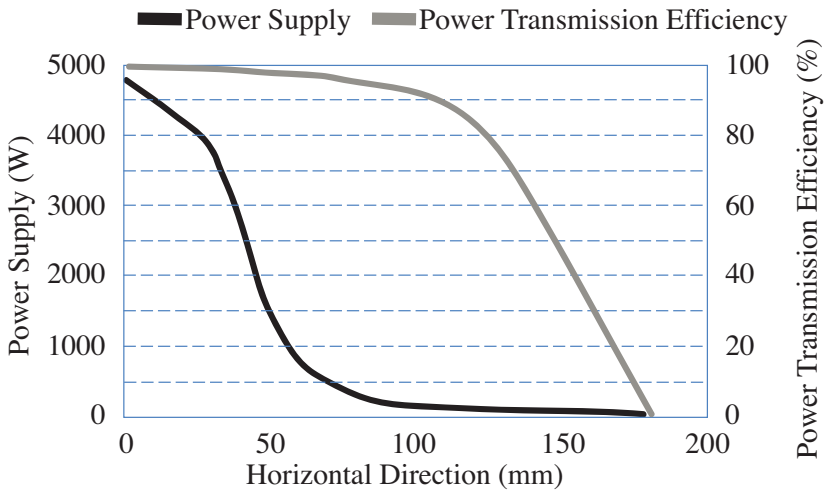

Figure 6.3. Efficiency and power supply versus horizontal distance.

considered 0, and the distance that it moves in the horizontal direction (horizontal distance) is defined as displacement in the horizontal direction. As the horizontal distance between the TX and RX coil gets larger and displaced, both power supply and power transmitting efficiency will decrease.

6.2 Efficiency Analysis and Proposed System with Dynamic Positioning

As mentioned in the introduction, this chapter presents a WPT with a dynamic positioning mechanism that would allow for efficient power transfer for a wider range of relative position between the TX and RX coils. Figure 6.4 presents a model of a WPT system that was used to simulate the system. Herein, k is the coupling coefficient between the coils; V is the phasor of the voltage source in the 1st coil; L_1 and L_2 are the self-inductance of the two coils; and R_1 and R_2 are the parasitic resistances of the two coils. Also, C_1 and C_2 are the capacitance of the coils respectively, where ω_0 is the resonant frequency of the WPT system. R_s is the source resistance, and R_L is the load resistance. Notice that the coupling coefficient k is also a function of the angle θ.

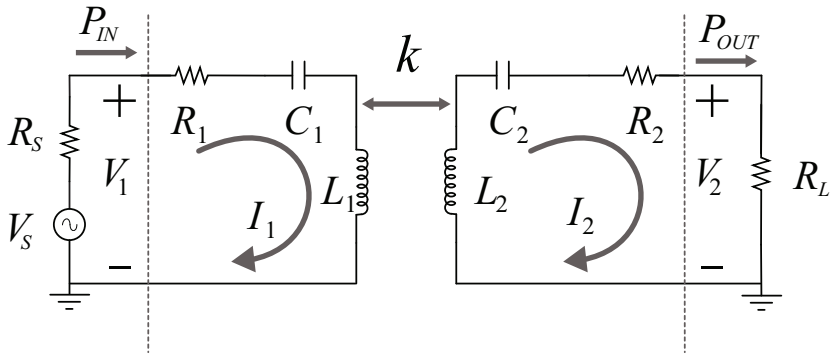

(a)

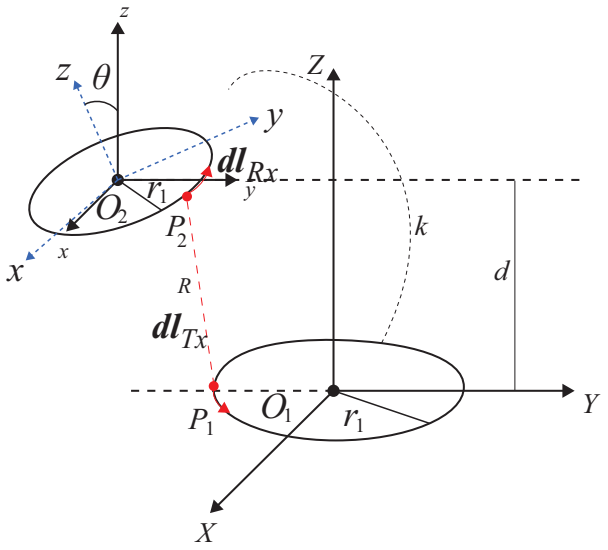

(b)

Figure 6.4. (a) Circuit model of WPT system with a single TX and RX. (b) WPT system with angle and horizontal misalignment.

Considering the circuit presented in Figure 6.4, applying phasor analysis using Kirchhoff's voltage laws for the transmitter and receiver loops yields to:

$$(R_s + R_1 + \frac{1}{\mathrm{j}\omega_0 C_1} + \mathrm{j}\omega_0 L_1)I_1 + (k\mathrm{j}\omega_0\sqrt{L_1 L_2})I_2 = 0 \tag{6.1}$$

and

$$(\mathrm{j}\omega_0 L_2 + \frac{1}{\mathrm{j}\omega_0 C_2} + R_2 + R_L)I_2 + (k\mathrm{j}\omega_0\sqrt{L_1 L_2})I_1 = 0 \tag{6.2}$$

where ω_0 is angular resonance frequency, and the term $kj\omega_0\sqrt{L_1L_2}$ is the phasor mutual impedance of the two coils. The power transfer efficiency relating the output power with the input power can be described as:

$$\eta = \frac{P_{out}}{P_{in}} = \frac{Re[V_1 I_1^*]}{Re[V_2 I_2^*]} \tag{6.3}$$

Solving for the two phasor currents in (6.1) and (6.2), then substituting that back into (6.3) to get:

$$\eta = \frac{k^2\omega_0^2 L_1 L_2}{R_1(R_2+R_L)^2 + k^2\omega_0^2 L_1 L_2(R_1+R_2)} \tag{6.4}$$

It is important to note that from (6.4), k and ω_0 play an important role in affecting the total system efficiency. The resonant frequency ω_0 is a programmable input, whereas k is affected by the relationship of the mutual inductance between the RX and TX coil. The authors in [144] calculate the mutual inductance using Neumann formula, and they clearly

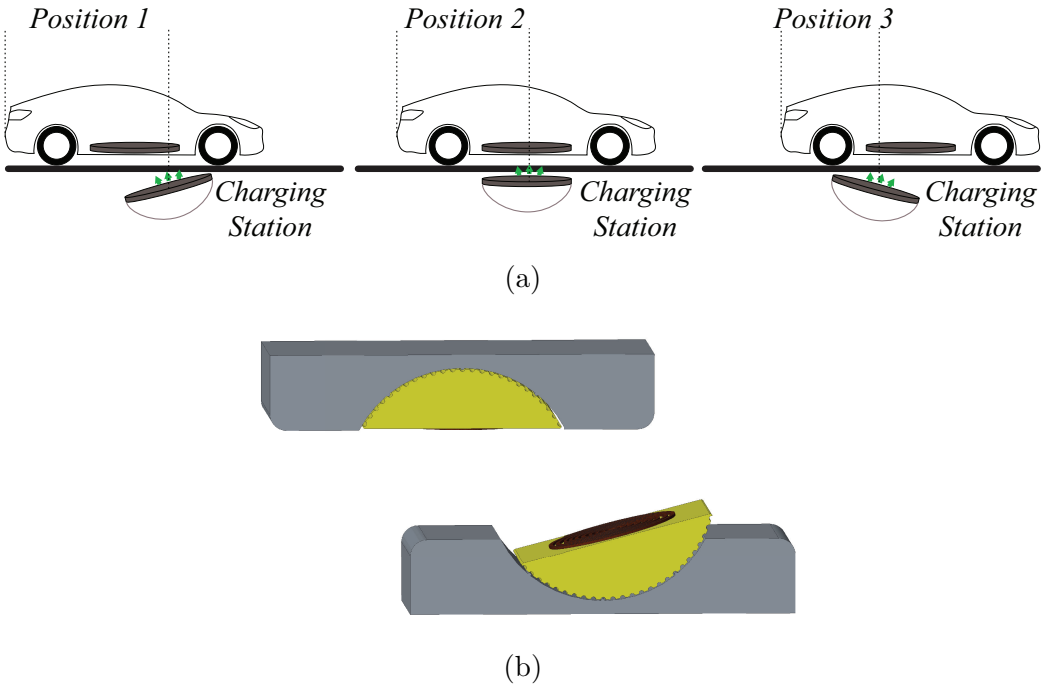

Figure 6.5. (a) Different relative position between vehicle and a charging station with dynamic self-alignment system. (b) 3D view in perspective.

show that for such a system presented in this paper, k is affected by the tilt angle between the RX and TX coils.

The proposed system should allow for a dynamic alignment towards a spot that guarantees a condition with maximum efficiency. The idea is that as the vehicle comes closer to the sweet spot, the mechanism would ensure that the TX coil is at an optimal tilt angle and resonant frequency for the current position of the vehicle to obtain higher WPT efficiency. Figure 6.5(a) illustrates schematically how the self-alignment mechanism of the proposed system works, with the coil placed on the charging station moving freely between two angle limits. Instead of placing the coils on a surface that moves on a parallel position from each other (as shown in Figure 6.1), one of the coils will have freedom to find a position that is of better alignment.

The self alignment can be accomplished by injecting DC voltages on auxiliary coils such that the same magnetic pole is created. Notice that this DC voltage applied to the auxiliary will not affect the AC power transfer from one coil to another. Both north poles will repel each other creating the desirable alignment position. As the plate self-aligns the effective distance between the coils will naturally increase, which will affect the efficiency. A feedback controller will be used to change the resonant frequency of the input source to compensate for the drop in efficiency.

6.3 Results

MATLAB® and Simulink® was used to simulate the WPT system presented in Figure 6.4. The parameters used for this circuit is presented in Table 6.1. As mentioned earlier and in Figure 6.4, the coupling coefficient k plays an important role in the efficiency, which is also a function of the tilt angle between the TX and RX coils. Figure 6.6 shows a relationship between the coupling coefficient k and the system efficiency when the resonant frequency f_0 was kept constant at 110 kHz.

It is also noticeable that the system at a given angle and position does indeed have a resonant frequency f_0 that is optimal in terms of efficiency. Figure 6.7 shows the range of frequency f_0 applied vs the efficiency η. Note that for this given position and tilt angle

Table 6.1. WPT system parameters

Parameter	Symbol	Value
TX coil inductance/radius	L_1/r_1	217.5 μH / 0.15 m
TX coil resistance	R_1	4.5 Ω
TX capacitance	C_1	11.65 nF
RX coil inductance/radius	L_2/r_2	80.3 μH / 0.075 m
RX coil resistance	R_2	2.1 Ω
RX Capacitance	C_2	31.54 nF
Load resistance	R_L	20 Ω
Source resistance	R_s	50 Ω
Input voltage source	V_1	212 $Vrms$

(coupling coefficient was kept constant at $k = 0.7$), the frequency at which the system is most efficient is at about 105 kHz. Figure 6.8 shows the effects of frequency and coupling coefficient on the efficiency of the simulated system. Figure 6.8 highlights how the change in resonant frequency can affect the WPT efficiency for a given tilt and relative position between the RX and TX coils. It also shows that the physical design should be chosen to maximize the coupling coefficient, while the resonant frequency can change dynamically to optimize the WPT.

Figure 6.9 shows pictures of a test-bed used to collect experimental results of the proposed system. This is a small-scale proof of concept prototype that allows testing the scenarios pre-

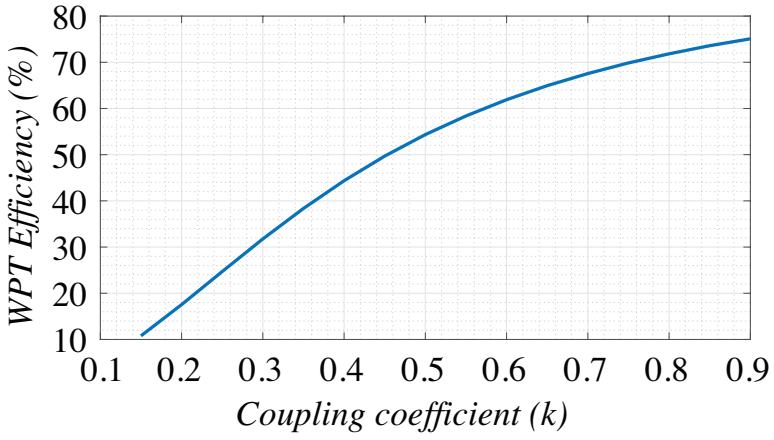

Figure 6.6. Coupling coefficient vs WPT efficiency.

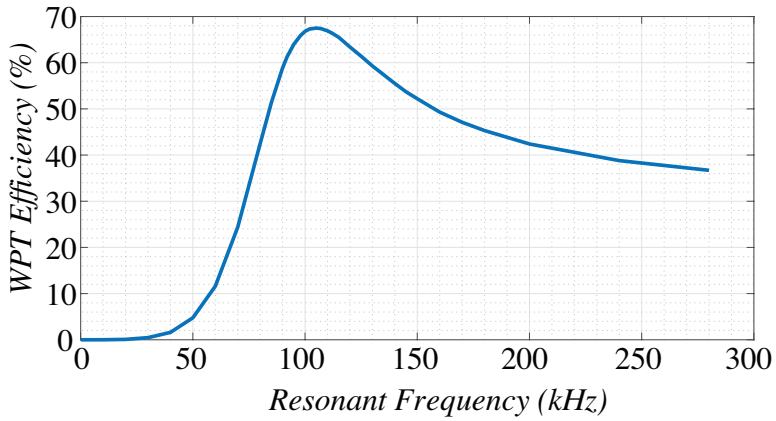

Figure 6.7. Resonant frequency vs WPT efficiency.

sented in Figure 6.5(a), with both changes in the horizontal and angular direction. Table 6.2 shows preliminary results collected with the current setup presented in Figure 6.9, within a constant load of 20Ω. Herein, it is evident that for the same vertical and horizontal distance, the efficiency of the WPT system changes as the angle between the two pads changes.

The direct evolution of the proposed system in Figure 6.5 is the solution presented in Figure 6.10 where the vehicle would also incorporate such a dynamic positioning mechanism. Such an evolved system (Figure 6.10) would allow for more freedom in angular rotation to

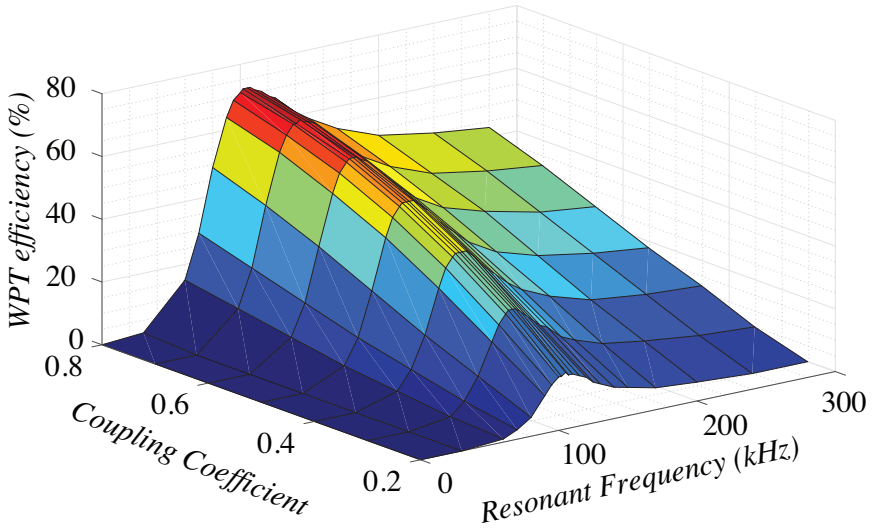

Figure 6.8. Effects of coupling coefficient and frequency on the efficiency of the WPT system.

Table 6.2. Experimental results of WPT with different angles

Vertical Distance	**Horizontal Distance**	**Angle (Degrees)**	**Input Power (W)**	**Output Power (W)**	**Efficiency (%)**
3.5 *cm*	1.75 *cm*	5	4.19	2.24	53.45
3.5 *cm*	1.75 *cm*	15	2.96	1.45	48.98
3.5 *cm*	3.5 *cm*	5	3.04	1.06	34.98
3.5 *cm*	3.5 *cm*	15	2.42	0.15	6.28

achieve an optimal angle for a higher WPT efficiency. This type of system would also be an optimal solution if implemented in the VVR system presented in Chapter 3, since the movement of the vehicles would continuously cause a change in distance and alignment.

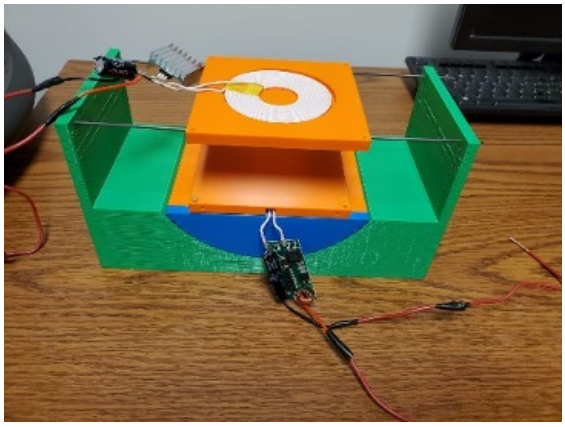

(a)

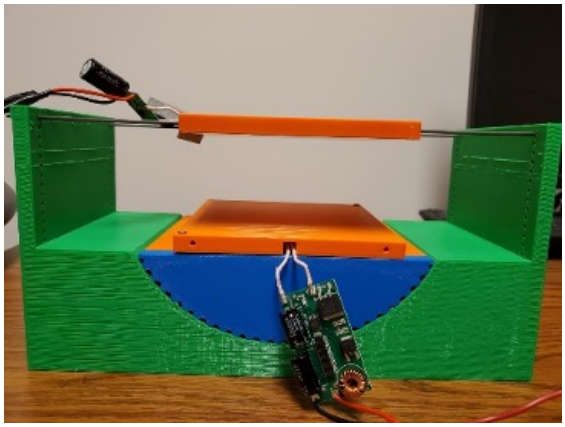

(b)

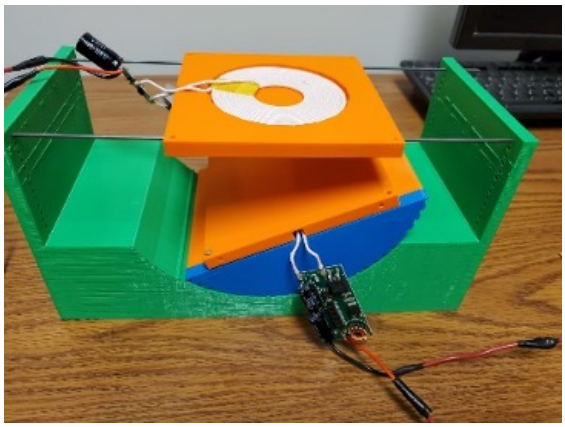

(c)

Figure 6.9. Test-bed photos: (a) perspective view with zero angle, (b) lateral view with zero angle, and (c) perspective view with 15 degree angle.

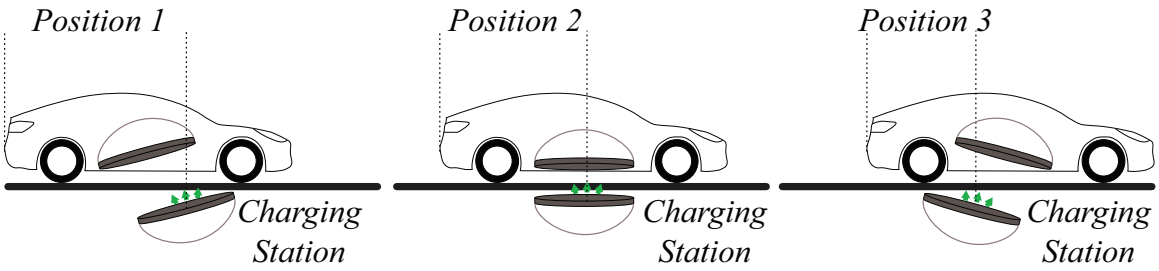

Figure 6.10. Alignment freedom on both the charging station and on the vehicle.

7. MULTI-MOTOR ARCHITECTURE FOR ELECTRIC VEHICLES

7.1 Proposed Multi-Motor Architecture

A typical architecture of an EV with a single motor is reintroduced in Figure 7.1a, to make it easier on the reader. Considering that it's a single motor, its efficiency map would have a single region of high efficiency. This means that unless the motor is running at the desired optimal speed and torque, it would be operating in regions that are not considered highly efficient. This paper proposes a multi-motor approach for an EV powertrain shown in Figs. 7.1b and 7.1c with three and n-motors respectively.

In this proposed architecture, three or more different motors with different operating regions are chosen. The goal is to ensure that each motors' highest efficiency region on its map is different. This way, a controller can decide which motor to operate based on its efficiency map at the demanded torque and speed. The controller can also decide if a combination of motors would be more efficient to operate than a single motor for a given operating region. This method produces a larger high efficiency region seen by the powertrain, which translates to less losses and consequently improves the SOC.

7.2 Proposed EV Modeling

Similar to the model presented in Chapter 4, the modeling employed in this chapter is a forward-facing model and was implemented in MATLAB®/Simulink ®. Figure 7.2 shows the main block diagram representing the model of a typical EV. Similar to Chapter 4, the drive cycle data (reference vehicle speed) is compared with the actual vehicle speed in the driver model block, and the difference (error) is applied to a PID controller to define the accelerator pedal position (APP) along with the brake pedal position (BPP). The APP then goes to the motor block shown with more details in Figure 7.3. Herein, the APP requests the amount of torque to reduce the speed difference, but is limited by a one-dimensional lookup table that defines how much maximum torque is allowed at the current motor speed. The output of the limiter is the positive torque needed for traction. The controller should

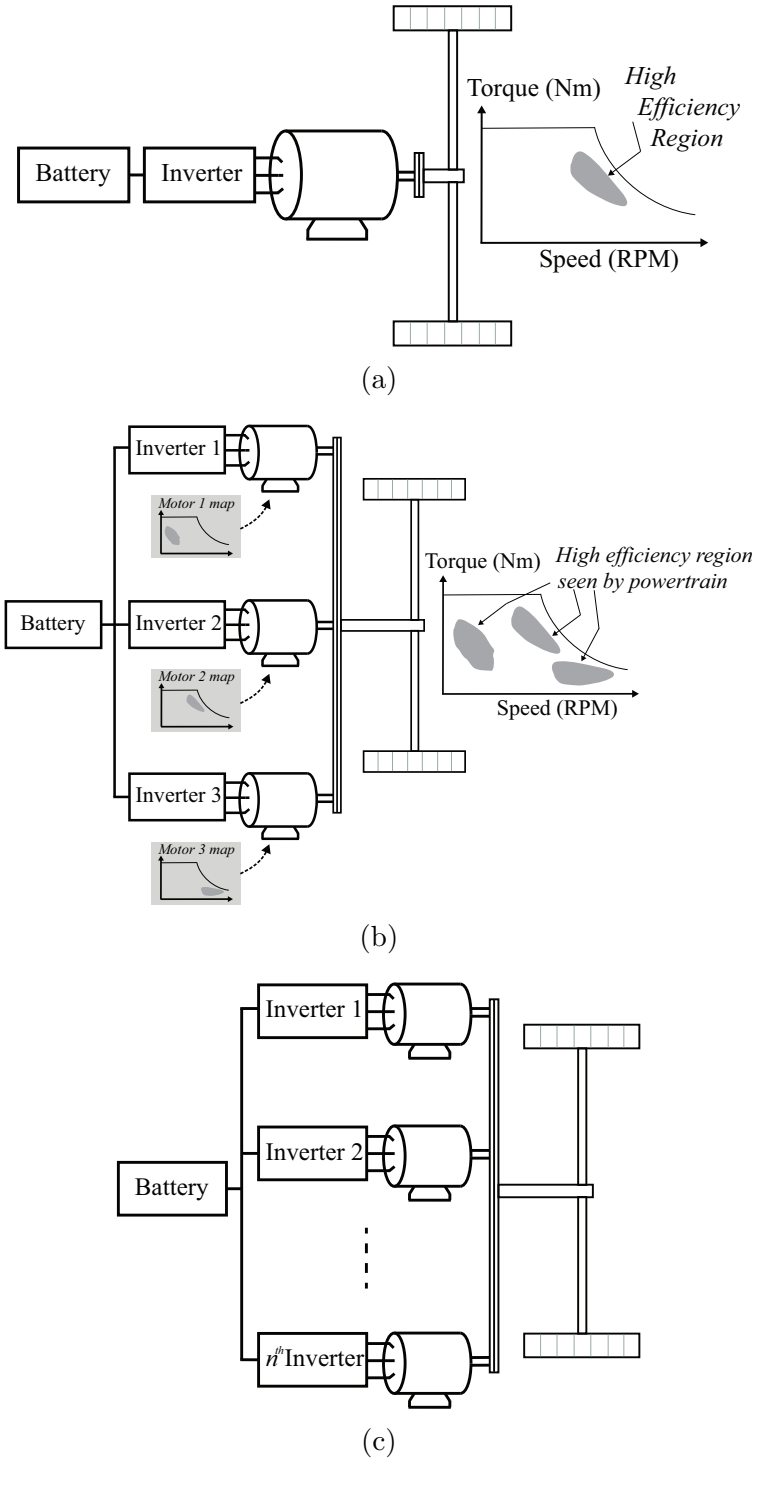

Figure 7.1. (a) Single motor EV architecture, (b) proposed three-motor architecture, and (c) proposed multi-motor architecture with n-motors.

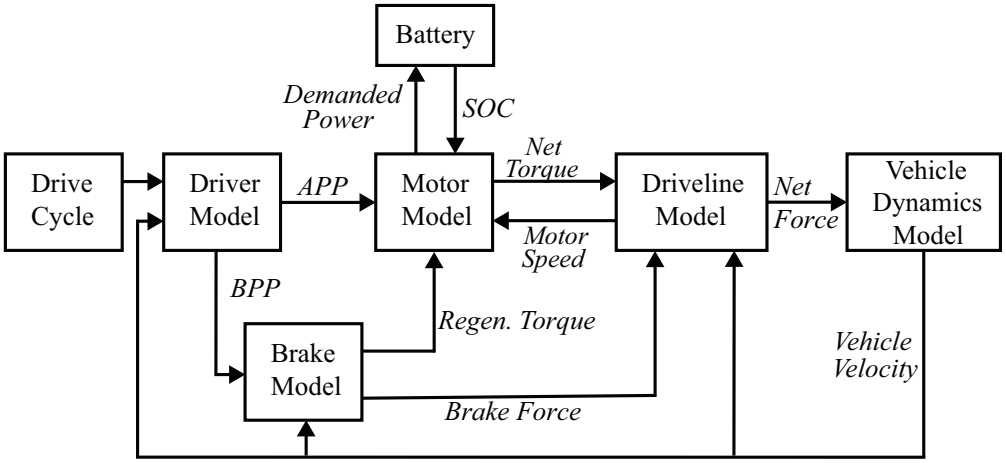

Figure 7.2. Block diagram of the proposed EV.

then decide which motor (or combination of motors) would be appropriate to use based off its efficiency map, and request that power from the battery.

Figure 7.4 shows a flowchart of the controller logic when a simple rule based strategy (RBS) is employed. As seen in the figure, once the program starts, the controller first checks to see if the SOC is at an appropriate level to continue. If the SOC is at an acceptable level, the controller will then check the demanded torque at the current vehicle speed to determine the operating region. It will then decide which motor to use, based on who has the highest efficiency at the current operating region. From there, the controller will go back

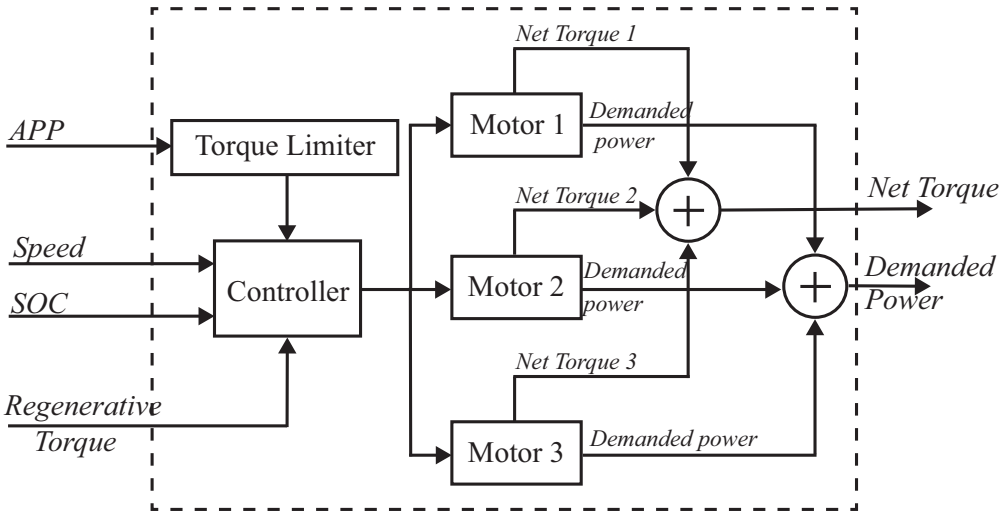

Figure 7.3. Block diagram of the motor model with a three-motor configuration.

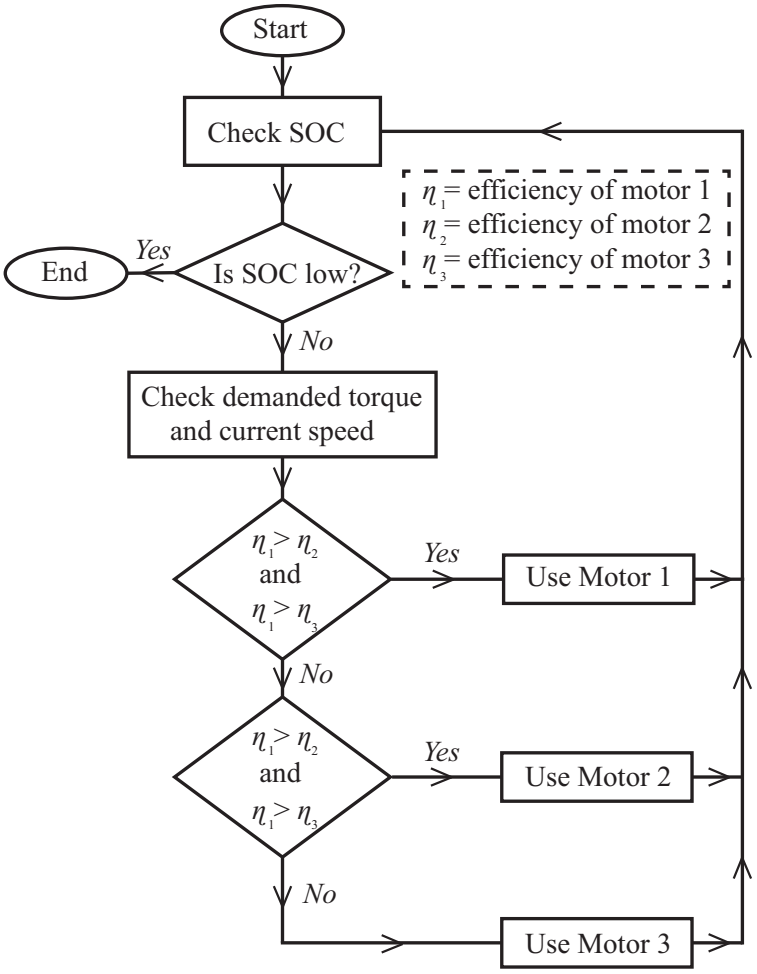

Figure 7.4. Flowchart of motor controller implementing RBS.

to check the SOC again and continue doing the same process until the SOC is too low, or the simulation is complete. Of course, to improve the performance of the model, a more complex optimization technique is to be used to help prolong the SOC of the battery for the same given drive cycle. In the simulation results, an optimized rule based strategy (ORBS) is presented and compared to that of the RBS employed here.

The SOC in this chapter was also calculated using the coulomb counting method as shown in [134]. This was presented in Chapter 4 in equation (4.1), with the current derived from Figure 4.4 and shown in equation (4.2). Similarly, the net tractive torque from the motor model is converted to net tractive force in the driveline block, which is sent to the vehicle dynamics model block to obtain the current vehicle speed.

7.3 Results

This section provides a comparison between the proposed methodology and current existing architectures. Figs. 7.5a-7.5b and Figs. 7.6a-7.6b show the maps of three different motors with high efficiency regions that are different. Each motor was simulated separately to see its behaviour with different drive cycles, and then compared with the proposed combined multi-motor architecture. Figure 7.5a will be denoted herein as the Motor 1 efficiency map, which is similar to an induction motor used in the Tesla Model S as presented in Chapter 4. Figure 7.5b and Figure 7.6a represent the efficiency maps of Motor 2 and Motor 3, respectively. Both those motors represent maps of permanent magnet synchronous machines (PMSMs), and were chosen because of the different positions of the highest efficiency region. In the combined architecture, since the controller decides which motor to operate, the powertrain views an efficiency map that is the combination of the three motors' maps, shown in Figure 7.6b.

For this simulation, the vehicle dynamics used are presented in Table 7.1. The drive cycles in Figs. 7.7a-7.7b and Figs. 7.7c-7.7d (obtained from [145]) were used to observe the behavior of SOC under different driving conditions. Figure 7.7a is derived from the Federal Test Procedure (FTP) drive cycle and represents city driving conditions followed by a short pause, then repeats the first 505 seconds again. Figure 7.7b is a portion of the drive cycle known as "Supplemental FTP" (US06) repeated 4 times, which represents a highway drive cycle. Figure 7.7c is the Urban Dynamometer Driving Schedule (UDDS), and

Table 7.1. Vehicle dynamic parameters.

Parameter	**Value**
Air density	1.23 kg/m^3
Drag coefficient	0.38
Vehicle frontal area	2.1 m^2
Vehicle mass	1560 kg
Gravitational acceleration	9.81 m/s^2
Road angle	0 $Degrees$
Rolling resistance coefficient	0.01

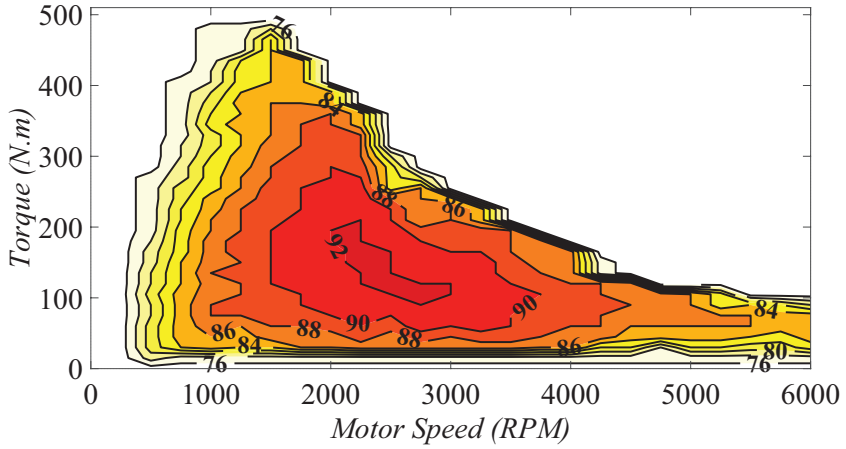

(a)

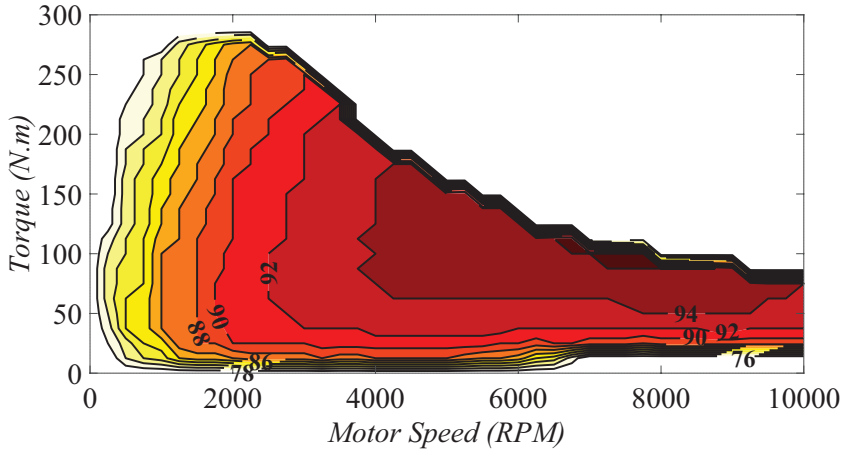

(b)

Figure 7.5. Motor efficiency maps of (a) Motor 1 and (b) Motor 2.

Figure 7.7d is a combination of Figure 7.7a and 7.7b. Figs. 7.8(a)-7.8(d) shows the compared battery's SOC for each drive cycle, and Figs. 7.9(a)-7.9(d) are the operating regions for those drive cycles respectively. It can be seen that the proposed architecture performs better in all cases with just an RBS strategy, which translates to longer range for the same given battery capacity. The first drive cycle tested was the FTP drive cycle. The corresponding Figure 7.8(a) shows that after 2500 seconds, the proposed multi-motor architecture has an SOC that is approximately 0.4% higher than Motor 3, 0.6% higher than Motor 1, and 1.5% higher than Motor 2. Although the operating regions of this drive cycle (Figure 7.9(a)) is primarily within within the high efficient region of Motor 3 and Motor 1, there are still some

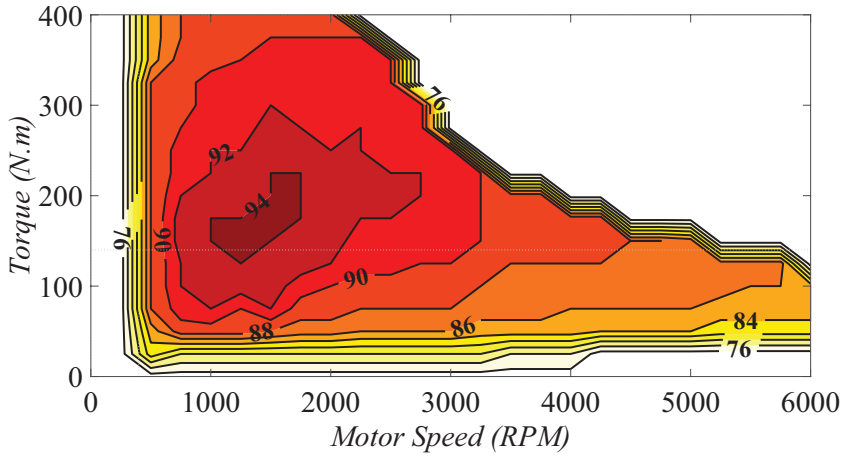

(a)

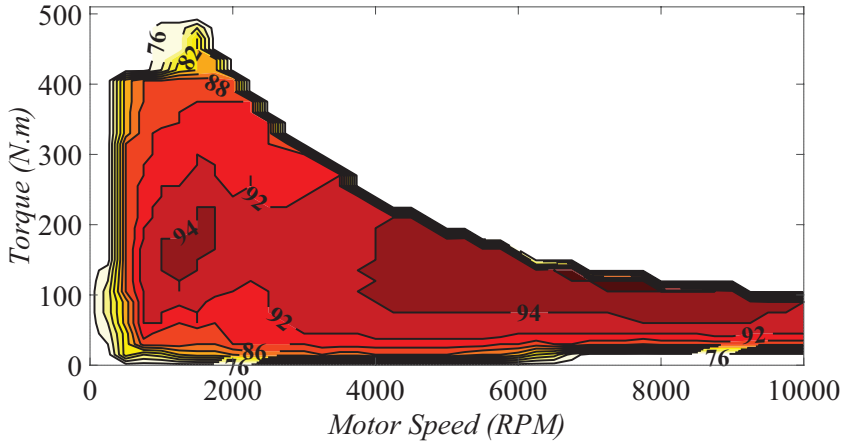

(b)

Figure 7.6. Motor efficiency maps of (a) Motor 3 and (b) combined motors.

regions that motor 2 is considered more efficient, hence the SOC level is a bit higher for the multi-motor architecture.

The second drive cycle focused mainly on highway driving conditions. The test was repeated 4 times to observe the effects of longer highway drives on the SOC when comparing the four configurations. Herein (Figure 7.8(b)), after 1500 seconds, the proposed multi-motor architecture is about 1.1% higher than Motor 2, 4.4% higher than Motor 1, and 4.8% higher than Motor 3. By observing Figure 7.9(b), it can be seen that Motor 2 would also do a good job in terms of SOC since it is most efficient at higher speeds.

The third drive cycle tested was the well known UDDS, which observes the behaviour of typical city driving conditions. It can be seen from Figure 7.8(c) that after 1400 seconds

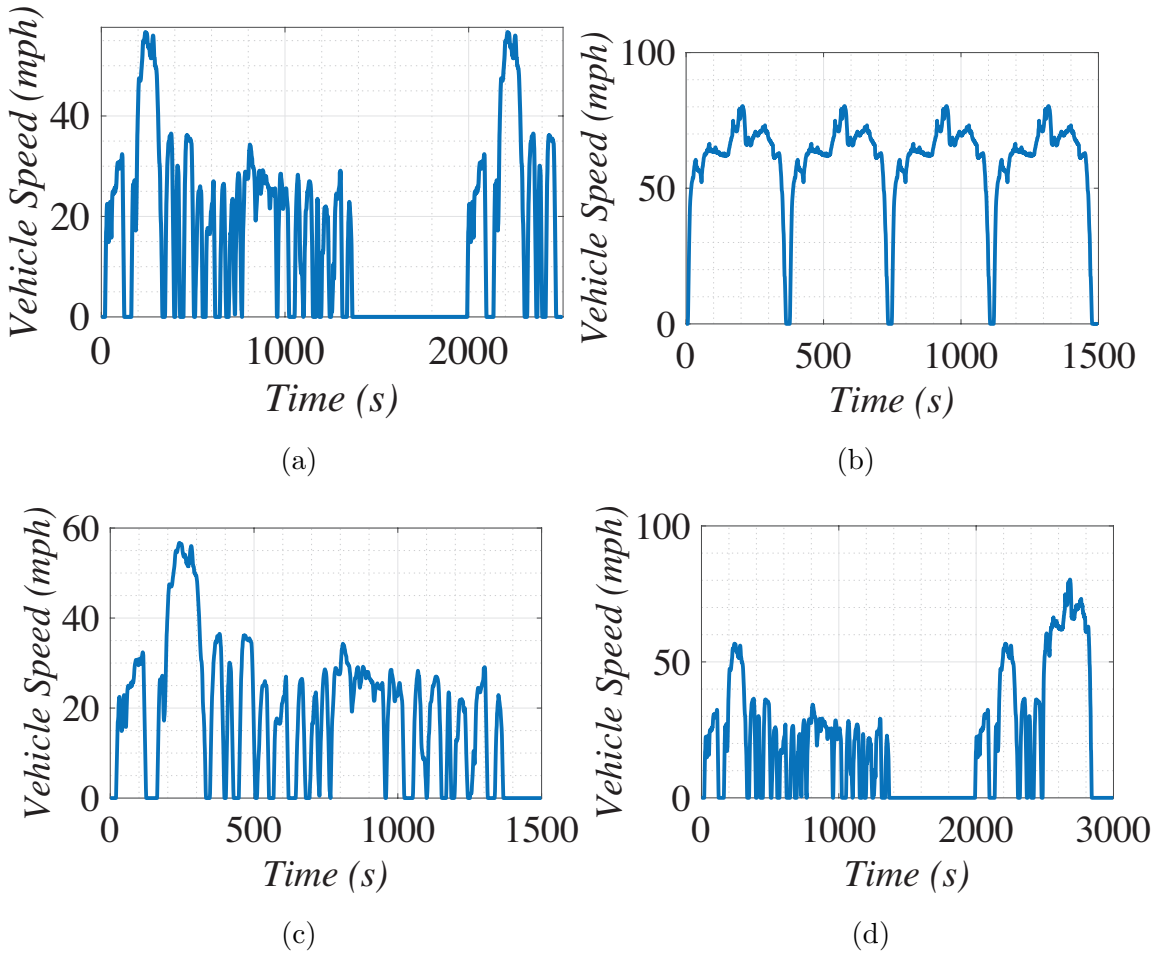

Figure 7.7. Drive cycles compared: (a) FTP, (b) US06Hwy (repeated), (c) UDDS, and (d) a combined FTP and US06Hwy.

the proposed architecture has an SOC that is 0.25% higher than Motor 3, 0.4% higher than Motor 1, and 1.5% higher than Motor 2. Figure 7.9(c) shows the operating region of this drive cycle is similar to that of the first test, hence similar results in terms of SOC performance. The final drive cycle tested was a combination of the FTP and US06. It is clear in Figure 7.8(d) that after 2848 seconds, the proposed architecture has an SOC that is 1.6% better than Motor 1 and 3, and 1.7% better than Motor 2. Looking at the operating regions of this mixed drive cycle shown in Figure 7.9(d), it is evident that it is a combination of the other three drive cycles. By applying a simple RBS strategy to the controller of the multi-motor architecture, it will always choose the motor with the highest efficiency at the current operating region, thus improving the total system efficiency which yields to higher

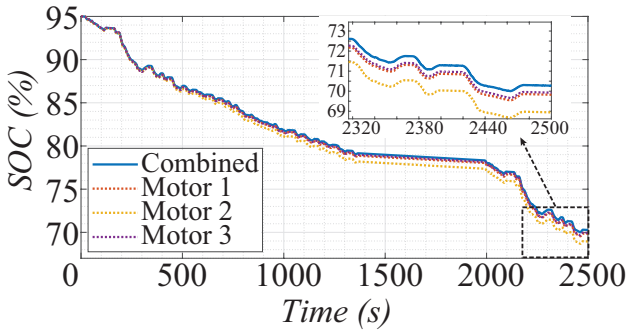

(a)

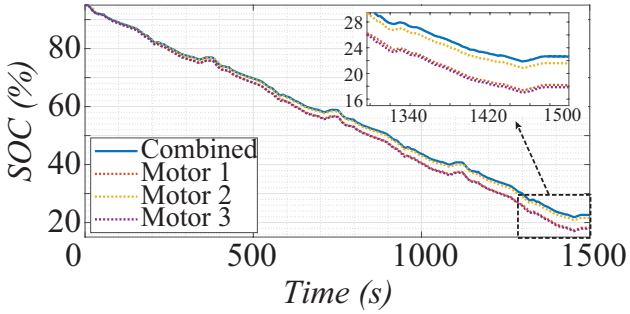

(b)

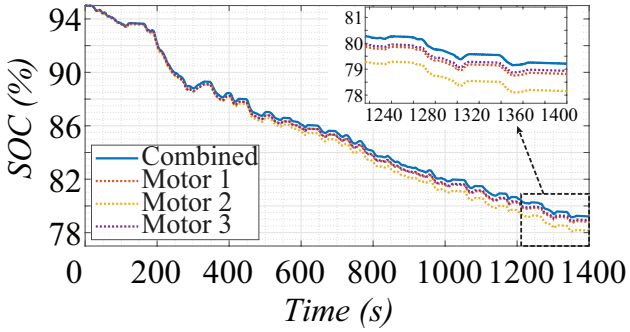

(c)

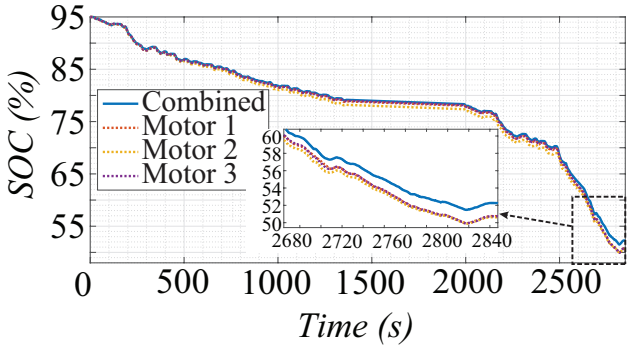

(d)

Figure 7.8. SOC using RBS for (a) FTP, (b) US06Hwy, (c) UDDS, and (d) the combined FTP and US06Hwy drive cycle.

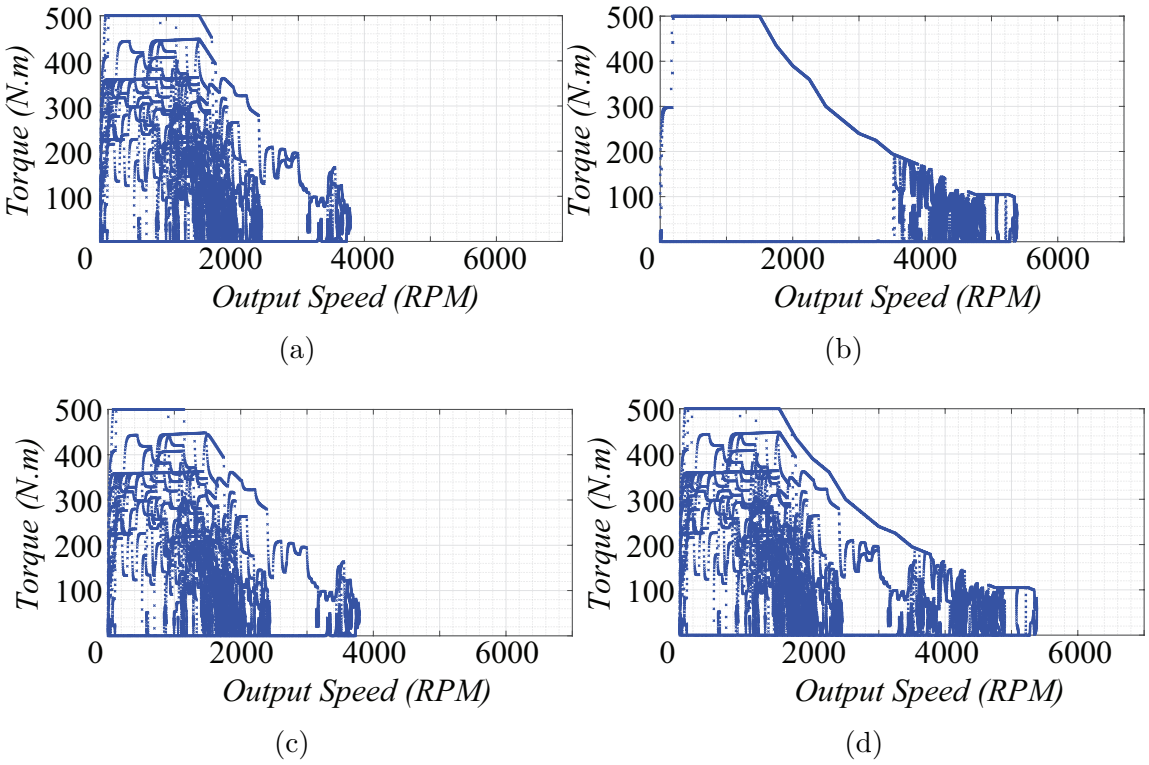

Figure 7.9. Operating regions for (a) FTP, (b) US06Hwy, (c) UDDS, and (d) the combined FTP and US06Hwy drive cycle.

SOC levels. Table 7.2 shows the SOC of the battery at the end of the aforementioned drive cycles.

7.3.1 Optimized Rule Based Strategy

As mentioned before, the purpose of the RBS was to show that the efficiency is indeed better with this type of multi-motor architecture when compared to a single motor archi-

Table 7.2. Battery SOC comparison

Drive Cycle	Motor 1	Motor 2	Motor 3	Three Motors
FTP	69.7%	68.8%	69.9%	70.3%
US06	18.2%	21.5%	17.8%	22.6%
UDDS	78.8%	77.7%	78.9%	79.2%
Mixed	50.7%	50.6%	50.7%	52.3%

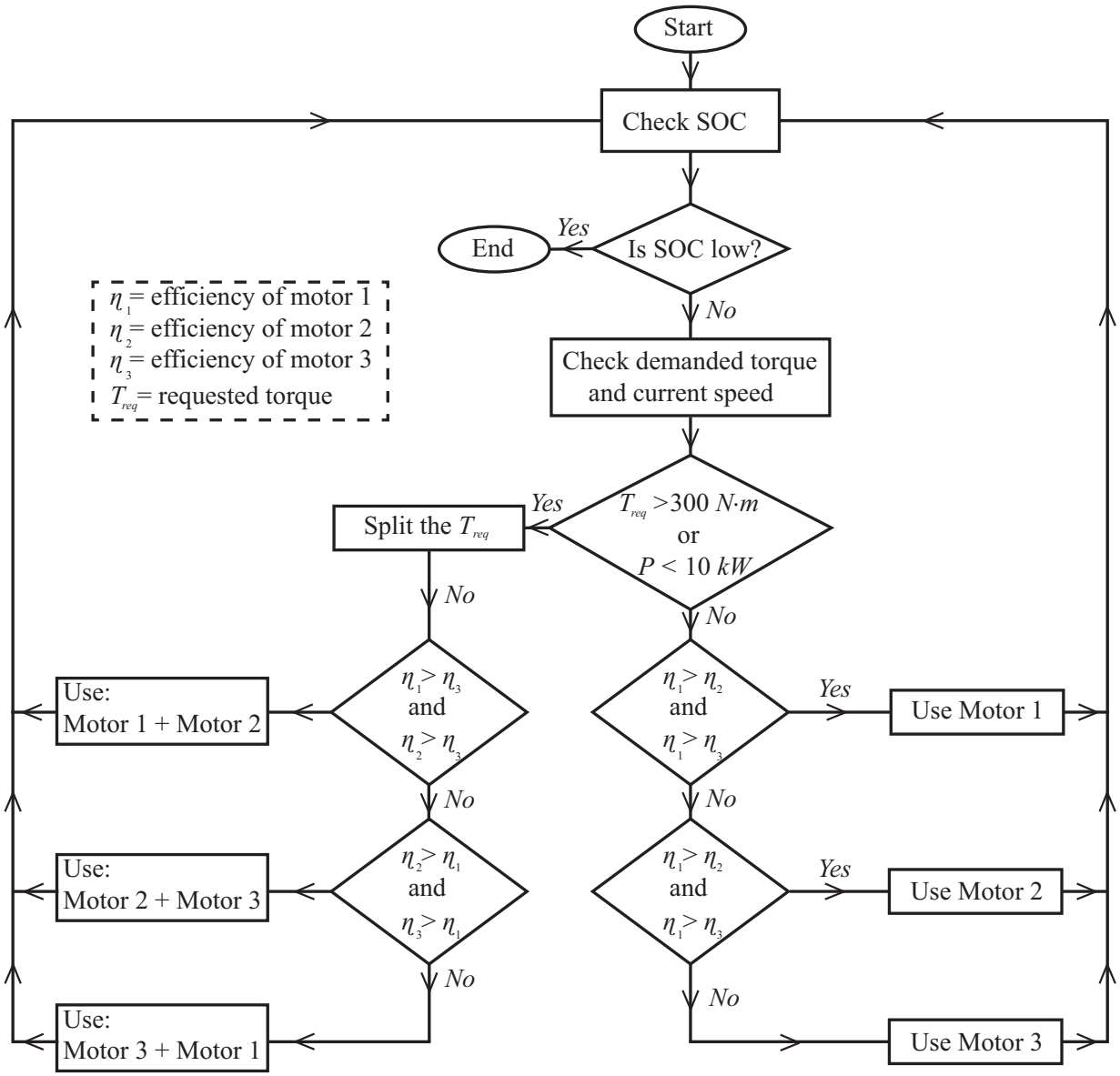

Figure 7.10. Multi-motor architecture with 5 motors.

tecture. If the controller would employ a more advanced optimization technique, the SOC of the battery can improve drastically on longer trips. Figure 7.10 shows an optimized rule based strategy (ORBS) that was used to compare model performance.

Similar to the RBS, the controller again first checks to see if the SOC is at an appropriate level to continue. If so, the controller will then check the demanded torque at the current vehicle speed to determine the operating region. As seen in the Figure 7.11, if the requested torque is below 300 Nm or above 10 kW of power, then it would fall in region 2

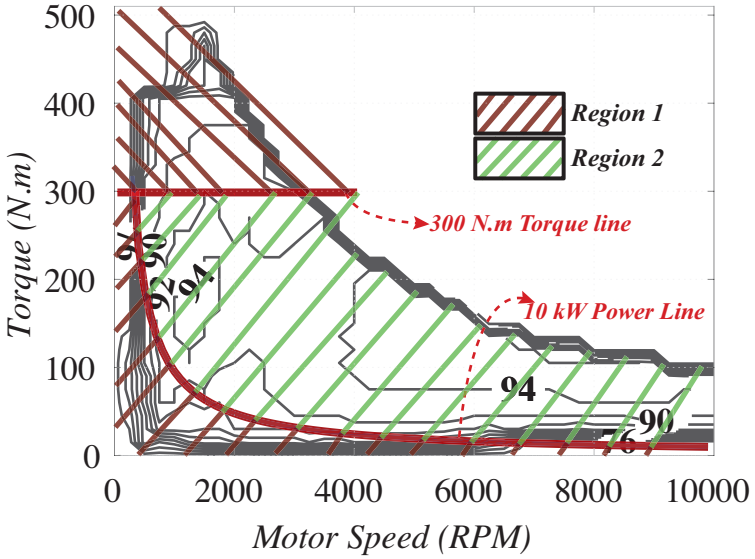

Figure 7.11. Multi-motor architecture with 5 motors.

and employ the previously discussed RBS method. Otherwise, the current operating region would be considered region 1, and the controller will split requested torque, and decide which combination of motors would provide higher efficiency for propulsion. Finally, the controller will again go back to check the SOC and continue doing so until the SOC is too low, or the simulation is complete. Note that in region 1, the operation of the controller can be described mathematically by the following equations:

$$T_{req} = T_{Motor\_\mathrm{i}} + T_{Motor\_\mathrm{j}} \tag{7.1}$$

$$T_{req} = T_{req}(k_{Motor\_\mathrm{i}}) + T_{req}(k_{Motor\_\mathrm{j}}) \tag{7.2}$$

where T_{req} represents the total requested torque for propulsion, T_{Motor_i} and T_{Motor_j} represent the torque obtained from motor i and j respectively, and finally k_{Motor_i} and k_{Motor_j} are percentages of the total requested torque and are bound by $k_{Motor\_\mathrm{i}} = 1 - k_{Motor\_\mathrm{j}}$. For this current architecture presented, i and j are defined as:

$$\mathrm{i}, \mathrm{j} \in \{1, 2, 3\} \mid \mathrm{i} \neq \mathrm{j} \tag{7.3}$$

With the ORBS employed as the controllers optimization technique, the performance of the multi-motor architecture improves in terms of efficiency. Although the ORBS has a lot of room for improvement, it was used to illustrate that any optimization technique can improve the current performance of the proposed EV architecture. Figure 7.12 shows the SOC of the multi-motor architecture when employing the ORBS vs the RBS with respect to the drive cycles presented in Figure 7.7.

For the FTP drive cycle, it can be seen from Figure 7.12a that the ORBS ends up with an SOC of approximately 71%, which is roughly 0.8% greater than the SOC when the RBS is employed. The second drive cycle in Figure 7.12b, which has a portion of the US06Hwy repeated, shows the SOC comparison with the UDDS drive cycle where the ORBS outperforms the RBS by 0.9% at about 25.1%. Figure 7.12c shows that after 1400 seconds, the ORBS provides an SOC that is about 0.5% higher than the RBS (at around 79.5%). Finally, Figure 7.12d shows the comparison of the SOC for the combined FTP and US06Hwy drive cycle, where the ORBS ends up with 53.7%, that is approximately 1.2% higher than the RBS. It is worth mentioning that this type of strategy was tailored to the current motor maps employed in this architecture, which is why a more complex optimization technique should be considered to accommodate more variations.

7.4 Generalized Architecture

The multi-motor architecture proposed in this paper incorporates motors with different high efficiency operating regions. Of course theoretically, as the number of motors increase, the high efficiency region seen by the powertrain becomes larger. The objective here is to observe the effects of more motors to the total overall efficiency of the system. Figure 7.13 shows a set up of five motors, with a corresponding map seen by the powertrain shown in Figure 7.14(a). Although the efficiency map can still be improved with more motors, the results indicate that there is no tangible difference in efficiency after five motors. Figure 7.14(b) highlights this by comparing the SOC of a three-motor, five-motor, and a n-motor architecture all employing an RBS strategy. Herein, the difference between a three-motor and a five-motor configuration after 1400 seconds is about 0.47%, whereas the difference between

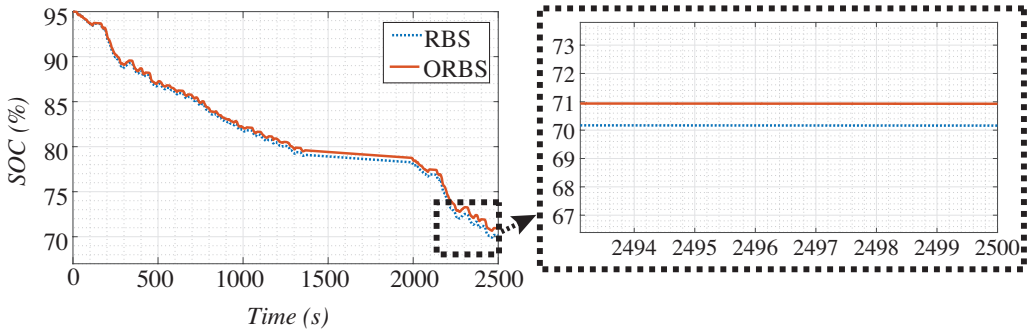

(a)

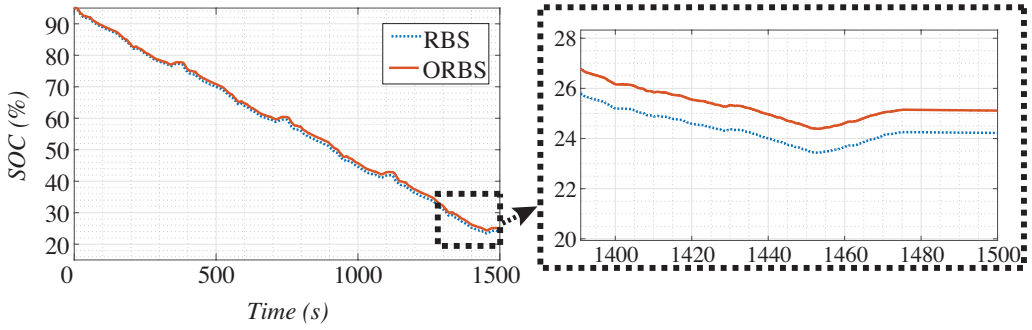

(b)

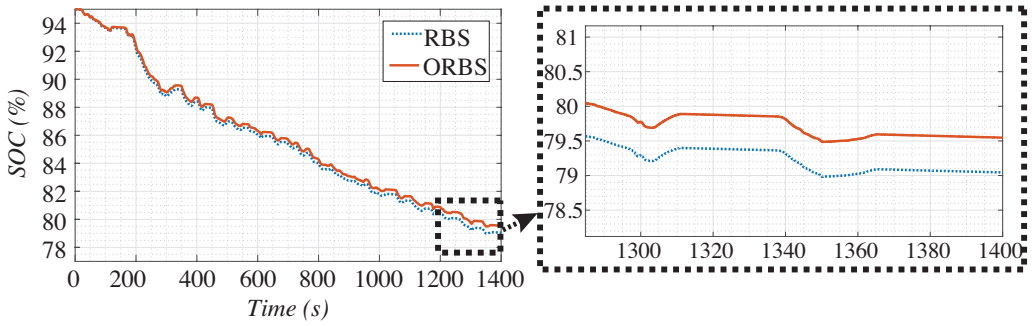

(c)

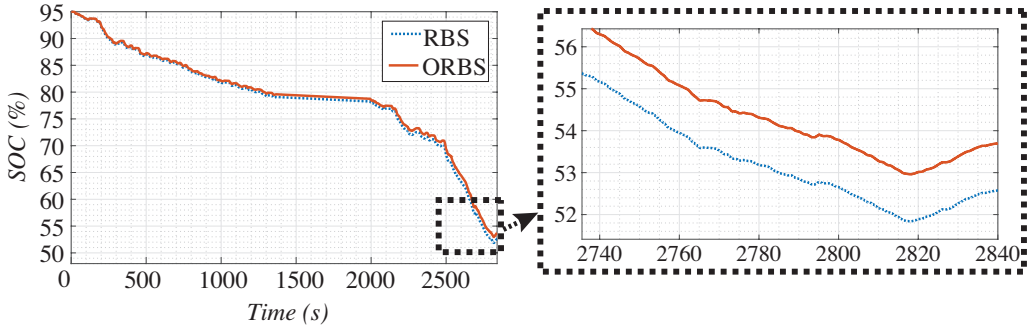

(d)

Figure 7.12. SOC using ORBS vs RBS for (a) FTP, (b) US06Hwy, (c) UDDS, and (d) the combined FTP and US06Hwy drive cycle.

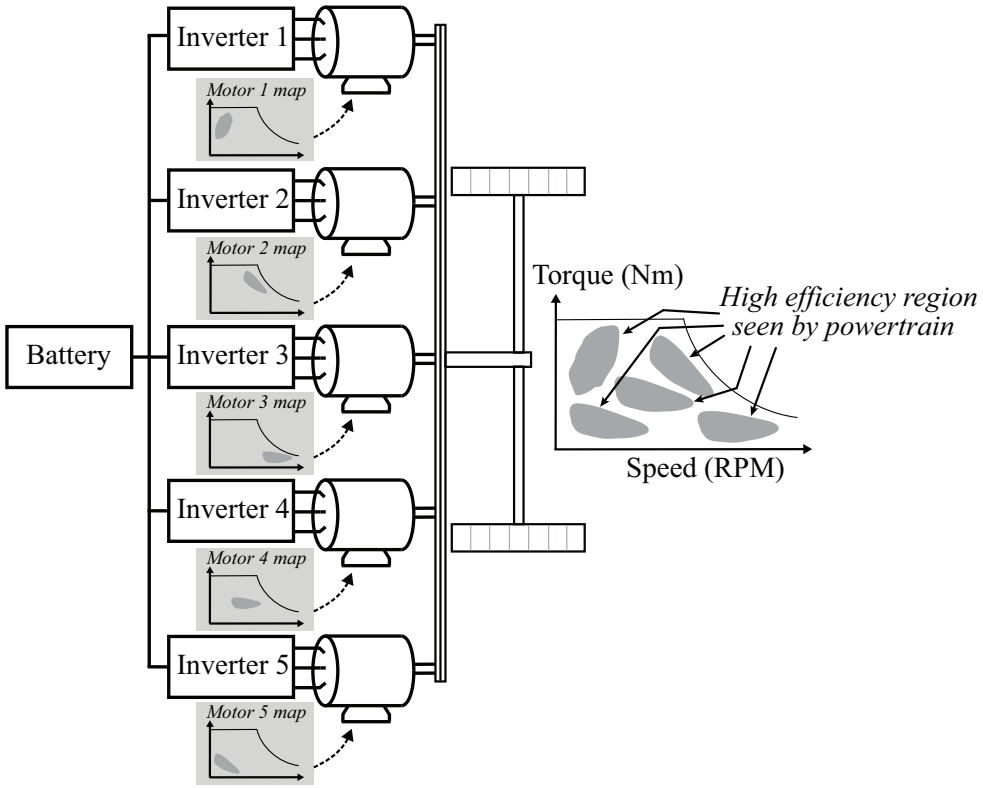

Figure 7.13. Multi-motor architecture with 5 motors.

the five-motor and n-motor configuration is about 0.03%. In this case, the n-motor architecture map was assumed with a minimum efficiency of 90% and a majority of 95% across the entire torque-speed region.

The results presented here indicate that after some point, it does not make sense to add more motors. If no optimization technique is employed, having more motors would improve the efficiency, however this would probably never be the case. With just a simple ORBS optimization technique applied to the motor controller, a vehicle with 3 motors can compete with that of 5 motors that has an RBS strategy. Perhaps a more complex optimization technique can improve the efficiency further, which would eliminate the need to add more motors to improve the efficiency of the vehicle.

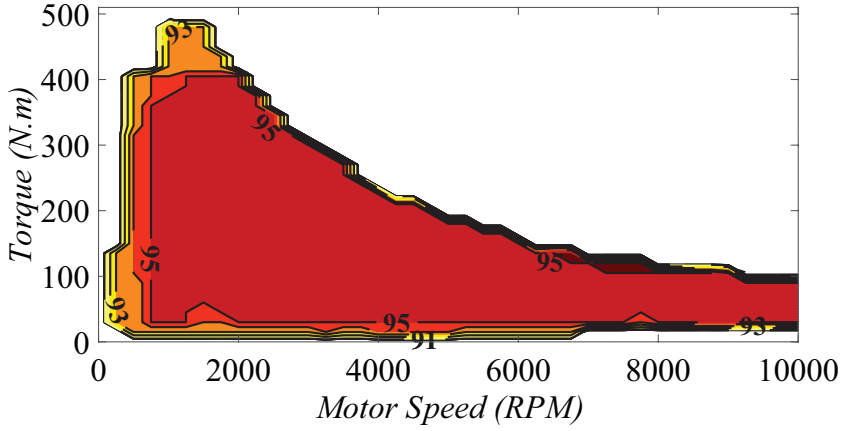

(a)

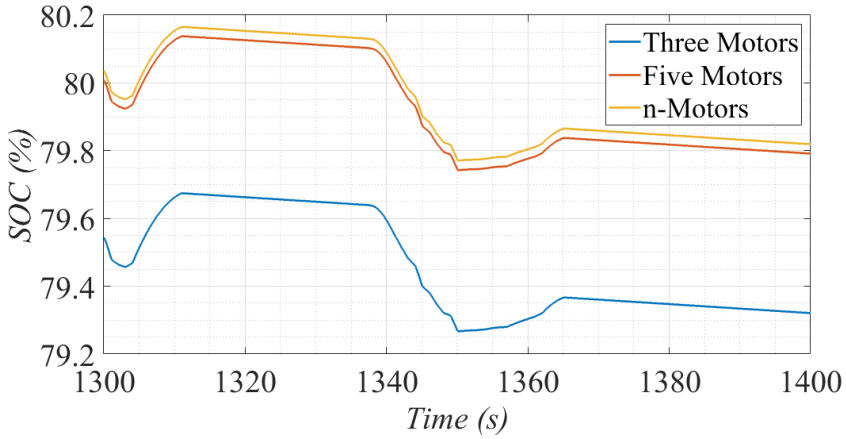

(b)

Figure 7.14. (a)An n-motor efficiency map seen by the power train. (b) SOC of 3 motors, 5 motors, and n-motors.

8. SUMMARY

It is inevitable that EVs will be the norm of transportation in the near future. The struggle that EVs face right now is the inconvenience in terms of how long it takes to charge while on a trip. This dissertation proposed two solutions for an electric vehicle to increase its range: the VVR system and a multi-motor architecture for EVs. The VVR was presented as a charging system that allows an EV to charge its battery while en route. The process of transferring electric power from one specialized vehicle (charger vehicle) to another (user vehicle) during a trip is implemented wirelessly. This VVR system will allow EVs to drive further distances without the need for a pit-stop.

In addition to the VVR system, a dynamic wireless charging system where high efficiency power transfer is still achievable at different alignment positions was presented. This would be suitable for the VVR system, as well as electric vehicle charging stations that will incorporate wireless charging. Vehicles in such a system would no longer need to find the sweet charging spot in order to achieve high WPT efficiency. Instead, a vehicle charging its battery wirelessly would have higher efficiencies at a wider range of relative position with respect to the wireless pad.

The second solution presented was a multi-motor architecture for EVs that incorporates motors with different high efficiency operating regions. Based on the current vehicle speed and demanded torque, a controller decides which motor, or combination of motors, would be most efficient to run for the given operating condition. With this architecture, the powertrain observes a combined efficiency map that incorporates the best of each motor. This offers more range for an EV with the same battery capacity when compared to other architectures.

In addition to modeling, analysis, and simulation of the proposed systems, this dissertation also presented an extensive state-of-the-art study highlighting the prospective solutions to mitigate the EVs major problem with range, i.e., (1) infrastructure changes, (2) device level innovations, (3) autonomous vehicles, and (4) electric vehicles.

8.1 Future work

This dissertation has the potential to expand in several areas in terms of either modeling, experimental results, or optimization techniques. The modeling here implies the battery model discussed in the simulation of the EVs presented in this dissertation. The experimental results is regarding the WPT system presented in Chapter 6. And finally, the optimization technique refers to motor controller presented Chapter 7. The aforementioned points will elaborate the following subsections.

8.1.1 Improvements on the battery model of the EVs

The battery model presented in this dissertation for the VVR system and the multi-motor architecture was defined from an internal voltage in series with an internal resistance as presented in Figure 4.4. From there, the equation of the battery current can be calculated as shown in equation (4.2) and used in the SOC equation in (4.1). This model works great in illustrating the effects of other parts of the vehicle on the SOC of the battery. However, the model can be improved and derived based on a more complex battery model for a specific type of battery (e.g., lead-acid, nickel-cadmium, nickel-metal hydride, or Li-ion).

8.1.2 Improvement in the experimental results of the WPT system

For the experimental setup presented in Chapter 6 (in Figure 6.9), the wireless power transfer circuits were bought off the shelf to demonstrate the proof of concept. A better RX and TX circuit can be designed in which the resonant frequency (f_0) can be adjusted. With that, a controller can decide which frequency would provide the highest efficiency for the given relative position between the TX and RX coil. Also, a new test-bed that allows both RX and TX coils in achieving an angular movement would provide a more comprehensive experimental results.

8.1.3 Improvement in the optimization technique employed in the multi-motor architecture EV

In the chapter highlighting the multi-motor architecture, an optimized version of a rule based strategy was presented and implemented. This was a simplistic model to prove that any optimization technique can help the efficiency of the system. The current model presented in this dissertation can be expressed as a somewhat ”hybrid model”, and can be converted to an equation based model. If done so properly, a better optimization technique can be explored to improve the selection of motors that turn on based on the current operating region. Also, a comparison of different optimization techniques to be implemented can be discussed in further detail.

REFERENCES

[1] S. Rastogi, A. Sankar, K. Manglik, S. Mishra, and S. Mohanty, "Toward the vision of all-electric vehicles in a decade [energy and security]," *IEEE Consumer Electronics Magazine*, vol. 8, pp. 103–107, Mar. 2019. DOI: 10.1109/MCE.2018.2880848.

[2] B. Sarlioglu, C. T. Morris, D. Han, and S. Li, "Driving toward accessibility: A review of technological improvements for electric machines, power electronics, and batteries for electric and hybrid vehicles," *IEEE Industry Applications Magazine*, vol. 23, no. 1, pp. 14–25, Jan. 2017, ISSN: 1558-0598. DOI: 10.1109/MIAS.2016.2600739.

[3] S. Shafiee and E. Topal, "An econometrics view of worldwide fossil fuel consumption and the role of us," *Energy Policy*, vol. 36, no. 2, pp. 775–786, 2008, ISSN: 0301-4215. DOI: https://doi.org/10.1016/j.enpol.2007.11.002. [Online]. Available: http://www.sciencedirect.com/science/article/pii/S0301421507004934.

[4] J. Liu, "Research on electric vehicle fast charging station billing and settlement system," in *2017 2nd IEEE International Conference on Intelligent Transportation Engineering (ICITE)*, Sep. 2017, pp. 223–226. DOI: 10.1109/ICITE.2017.8056913.

[5] R. Pawełek, P. Kelm, and I. Wasiak, "Experimental analysis of dc electric vehicles charging station operation and its impact on the supplying grid," in *2014 IEEE International Electric Vehicle Conference (IEVC)*, Dec. 2014, pp. 1–4. DOI: 10.1109/IEVC.2014.7056152.

[6] J. Channegowda, V. K. Pathipati, and S. S. Williamson, "Comprehensive review and comparison of dc fast charging converter topologies: Improving electric vehicle plug-to-wheels efficiency," in *2015 IEEE 24th International Symposium on Industrial Electronics (ISIE)*, 2015, pp. 263–268.

[7] M. J. Gielniak and Z. J. Shen, "Power management strategy based on game theory for fuel cell hybrid electric vehicles," in *IEEE 60th Vehicular Technology Conference, 2004. VTC2004-Fall. 2004*, vol. 6, Sep. 2004, 4422–4426 Vol. 6. DOI: 10.1109/VETECF.2004.1404915.

[8] K. C. Aguirre, L. Eisenhardt, C. Lim, B. H. Nelson, A. Norring, P. Slowik, and N. Tu, "Lifecycle analysis comparison of a battery electric vehicle and a conventional gasoline vehicle," 2012.

[9] P. Cazzola. (Jul. 1, 2018). "The global ev outlook 2018." Last accessed: January 12, 2019, [Online]. Available: http://movelatam.org/wp-content/uploads/2018/07/GEVO-2018-MOVE-webinar.pdf.

[10] M. Etezadi-Amoli, K. Choma, and J. Stefani, "Rapid-charge electric-vehicle stations," *IEEE Transactions on Power Delivery*, vol. 25, no. 3, pp. 1883–1887, Jul. 2010, ISSN: 1937-4208. DOI: 10.1109/TPWRD.2010.2047874.

[11] Z. Duan, B. Gutierrez, and L. Wang, "Forecasting plug-in electric vehicle sales and the diurnal recharging load curve," *IEEE Transactions on Smart Grid*, vol. 5, no. 1, pp. 527–535, Jan. 2014, ISSN: 1949-3061. DOI: 10.1109/TSG.2013.2294436.

[12] C. Liu, K. T. Chau, D. Wu, and S. Gao, "Opportunities and challenges of vehicle-to-home, vehicle-to-vehicle, and vehicle-to-grid technologies," *Proceedings of the IEEE*, vol. 101, no. 11, pp. 2409–2427, Nov. 2013, ISSN: 1558-2256. DOI: 10.1109/JPROC.2013.2271951.

[13] K. J. Dyke, N. Schofield, and M. Barnes, "The impact of transport electrification on electrical networks," *IEEE Transactions on Industrial Electronics*, vol. 57, no. 12, pp. 3917–3926, Dec. 2010, ISSN: 1557-9948. DOI: 10.1109/TIE.2010.2040563.

[14] S. Habib, M. Khan, F. Abbas, L. Sang, M. Shahid, and H. Tang, "A comprehensive study of implemented international standards, technical challenges, impacts and prospects for electric vehicles," *IEEE Access*, vol. PP, pp. 1–1, Mar. 2018. DOI: 10.1109/ACCESS.2018.2812303.

[15] A. G. Boulanger, A. C. Chu, S. Maxx, and D. L. Waltz, "Vehicle electrification: Status and issues," *Proceedings of the IEEE*, vol. 99, no. 6, pp. 1116–1138, Jun. 2011, ISSN: 1558-2256. DOI: 10.1109/JPROC.2011.2112750.

[16] M. Z. Fortes, D. F. Silva, T. P. Abud, P. P. Machado, R. S. Maciel, and D. H. N. Dias, "Impact analysis of plug-in electric vehicle connected in real distribution network," *IEEE Latin America Transactions*, vol. 14, no. 5, pp. 2239–2245, May 2016, ISSN: 1548-0992. DOI: 10.1109/TLA.2016.7530419.

[17] P. Kong and G. K. Karagiannidis, "Charging schemes for plug-in hybrid electric vehicles in smart grid: A survey," *IEEE Access*, vol. 4, pp. 6846–6875, 2016, ISSN: 2169-3536. DOI: 10.1109/ACCESS.2016.2614689.

[18] N. Leemput, F. Geth, J. Van Roy, A. Delnooz, J. Büscher, and J. Driesen, "Impact of electric vehicle on-board single-phase charging strategies on a flemish residential grid," *IEEE Transactions on Smart Grid*, vol. 5, no. 4, pp. 1815–1822, Jul. 2014, ISSN: 1949-3061. DOI: 10.1109/TSG.2014.2307897.

[19] K. Clement-Nyns, E. Haesen, and J. Driesen, "The impact of charging plug-in hybrid electric vehicles on a residential distribution grid," *IEEE Transactions on Power Systems*, vol. 25, no. 1, pp. 371–380, Feb. 2010, ISSN: 1558-0679. DOI: 10.1109/TPWRS.2009.2036481.

[20] M. Yilmaz and P. T. Krein, "Review of the impact of vehicle-to-grid technologies on distribution systems and utility interfaces," *IEEE Transactions on Power Electronics*, vol. 28, no. 12, pp. 5673–5689, Dec. 2013, ISSN: 1941-0107. DOI: 10.1109/TPEL.2012.2227500.

[21] F. Lambert. (Jan. 1, 2020). "Tesla updates 2020 Supercharger map with new locations." Last accessed: March 23, 2020, [Online]. Available: https://electrek.co/2020/01/01/tesla-updates-2020-supercharger-map/.

[22] R. Stumpf. (Feb. 19, 2018). "Fully Electric Cars Not Useful for Local Police Stations...Yet." Last accessed: December 03, 2019, [Online]. Available: https://www.thedrive.com/tech/18534/fully-electric-cars-not-useful-for-local-police-stations-yet.

[23] J. Shin, B. Song, S. Shi, S. Chun, Y. Kim, G. Jung, and S. Jeon, "Design of buried power line for roadway-powered electric vehicle system," in *2013 IEEE Wireless Power Transfer (WPT)*, 2013, pp. 56–57. DOI: 10.1109/WPT.2013.6556880.

[24] G. Ombach, "Design considerations for wireless charging system for electric and plug-in hybrid vehicles," in *IET Hybrid and Electric Vehicles Conference 2013 (HEVC 2013)*, Nov. 2013, pp. 1–4. DOI: 10.1049/cp.2013.1904.

[25] O. C. Onar, M. Chinthavali, S. L. Campbell, L. E. Seiber, and C. P. White, "Vehicular integration of wireless power transfer systems and hardware interoperability case studies," *IEEE Transactions on Industry Applications*, vol. 55, no. 5, pp. 5223–5234, Sep. 2019, ISSN: 1939-9367. DOI: 10.1109/TIA.2019.2928482.

[26] Y. Bu, S. Endo, and T. Mizuno, "Improvement in the transmission efficiency of ev wireless power transfer system using a magnetoplated aluminum pipe," *IEEE Transactions on Magnetics*, vol. 54, no. 11, pp. 1–5, Nov. 2018, ISSN: 1941-0069. DOI: 10.1109/TMAG.2018.2840109.

[27] Y. Huang, C. Liu, Y. Zhou, Y. Xiao, and S. Liu, "Power allocation for dynamic dual-pickup wireless charging system of electric vehicle," *IEEE Transactions on Magnetic*, vol. 55, no. 7, pp. 1–6, Jul. 2019, ISSN: 1941-0069. DOI: 10.1109/TMAG.2019.2894163.

[28] Z. Danping, L. juan, C. Yuchun, L. Yuhang, and C. Zhongjian, "Research on electric energy metering and charging system for dynamic wireless charging of electric vehicle," in *2019 4th International Conference on Intelligent Transportation Engineering (ICITE)*, Sep. 2019, pp. 252–255. DOI: 10.1109/ICITE.2019.8880214.

[29] H. Grünjes and M. Birkner, "Electro mobility for heavy duty vehicles (hdv): The siemens ehighway system," in *HVTT12: 12th International Symposium on Heavy Vehicle Transport Technology*, 2012.

[30] D. Nicolaides, R. McMahon, D. Cebon, and J. Miles, "A national power infrastructure for charge-on-the-move: An appraisal for great britain," *IEEE Systems Journal*, vol. 13, no. 1, pp. 720–728, Mar. 2019, ISSN: 2373-7816. DOI: 10.1109/JSYST.2018.2792939.

[31] D. Nicolaides, D. Cebon, and J. Miles, "Prospects for electrification of road freight," *IEEE Systems Journal*, vol. 12, no. 2, pp. 1838–1849, Jun. 2018, ISSN: 2373-7816. DOI: 10.1109/JSYST.2017.2691408.

[32] Seungyoung Ahn and Joungho Kim, "Magnetic field design for high efficient and low emf wireless power transfer in on-line electric vehicle," in *Proceedings of the 5th European Conference on Antennas and Propagation (EUCAP)*, Apr. 2011, pp. 3979–3982.

[33] Y. Hori, "Novel ev society based on motor/ capacitor/ wireless — application of electric motor, supercapacitors, and wireless power transfer to enhance operation of future vehicles," in *2012 IEEE MTT-S International Microwave Workshop Series on Innovative Wireless Power Transmission: Technologies, Systems, and Applications*, May 2012, pp. 3–8. DOI: 10.1109/IMWS.2012.6215827.

[34] X. Zhang, Z. Yuan, Q. Yang, Y. Li, J. Zhu, and Y. Li, "Coil design and efficiency analysis for dynamic wireless charging system for electric vehicles," *IEEE Transactions on Magnetics*, vol. 52, no. 7, pp. 1–4, Jul. 2016, ISSN: 1941-0069. DOI: 10.1109/TMAG.2016.2529682.

[35] Y. Suzuki, T. Sugiura, N. Sakai, M. Hanazawa, and T. Ohira, "Dielectric coupling from electrified roadway to steel-belt tires characterized for miniature model car running demonstration," in *2012 IEEE MTT-S International Microwave Workshop Series on Innovative Wireless Power Transmission: Technologies, Systems, and Applications*, May 2012, pp. 35–38. DOI: 10.1109/IMWS.2012.6215814.

[36] L. A. Maglaras, J. Jiang, A. L. Maglaras, and F. V. Topalis, "Mobile energy disseminators increase electrical vehicles range in a smart city," in *5th IET Hybrid and Electric Vehicles Conference (HEVC 2014)*, Nov. 2014, pp. 1–6. DOI: 10.1049/cp.2014.0947.

[37] L. A. Maglaras, F. V. Topalis, and A. L. Maglaras, "Cooperative approaches for dynamic wireless charging of electric vehicles in a smart city," in *2014 IEEE International Energy Conference (ENERGYCON)*, May 2014, pp. 1365–1369. DOI: 10.1109/ENERGYCON.2014.6850600.

[38] S. Das, K. Pal, P. Goswami, and M. Kerawalla, "Wireless power transfer in electric vehicles," *International Journal of Applied Environmental Sciences*, vol. 13, no. 7, pp. 643–659, Jan. 2018.

[39] T. M. Fisher, K. B. Farley, Y. Gao, H. Bai, and Z. T. H. Tse, "Electric vehicle wireless charging technology: A state-of-the-art review of magnetic coupling systems," *Wireless Power Transfer*, vol. 1, no. 2, pp. 87–96, 2014.

[40] M. Debbou and F. Colet, "Inductive wireless power transfer for electric vehicle dynamic charging," in *2016 IEEE PELS Workshop on Emerging Technologies: Wireless Power Transfer (WoW)*, Oct. 2016, pp. 118–122. DOI: 10.1109/WoW.2016.7772077.

[41] D. Kishan and P. S. R. Nayak, "Wireless power transfer technologies for electric vehicle battery charging — a state of the art," in *2016 International Conference on Signal Processing, Communication, Power and Embedded System (SCOPES)*, Oct. 2016, pp. 2069–2073. DOI: 10.1109/SCOPES.2016.7955812.

[42] P. Ning, J. M. Miller, O. C. Onar, and C. P. White, "A compact wireless charging system for electric vehicles," in *2013 IEEE Energy Conversion Congress and Exposition*, IEEE, 2013, pp. 3629–3634.

[43] S. Chopra and P. Bauer, "Driving range extension of ev with on-road contactless power transfer—a case study," *IEEE Transactions on Industrial Electronics*, vol. 60, no. 1, pp. 329–338, Jan. 2013, ISSN: 1557-9948. DOI: 10.1109/TIE.2011.2182015.

[44] S. Li and C. C. Mi, "Wireless power transfer for electric vehicle applications," *IEEE Journal of Emerging and Selected Topics in Power Electronics*, vol. 3, no. 1, pp. 4–17, Mar. 2015, ISSN: 2168-6785. DOI: 10.1109/JESTPE.2014.2319453.

[45] M. S. A. Chowdhury and X. Liang, "Power transfer efficiency evaluation of different power pads for electric vehicle's wireless charging systems," in *2019 IEEE Canadian Conference of Electrical and Computer Engineering (CCECE)*, May 2019, pp. 1–4. DOI: 10.1109/CCECE.2019.8861757.

[46] D. Niculae, M. Iordache, M. Stanculescu, M. L. Bobaru, and S. Deleanu, "A review of electric vehicles charging technologies stationary and dynamic," in *2019 11th International Symposium on Advanced Topics in Electrical Engineering (ATEE)*, Mar. 2019, pp. 1–4. DOI: 10.1109/ATEE.2019.8724943.

[47] N. Shinohara, "Beam efficiency of wireless power transmission via radio waves from short range to long rangefpr," *Journal of electromagnetic engineering and science*, vol. 10, Jan. 2010. DOI: 10.5515/JKIEES.2010.10.4.224.

[48] N. Shinohara, "Wireless power transmission progress for electric vehicle in japan," in *2013 IEEE Radio and Wireless Symposium*, Jan. 2013, pp. 109–111. DOI: 10.1109/RWS.2013.6486657.

[49] Y. Wang, J. Song, L. Lin, X. Wu, and W. Zhang, "Research on magnetic coupling resonance wireless power transfer system with variable coil structure," in *2017 IEEE PELS Workshop on Emerging Technologies: Wireless Power Transfer (WoW)*, May 2017, pp. 1–6. DOI: 10.1109/WoW.2017.7959403.

[50] S. Masuda, T. Hirose, Y. Akihara, N. Kuroki, M. Numa, and M. Hashimoto, "Impedance matching in magnetic-coupling-resonance wireless power transfer for small implantable devices," in *2017 IEEE Wireless Power Transfer Conference (WPTC)*, May 2017, pp. 1–3. DOI: 10.1109/WPT.2017.7953839.

[51] Cheng Yang and K. Tsunekawa, "A novel parallel double-layer spiral coil for coupled magnetic resonance wireless power transfer," in *2015 IEEE Wireless Power Transfer Conference (WPTC)*, May 2015, pp. 1–3. DOI: 10.1109/WPT.2015.7140115.

[52] K. Miwa, H. Mori, N. Kikuma, H. Hirayama, and K. Sakakibara, "A consideration of efficiency improvement of transmitting coil array in wireless power transfer with magnetically coupled resonance," in *2013 IEEE Wireless Power Transfer (WPT)*, 2013, pp. 13–16. DOI: 10.1109/WPT.2013.6556870.

[53] L. Tong, H. Zeng, and F. Peng, "A study of the self-coupling magnetic resonance coupled wireless power transfer," in *2015 IEEE Applied Power Electronics Conference and Exposition (APEC)*, Mar. 2015, pp. 3138–3142. DOI: 10.1109/APEC.2015.7104800.

[54] V. Jiwariyavej, T. Imura, and Y. Hori, "Coupling coefficients estimation of wireless power transfer system via magnetic resonance coupling using information from either side of the system," *IEEE Journal of Emerging and Selected Topics in Power Electronics*, vol. 3, no. 1, pp. 191–200, Mar. 2015, ISSN: 2168-6785. DOI: 10.1109/JESTPE.2014.2332056.

[55] A. Kurs, A. Karalis, R. Moffatt, J. D. Joannopoulos, P. Fisher, and M. Soljačić, "Wireless power transfer via strongly coupled magnetic resonances," *Science*, vol. 317, no. 5834, pp. 83–86, 2007, ISSN: 0036-8075. DOI: 10.1126/science.1143254. eprint: https://science.sciencemag.org/content/317/5834/83.full.pdf. [Online]. Available: https://science.sciencemag.org/content/317/5834/83.

[56] D. Naberezhnykh, N. Reed, F. Ognissanto, T. Theodoropoulos, and H. Bludszuweit, "Operational requirements for dynamic wireless power transfer systems for electric vehicles," in *2014 IEEE International Electric Vehicle Conference (IEVC)*, Dec. 2014, pp. 1–8. DOI: 10.1109/IEVC.2014.7056236.

[57] Z. Bin and H. Xiao-hong, "Modeling and analysis of wireless power transmission system via strongly coupled magnetic resonances," in *2014 International Conference on Mechatronics and Control (ICMC)*, Jul. 2014, pp. 70–75. DOI: 10.1109/ICMC.2014.7231519.

[58] T. Sasatani, Y. Narusue, and Y. Kawahara, "Dynamic complex impedance tuning method using a multiple-input dc/dc converter for wireless power transfer," in *2018 IEEE Wireless Power Transfer Conference (WPTC)*, Jun. 2018, pp. 1–4. DOI: 10.1109/WPT.2018.8639301.

[59] D. Kobayashi, T. Imura, and Y. Hori, "Real-time coupling coefficient estimation and maximum efficiency control on dynamic wireless power transfer for electric vehicles," in *2015 IEEE PELS Workshop on Emerging Technologies: Wireless Power (2015 WoW)*, Jun. 2015, pp. 1–6. DOI: 10.1109/WoW.2015.7132799.

[60] K. Hata, T. Imura, and Y. Hori, "Dynamic wireless power transfer system for electric vehicles to simplify ground facilities - power control and efficiency maximization on the secondary side," in *2016 IEEE Applied Power Electronics Conference and Exposition (APEC)*, Mar. 2016, pp. 1731–1736. DOI: 10.1109/APEC.2016.7468101.

[61] T. A. Khan, A. Yazdan, and R. W. Heath, "Optimization of power transfer efficiency and energy efficiency for wireless-powered systems with massive mimo," *IEEE Transactions on Wireless Communications*, vol. 17, no. 11, pp. 7159–7172, Nov. 2018, ISSN: 1558-2248. DOI: 10.1109/TWC.2018.2865727.

[62] J. Shin, S. Shin, Y. Kim, S. Ahn, S. Lee, G. Jung, S. Jeon, and D. Cho, "Design and implementation of shaped magnetic-resonance-based wireless power transfer system for roadway-powered moving electric vehicles," *IEEE Transactions on Industrial Electronics*, vol. 61, no. 3, pp. 1179–1192, Mar. 2014, ISSN: 1557-9948. DOI: 10.1109/TIE.2013.2258294.

[63] Z. Yan, B. Song, Y. Zhang, K. Zhang, Z. Mao, and Y. Hu, "A rotation-free wireless power transfer system with stable output power and efficiency for autonomous underwater vehicles," *IEEE Transactions on Power Electronics*, vol. 34, no. 5, pp. 4005–4008, May 2019, ISSN: 1941-0107. DOI: 10.1109/TPEL.2018.2871316.

[64] J. Choi, S. Yeo, S. Park, J. Lee, and G. Cho, "Resonant regulating rectifiers (3r) operating for 6.78 mhz resonant wireless power transfer (rwpt)," *IEEE Journal of Solid-State Circuits*, vol. 48, no. 12, pp. 2989–3001, Dec. 2013, ISSN: 1558-173X. DOI: 10.1109/JSSC.2013.2287592.

[65] D. Seo and J. Lee, "Frequency-tuning method using the reflection coefficient in a wireless power transfer system," *IEEE Microwave and Wireless Components Letters*, vol. 27, no. 11, pp. 959–961, Nov. 2017, ISSN: 1558-1764. DOI: 10.1109/LMWC.2017.2750023.

[66] J. Kim, H. Son, K. Kim, and Y. Park, "Efficiency analysis of magnetic resonance wireless power transfer with intermediate resonant coil," *IEEE Antennas and Wireless Propagation Letters*, vol. 10, pp. 389–392, 2011, ISSN: 1548-5757. DOI: 10.1109/LAWP.2011.2150192.

[67] C. Cui, K. Song, C. Zhu, Q. Zhang, Y. Liu, and S. Dong, "State feedback controller design of dynamic wireless power transfer system," in *2018 IEEE PELS Workshop on Emerging Technologies: Wireless Power Transfer (Wow)*, Jun. 2018, pp. 1–5. DOI: 10.1109/WoW.2018.8450915.

[68] K. H. Huang Wei, "Analysis and optimization of wireless power transfer efficiency considering the tilt angle of a coil," *J Electromagn Eng Sci*, vol. 18, no. 1, pp. 13–19, 2018. DOI: 10.26866/jees.2018.18.1.13. eprint: http://jees.kr/journal/view.php?number=3286. [Online]. Available: http://jees.kr/journal/view.php?number=3286.

[69] Y. Wang, R. Yuan, Z. Jiang, S. Zhao, W. Zhao, and X. Huang, "Research on dynamic wireless ev charging power control method based on parameter adjustment according to driving speed," in *2019 IEEE 2nd International Conference on Electronics Technology (ICET)*, May 2019, pp. 305–309. DOI: 10.1109/ELTECH.2019.8839356.

[70] N. T. Diep, N. K. Trung, and T. T. Minh, "Power control in the dynamic wireless charging of electric vehicles," in *2019 10th International Conference on Power Electronics and ECCE Asia (ICPE 2019 - ECCE Asia)*, May 2019, pp. 1–6.

[71] Y. Liangyi, S. Dihua, X. Fei, and Z. Jian, "Study of autonomous platoon vehicle longitudinal modeling," in *IET International Conference on Intelligent and Connected Vehicles (ICV 2016)*, Sep. 2016, pp. 1–10. DOI: 10.1049/cp.2016.1176.

[72] C. Tang and Y. Li, "Consensus-based platoon control for non-lane-discipline connected autonomous vehicles considering time delays," in *2018 37th Chinese Control Conference (CCC)*, Jul. 2018, pp. 7713–7718. DOI: 10.23919/ChiCC.2018.8484016.

[73] Y. Li and C. He, "Connected autonomous vehicle platoon control considering vehicle dynamic information," in *2018 37th Chinese Control Conference (CCC)*, Jul. 2018, pp. 7834–7839. DOI: 10.23919/ChiCC.2018.8483514.

[74] J. Axelsson, "Safety in vehicle platooning: A systematic literature review," *IEEE Transactions on Intelligent Transportation Systems*, vol. 18, no. 5, pp. 1033–1045, 2017.

[75] S. Medawar, D. Scholle, and I. Šljivo, "Cooperative safety critical cps platooning in safecop," in *2017 6th Mediterranean Conference on Embedded Computing (MECO)*, 2017, pp. 1–5.

[76] H. Suzuki and K. Matsunaga, "New approach to evaluating macroscopic safety of platooned vehicles based on shockwave theory," in *Proceedings of SICE Annual Conference 2010*, 2010, pp. 925–929.

[77] S. Lee, C. Oh, and S. Hong, "Exploring lane change safety issues for manually driven vehicles in vehicle platooning environments," *IET Intelligent Transport Systems*, vol. 12, no. 9, pp. 1142–1147, 2018.

[78] E. van Nunen, F. Esposto, A. K. Saberi, and J. Paardekooper, "Evaluation of safety indicators for truck platooning," in *2017 IEEE Intelligent Vehicles Symposium (IV)*, 2017, pp. 1013–1018.

[79] Tae Soo no, Kil-To Chong, and Do-Hwan Roh, "A lyapunov function approach to longitudinal control of vehicles in a platoon," *IEEE Transactions on Vehicular Technology*, vol. 50, no. 1, pp. 116–124, Jan. 2001, ISSN: 1939-9359. DOI: 10.1109/25.917894.

[80] T. Fujioka, "Longitudinal vehicle following control for autonomous driving," in *Proceedings of the International Symposium on Advanced Vehicle Control, 1996*, 1996.

[81] S. Sheikholeslam and C. A. Desoer, "Longitudinal control of a platoon of vehicles with no communication of lead vehicle information," in *1991 American Control Conference*, Jun. 1991, pp. 3102–3106. DOI: 10.23919/ACC.1991.4791979.

[82] S. Sheikholeslam and C. A. Desoer, "Longitudinal control of a platoon of vehicles i: Linear model," in *UC Berkeley: California Partners for Advanced Transportation Technology.*, 1989. [Online]. Available: https://escholarship.org/uc/item/7ns408fp.

[83] S. Sheikholeslam and C. A. Desoer, "Longitudinal control of a platoon of vehicles. iii, nonlinear model," in *UC Berkeley: California Partners for Advanced Transportation Technology.*, 1990. [Online]. Available: https://escholarship.org/uc/item/0dx8t12z.

[84] S. E. Shladover, "Longitudinal Control of Automotive Vehicles in Close-Formation Platoons," *Journal of Dynamic Systems, Measurement, and Control*, vol. 113, no. 2, pp. 231–241, Jun. 1991, ISSN: 0022-0434. DOI: 10.1115/1.2896370. eprint: https://asmedigitalcollection.asme.org/dynamicsystems/article-pdf/113/2/231/5778576/231_1.pdf. [Online]. Available: https://doi.org/10.1115/1.2896370.

[85] S. E. Shladover, "Longitudinal Control of Automated Guideway Transit Vehicles Within Platoons," *Journal of Dynamic Systems, Measurement, and Control*, vol. 100, no. 4, pp. 302–310, Dec. 1978, ISSN: 0022-0434. DOI: 10.1115/1.3426382. eprint: https://asmedigitalcollection.asme.org/dynamicsystems/article-pdf/100/4/302/5528451/302_1.pdf. [Online]. Available: https://doi.org/10.1115/1.3426382.

[86] M. Li, Y. Xu, M. Lei, and B. Zhou, "Velocity tracking control based on throttle-pedal-moving data mapping for the autonomous vehicle," *IEEE Access*, vol. 7, pp. 176 712–176 718, 2019, ISSN: 2169-3536. DOI: 10.1109/ACCESS.2019.2956547.

[87] H. J. Kim and J. H. Yang, "Takeover requests in simulated partially autonomous vehicles considering human factors," *IEEE Transactions on Human-Machine Systems*, vol. 47, no. 5, pp. 735–740, Oct. 2017, ISSN: 2168-2305. DOI: 10.1109/THMS.2017.2674998.

[88] M. Aldibaja, N. Suganuma, and K. Yoneda, "Robust intensity-based localization method for autonomous driving on snow–wet road surface," *IEEE Transactions on Industrial Informatics*, vol. 13, no. 5, pp. 2369–2378, Oct. 2017, ISSN: 1941-0050. DOI: 10.1109/TII.2017.2713836.

[89] K. P. Divakarla, A. Emadi, and S. Razavi, "A cognitive advanced driver assistance systems architecture for autonomous-capable electrified vehicles," *IEEE Transactions on Transportation Electrification*, vol. 5, no. 1, pp. 48–58, Mar. 2019, ISSN: 2372-2088. DOI: 10.1109/TTE.2018.2870819.

[90] A. Y. S. Lam, J. J. Q. Yu, Y. Hou, and V. O. K. Li, "Coordinated autonomous vehicle parking for vehicle-to-grid services: Formulation and distributed algorithm," *IEEE Transactions on Smart Grid*, vol. 9, no. 5, pp. 4356–4366, Sep. 2018, ISSN: 1949-3061. DOI: 10.1109/TSG.2017.2655299.

[91] D. Meltz and H. Guterman, "Functional safety verification for autonomous ugvs - methodology presentation and implementation on a full-scale system," *IEEE Transactions on Intelligent Vehicles*, vol. 4, no. 3, pp. 472–485, Sep. 2019, ISSN: 2379-8858. DOI: 10.1109/TIV.2019.2919460.

[92] D. Åsljung, J. Nilsson, and J. Fredriksson, "Using extreme value theory for vehicle level safety validation and implications for autonomous vehicles," *IEEE Transactions on Intelligent Vehicles*, vol. 2, no. 4, pp. 288–297, Dec. 2017, ISSN: 2379-8858. DOI: 10.1109/TIV.2017.2768219.

[93] A. Li, W. Zhao, X. Wang, and X. Qiu, "Act-r cognitive model based trajectory planning method study for electric vehicle's active obstacle avoidance system," *Energies*, vol. 11, no. 1, p. 75, 2018.

[94] C. Chatzikomis, A. Sorniotti, P. Gruber, M. Zanchetta, D. Willans, and B. Balcombe, "Comparison of path tracking and torque-vectoring controllers for autonomous electric vehicles," *IEEE Transactions on Intelligent Vehicles*, vol. 3, no. 4, pp. 559–570, Dec. 2018, ISSN: 2379-8858. DOI: 10.1109/TIV.2018.2874529.

[95] H. Marzbani, H. Khayyam, C. N. TO, Đ. V. Quoc, and R. N. Jazar, "Autonomous vehicles: Autodriver algorithm and vehicle dynamics," *IEEE Transactions on Vehicular Technology*, vol. 68, no. 4, pp. 3201–3211, Apr. 2019, ISSN: 1939-9359. DOI: 10.1109/TVT.2019.2895297.

[96] N. Li, D. W. Oyler, M. Zhang, Y. Yildiz, I. Kolmanovsky, and A. R. Girard, "Game theoretic modeling of driver and vehicle interactions for verification and validation of autonomous vehicle control systems," *IEEE Transactions on Control Systems Technology*, vol. 26, no. 5, pp. 1782–1797, Sep. 2018, ISSN: 2374-0159. DOI: 10.1109/TCST.2017.2723574.

[97] K. Lee, S. Jeon, H. Kim, and D. Kum, "Optimal path tracking control of autonomous vehicle: Adaptive full-state linear quadratic gaussian (lqg) control," *IEEE Access*, vol. 7, pp. 109 120–109 133, 2019, ISSN: 2169-3536. DOI: 10.1109/ACCESS.2019.2933895.

[98] S. Kuutti, S. Fallah, K. Katsaros, M. Dianati, F. Mccullough, and A. Mouzakitis, "A survey of the state-of-the-art localization techniques and their potentials for autonomous vehicle applications," *IEEE Internet of Things Journal*, vol. 5, no. 2, pp. 829–846, Apr. 2018, ISSN: 2372-2541. DOI: 10.1109/JIOT.2018.2812300.

[99] M. Obst, N. Mattern, R. Schubert, and G. Wanielik, "Car-to-car communication for accurate vehicle localization — the covel approach," in *International Multi-Conference on Systems, Signals Devices*, Mar. 2012, pp. 1–6. DOI: 10.1109/SSD.2012.6198050.

[100] M. H. Choi, B. Shirinzadeh, and R. Porter, "System identification-based sliding mode control for small-scaled autonomous aerial vehicles with unknown aerodynamics derivatives," *IEEE/ASME Transactions on Mechatronics*, vol. 21, no. 6, pp. 2944–2952, Dec. 2016, ISSN: 1941-014X. DOI: 10.1109/TMECH.2016.2578311.

[101] Z. Wei, H. Wu, S. Huang, and Z. Feng, "Scaling laws of unmanned aerial vehicle network with mobility pattern information," *IEEE Communications Letters*, vol. 21, no. 6, pp. 1389–1392, Jun. 2017, ISSN: 2373-7891. DOI: 10.1109/LCOMM.2017.2671861.

[102] L. Paull, C. Thibault, A. Nagaty, M. Seto, and H. Li, "Sensor-driven area coverage for an autonomous fixed-wing unmanned aerial vehicle," *IEEE Transactions on Cybernetics*, vol. 44, no. 9, pp. 1605–1618, Sep. 2014, ISSN: 2168-2275. DOI: 10.1109/TCYB.2013.2290975.

[103] C. Wang, J. Wang, X. Zhang, and X. Zhang, "Autonomous navigation of uav in large-scale unknown complex environment with deep reinforcement learning," in *2017 IEEE Global Conference on Signal and Information Processing (GlobalSIP)*, Nov. 2017, pp. 858–862. DOI: 10.1109/GlobalSIP.2017.8309082.

[104] Z. Wang, H. She, and W. Si, "Autonomous landing of multi-rotors uav with monocular gimbaled camera on moving vehicle," in *2017 13th IEEE International Conference on Control Automation (ICCA)*, Jul. 2017, pp. 408–412. DOI: 10.1109/ICCA.2017.8003095.

[105] F. Wang, B. Xian, G. Huang, and B. Zhao, "Autonomous hovering control for a quadrotor unmanned aerial vehicle," in *Proceedings of the 32nd Chinese Control Conference*, Jul. 2013, pp. 620–625.

[106] A. Kuzu, O. Songuler, and F. Ucan, "Fuzzy interval type ii lateral control of an autonomous uav," in *2014 6th International Congress on Ultra Modern Telecommunications and Control Systems and Workshops (ICUMT)*, Oct. 2014, pp. 214–219. DOI: 10.1109/ICUMT.2014.7002105.

[107] S. D. McPhail and M. Pebody, "Range-only positioning of a deep-diving autonomous underwater vehicle from a surface ship," *IEEE Journal of Oceanic Engineering*, vol. 34, no. 4, pp. 669–677, Oct. 2009, ISSN: 2373-7786. DOI: 10.1109/JOE.2009.2030223.

[108] J. Biggs and W. Holderbaum, "Optimal kinematic control of an autonomous underwater vehicle," *IEEE Transactions on Automatic Control*, vol. 54, no. 7, pp. 1623–1626, Jul. 2009, ISSN: 2334-3303. DOI: 10.1109/TAC.2009.2017966.

[109] W. Caharija, K. Y. Pettersen, M. Bibuli, P. Calado, E. Zereik, J. Braga, J. T. Gravdahl, A. J. Sørensen, M. Milovanović, and G. Bruzzone, "Integral line-of-sight guidance and control of underactuated marine vehicles: Theory, simulations, and experiments," *IEEE Transactions on Control Systems Technology*, vol. 24, no. 5, pp. 1623–1642, Sep. 2016, ISSN: 2374-0159. DOI: 10.1109/TCST.2015.2504838.

[110] C. Paliotta, E. Lefeber, K. Y. Pettersen, J. Pinto, M. Costa, and J. T. de Figueiredo Borges de Sousa, "Trajectory tracking and path following for underactuated marine vehicles," *IEEE Transactions on Control Systems Technology*, vol. 27, no. 4, pp. 1423–1437, Jul. 2019, ISSN: 2374-0159. DOI: 10.1109/TCST.2018.2834518.

[111] C. Sun, X. Zhang, Q. Zhou, and Y. Tian, "A model predictive controller with switched tracking error for autonomous vehicle path tracking," *IEEE Access*, vol. 7, pp. 53 103–53 114, 2019, ISSN: 2169-3536. DOI: 10.1109/ACCESS.2019.2912094.

[112] B. Zhang, C. Zong, G. Chen, and B. Zhang, "Electrical vehicle path tracking based model predictive control with a laguerre function and exponential weight," *IEEE Access*, vol. 7, pp. 17 082–17 097, 2019, ISSN: 2169-3536. DOI: 10.1109/ACCESS.2019.2892746.

[113] Liuping Wang, "Use of exponential data weighting in model predictive control design," in *Proceedings of the 40th IEEE Conference on Decision and Control (Cat. No.01CH37228)*, vol. 5, Dec. 2001, 4857–4862 vol.5. DOI: 10.1109/CDC.2001.980976.

[114] Liuping Wang, "Discrete time model predictive control design using laguerre functions," in *Proceedings of the 2001 American Control Conference. (Cat. No.01CH37148)*, vol. 3, Jun. 2001, 2430–2435 vol.3. DOI: 10.1109/ACC.2001.946117.

[115] C. Sun, X. Zhang, L. Xi, and Y. Tian, "Design of a path-tracking steering controller for autonomous vehicles," *Energies*, vol. 11, no. 6, p. 1451, 2018.

[116] C. Chatzikomis, A. Sorniotti, P. Gruber, M. Zanchetta, D. Willans, and B. Balcombe, "Comparison of path tracking and torque-vectoring controllers for autonomous electric vehicles," *IEEE Transactions on Intelligent Vehicles*, vol. 3, no. 4, pp. 559–570, Dec. 2018, ISSN: 2379-8858. DOI: 10.1109/TIV.2018.2874529.

[117] N. Li, D. W. Oyler, M. Zhang, Y. Yildiz, I. Kolmanovsky, and A. R. Girard, "Game theoretic modeling of driver and vehicle interactions for verification and validation of autonomous vehicle control systems," *IEEE Transactions on Control Systems Technology*, vol. 26, no. 5, pp. 1782–1797, Sep. 2018, ISSN: 2374-0159. DOI: 10.1109/TCST.2017.2723574.

[118] X. Na and D. J. Cole, "Game-theoretic modeling of the steering interaction between a human driver and a vehicle collision avoidance controller," *IEEE Transactions on Human-Machine Systems*, vol. 45, no. 1, pp. 25–38, Feb. 2015, ISSN: 2168-2305. DOI: 10.1109/THMS.2014.2363124.

[119] X. Na and D. J. Cole, "Modelling of a human driver s interaction with vehicle automated steering using cooperative game theory," *IEEE/CAA Journal of Automatica Sinica*, vol. 6, no. 5, pp. 1095–1107, Sep. 2019, ISSN: 2329-9274. DOI: 10.1109/JAS.2019.1911675.

[120] A. Zia, "A comprehensive overview on the architecture of hybrid electric vehicles (hev)," in *2016 19th International Multi-Topic Conference (INMIC)*, Dec. 2016, pp. 1–7. DOI: 10.1109/INMIC.2016.7840143.

[121] H. L. Husted, "A comparative study of the production applications of hybrid electric powertrains," in *Future Transportation Technology Conference & Exposition*, SAE International, Jun. 2003. DOI: https://doi.org/10.4271/2003-01-2307. [Online]. Available: https://doi.org/10.4271/2003-01-2307.

[122] Y. Tang, *Dual motors drive and control system for an electric vehicle.* U.S. Patent 8453770B2, Jun. 2013.

[123] S. Zhang, R. Xiong, and C. Zhang, "Pontryagin's minimum principle-based power management of a dual-motor-driven electric bus," *Applied energy*, vol. 159, pp. 370–380, 2015.

[124] H. Xiong, X. Zhu, and R. Zhang, "Energy recovery strategy numerical simulation for dual axle drive pure electric vehicle based on motor loss model and big data calculation," *Complexity*, vol. 2018, 2018.

[125] M. Hu, J. Zeng, S. Xu, C. Fu, and D. Qin, "Efficiency study of a dual-motor coupling ev powertrain," *IEEE Transactions on Vehicular Technology*, vol. 64, no. 6, pp. 2252–2260, Jun. 2015, ISSN: 0018-9545. DOI: 10.1109/TVT.2014.2347349.

[126] P. Xu, G. Guo, J. Cao, and B. Cao, "A novel fore axle whole-turning driving and control system for direct-wheel-driven electric vehicle," in *2008 IEEE International Conference on Automation and Logistics*, Sep. 2008, pp. 705–709. DOI: 10.1109/ICAL.2008.4636240.

[127] Y.-P. Yang and C.-P. Lo, "Current distribution control of dual directly driven wheel motors for electric vehicles," *Control Engineering Practice*, vol. 16, no. 11, pp. 1285–1292, 2008.

[128] S. D. Pinto, P. Camocardi, A. Sorniotti, P. Gruber, P. Perlo, and F. Viotto, "Torque-fill control and energy management for a four-wheel-drive electric vehicle layout with two-speed transmissions," *IEEE Transactions on Industry Applications*, vol. 53, no. 1, pp. 447–458, Jan. 2017, ISSN: 0093-9994. DOI: 10.1109/TIA.2016.2616322.

[129] S. Sakai, H. Sado, and Y. Hori, "Motion control in an electric vehicle with four independently driven in-wheel motors," *IEEE/ASME Transactions on Mechatronics*, vol. 4, no. 1, pp. 9–16, Mar. 1999, ISSN: 1083-4435. DOI: 10.1109/3516.752079.

[130] *The pros and cons of using in-wheel motors in electric cars*, https://www.plugincars.com/pros-and-cons-wheel-motors-127174.html, Last accessed: December 9, 2018.

[131] M. Biček, G. Gotovac, D. Miljavec, and S. Zupan, "Mechanical failure mode causes of in-wheel motors," *Strojniški vestnik - Journal of Mechanical Engineering*, vol. 61, no. 1, pp. 74–85, 2015, ISSN: 0039-2480. DOI: 10.5545/sv-jme.2014.2022. [Online]. Available: https://www.sv-jme.eu/article/mechanical-failure-mode-causes-of-in-wheel-motors/.

[132] O. Nezamuddin, R. Bagwe, and E. Dos Santos, "A multi-motor architecture for electric vehicles," in *2019 IEEE Transportation Electrification Conference and Expo (ITEC)*, Jun. 2019, pp. 1–6. DOI: 10.1109/ITEC.2019.8790582.

[133] G. Mohan, F. Assadian, and S. Longo, "Comparative analysis of forward-facing models vs backwardfacing models in powertrain component sizing," in *IET Hybrid and Electric Vehicles Conference 2013 (HEVC 2013)*, Nov. 2013, pp. 1–6. DOI: 10.1049/cp.2013.1920.

[134] S. Pickenhain and A. Burtchen, "Optimal energy control of hybrid vehicles," in *Modeling, Simulation and Optimization of Complex Processes HPSC 2015*, Springer, 2017, pp. 179–188.

[135] T. Liu, X. Tang, H. Wang, H. Yu, and X. Hu, "Adaptive hierarchical energy management design for a plug-in hybrid electric vehicle," *IEEE Transactions on Vehicular Technology*, vol. 68, no. 12, pp. 11 513–11 522, 2019.

[136] R. M. Bagwe, A. Byerly, E. C. dos Santos, and Z. Ben-Miled, "Adaptive rule-based energy management strategy for a parallel hev," *Energies*, vol. 12, no. 23, 2019, ISSN: 1996-1073. DOI: 10.3390/en12234472. [Online]. Available: https://www.mdpi.com/1996-1073/12/23/4472.

[137] D. Karbowski and S. Pagerit, "Autonomie, a plug-and-play software architecture," in *Proceedings of the Vehicle Power and Propulsion Conference, Lille, France*, 2010, pp. 1–3.

[138] A. Brooker, J. Gonder, L. Wang, E. Wood, S. Lopp, and L. Ramroth, "Fastsim: A model to estimate vehicle efficiency, cost and performance," SAE Technical Paper, Tech. Rep., 2015.

[139] F. Lu, H. Zhang, and C. Mi, "A two-plate capacitive wireless power transfer system for electric vehicle charging applications," *IEEE Transactions on Power Electronics*, vol. 33, no. 2, pp. 964–969, 2018.

[140] R. Mai, Y. Liu, Y. Li, P. Yue, G. Cao, and Z. He, "An active-rectifier-based maximum efficiency tracking method using an additional measurement coil for wireless power transfer," *IEEE Transactions on Power Electronics*, vol. 33, no. 1, pp. 716–728, 2018.

[141] K. Yoon, S. Lee, I. Cho, H. Lee, and G. Cho, "Dual receiver coils wireless power transfer system with interleaving switching," *IEEE Transactions on Power Electronics*, vol. 33, no. 12, pp. 10 016–10 020, 2018.

[142] F. Lu, H. Zhang, H. Hofmann, and C. C. Mi, "An inductive and capacitive combined wireless power transfer system with lc-compensated topology," *IEEE Transactions on Power Electronics*, vol. 31, no. 12, pp. 8471–8482, 2016.

[143] J. Hudecek, J. Küfen, O. Langen, J. Dankert, and L. Eckstein, "A system for precise positioning of vehicles aiming at increased inductive charging efficiency," in *MedPower 2014*, 2014, pp. 1–6.

[144] W. Huang and H. Ku, "Analysis and optimization of wireless power transfer efficiency considering the tilt angle of a coil," *Journal of Electromagnetic Engineering and Science*, vol. 18, pp. 13–19, Jan. 2018. DOI: 10.26866/jees.2018.18.1.13.

[145] *Dynamometer drive schedules*, https://www.epa.gov/vehicle-and-fuel-emissions-testing/dynamometer-drive-schedules, Last accessed: January 10, 2019.

VITA

Omar N. Nezamuddin received the B.S. degree in spring of 2012, the M.S. degree in Fall of 2014, both in Electrical and Computer Engineering from Purdue School of Engineering and Technology-Indianapolis. He started the PhD Program in the spring of 2015 at the same University, and at the time of this writing is a PhD candidate focusing on power electronics for the majority part of his PhD.

Omar has been working in the power electronics lab since 2015 and has done a lot of hands-on work on power converters along with PCB design, assembling and soldering. He has led some projects that included the designing of an inverter for solar application and for motor control. He has also worked and consulted for the Medical/Nursing school at IU to develop medical adherence devices that lead to a couple of patents in which he is a co-inventor.

Omar's research interests include power electronics, electrical drives, control, and energy efficiency. He is a student member of IEEE, and a member of the IEEE IAS chapter of IUPUI.